DISSERTATION

ROLE OF NEUROINFLAMMATORY NF-KB SIGNALING AND GLIAL CROSSTALK IN NEURODEGENERATION

Submitted by

Kelly Sullivan Kirkley

Department of Environmental and Radiological Health Sciences

In partial fulfillment of the requirements

For the Degree of Doctor of Philosophy

Colorado State University

Fort Collins, Colorado

Fall 2013

Doctoral Committee:

Advisor: Ronald Tjalkens

Anne Avery
Marie Legare
William Hanneman

ABSTRACT

ROLE OF NEUROINFLAMMATORY NF-KB SIGNALING AND GLIAL CROSSTALK IN NEURODEGENERATION

Neuroinflammation or inflammatory activation of astrocytes and microglia are considered pathological hallmarks and important mechanisms in debilitating neurodegenerative diseases. However, the signaling mechanisms underlying these neuroinflammatory changes are not fully understood and there is evidence that these inflammatory responses can serve both neuroprotective and neurotoxic roles. Few studies have begun to study the complicated communications occurring between activated glia and the contributions of these cells to neuronal injury. Furthermore, the importance of these pathways in environmentally relevant animal models is currently unknown. Therefore, in order to address these knowledge gaps, I utilized three different neurodegenerative diseases models, domoic acid induced seizures in sea lions, a mouse model of Parkinson's disease (PD), and an *in vitro* astrocyte-microglia culture model of Manganism, to decipher the contributions of microglia and astrocytes to neuronal injury and the pathways that dictate these responses. First, for the first time, I have identified significant correlations between severity of neuronal loss and glial activation in domoic acid exposed sea lions that were associated with significant changes in glutamate metabolism. This indicates that neuroinflammation is playing a never before described role in this disease and targeting this neuroinflammation may be a new source to limit progression of seizures in these animals. Secondly, by creating a mouse with an astrocyte specific deletion of the nuclear factor kappa B (NFκB) pathway, it was determined that neuroinflammatory activation of astrocytes through NFκB is important in the initiation and progression of dopaminergic cell loss in a chemical PD

model. Also, in a similar model of disease, we found that full and potent activation of astrocytes to the basal ganglia toxicant manganese (Mn) required soluble factors from Mn activated microglia. These studies indicate that glial release of inflammatory factors is not only affecting neuronal function and survival, but is important in glial crosstalk and resultant exacerbation of the inflammatory response. Targeting these glial interactions may play important roles in developing treatments to limit the neurotoxicity of neuroinflammation.

TABLE OF CONTENTS

LIST TABLES

Chapter 2

Chapter 4

LIST FIGURES

Chapter 2

Chapter 3

Chapter 4

CHAPTER 1

LITERATURE REVIEW

Physiological Roles of Glia

General Information

Glia represent a diverse class of cells grouped together due their status as non-excitable neural cells that lack the ability to form an action potential and thus transmit electrical signals (GribbinSimon, 2009). Within the central nervous system (CNS), glia represent 90% of all cells and are classified on the basis of morphology, function, and location consisting of astrocytes, microglia, oligodendrocytes, and ependymal cells (Verkhratsky & Butt, 2007). Early descriptions of these cells labeled them as "glue" with a primarily passive structural/supportive role. However, with the advent of patch clamping and fluorescent calcium dye techniques in the late 1980's and early 1990's, research over the past 30 years has found that the role of these cells is much more extensive and complex (Araque, Carmignoto, & Haydon, 2001). Glia are essential for neuronal survival and function, a role that is evolutionary conserved across different phyla, playing prominent roles in both development and pathology of the CNS (GribbinSimon, 2009).

Astrocytes

Description and Distribution

The term astrocyte encompasses a heterogeneous population of cells that can have vastly different morphological and physiological characteristics depending on their location with the brain (Matyash & Kettenmann, 2010; Verkhratsky & Butt, 2007). Their morphological forms range from the protoplasmic astrocyte with extensive arborization found in the gray matter to the more rod-like fibrous astrocyte located within the white matter (Perea & Araque, 2010; Sofroniew & Vinters, 2010). With their extensive processes, they make contacts with neuronal bodies, synapses, axons, blood vessels, and other astrocytes thereby creating a vast network that

allow them to serve a multitude of both structural and important physiological roles within the CNS (GribbinSimon, 2009).

Astrocytes are the most prominent type of cell in the CNS making up sixty to seventy percent of all cells in the brain and are also the most prominent glial type with ninety percent of all glia cells classified as astrocytes (Verkhratsky & Butt, 2007). These cells are found throughout the CNS in a contingent, but non-overlapping manner forming distinct microdomains (Sofroniew & Vinters, 2010). Astrocytes are morphologically characterized by their classic expression of the intermediate filament proteins glial fibrillary acidic protein (GFAP) and vimentin. Other known markers of astrocytes in the adult brain include glutamine synthetase (GS), S100 calcium binding protein β, and glutamate transporters GLT-1/EAAT2 and GLAST/EAAT1(Kimelberg, 2004); however, GFAP has been shown to be the most consistent marker in both physiological and pathological states (O'Callaghan & Sriram, 2005).

Functional Roles

The first noted function of astrocytes within the adult CNS was purely structural; astrocytes were described as a scaffold to arrange and contain the neuronal circuitry due to their relative abundance and formation of glial scars in disease(Verkhratsky & Butt, 2007). Although it is now known that astrocytes have more complex roles, their formation of a continuous syncytium is still important for the structural integrity of the brain. These vast networks help to create specific micro and macro domains and help to create physical barriers between neuronal synapses(GribbinSimon, 2009; Sofroniew & Vinters, 2010). Furthermore, astrocytic endfeet are an important component of the glial limitans, a barrier that helps to isolate the brain parenchyma from the vasculature and subarachnoid compartments (Nimmerjahn, 2009; Verkhratsky & Butt,

2007), as well as the blood-brain barrier (BBB) through the ensheathing of blood vessels throughout the CNS (Carmignoto & Gómez-Gonzalo, 2010).

Past their structural roles, astrocytes serve as important facilitators of neuronal homeostasis through nutritive and trophic support. As a primary component of the BBB, astrocytes that surround endothelial cells are enriched in glucose receptors and channels and act as the main vehicle for the movement of glucose and oxygen from the blood to neurons (GribbinSimon, 2009). Astrocytes, not neurons, are capable of storing glucose in the form of glycogen and of *de novo* synthesis of glutamate (Parpura, Heneka, & Montana, 2012). Glutamate, the primary excitatory neurotransmitter, is under tight control achieved primarily by astrocyte oversight producing, containing, and rapidly removing glutamate from synapses in the cycle known as the glutamate-glutamine cycle. Eighty percent of glutamate released into the synapse is removed by astrocytes and then converted to glutamine by GS. This glutamine is released and then taken up by neurons that convert glutamine into glutamate and γ-amino butyric acid (GABA). Additionally, production of lactate by astrocytes is used by neurons to produce pyruvate and generate adenosine triphosphate (ATP) via the tricarboxcylic acid cycle (TCA) (Verkhratsky & Butt, 2007). Without these shuttle pathways, neurons would not have the resources to continue functioning at the high rates of metabolism and would quickly run out of materials for neurotransmitter release.

In addition to being critical for neuronal metabolism, astrocytes are required for normal synaptic transmission through regulation of neurotransmitters, ions, water, and extracellular pH (Sofroniew & Vinters, 2010; Verkhratsky & Butt, 2007). Astrocytes enwrap pre and post-synaptic membranes forming what is known as the tripartite synapse which allows astrocytes to not only regulate neurotransmitters, but also actively respond to and modulate synaptic plasticity

through the release of gliotransmitters (Araque et al., 2001; Nedergaard & Verkhratsky, 2012; Perea & Araque, 2010; Perea, Navarrete, & Araque, 2009). Astrocytes express a wide assortment of functional neurotransmitters including glutamate, GABA, dopamine, adrenalin/epinephrine, histamine, and glycine, the expression of which varies depending on the local microenvironment to match the physiology of their neuronal neighbors(Parpura et al., 2012; Verkhratsky & Butt, 2007). Majority of the neurotransmitter receptors expressed are metabotropic receptors coupled to G-proteins whose activation results in the generation of inositol triphosphate (IP3) and the release of calcium (Ca2+). However, astrocytes express at least three types of ionotrophic receptors: α-amino-3-hydroxy-5-methyl-isoxazole propionate (AMPA), N-methyl-D-aspartate (NMDA) types of tetrameric glutamate receptors, and P2X trimeric purinoreceptors(Lalo et al., 2008). Activation of glia metabotropic and inotropic receptors results in the generation of Ca2+ waves within astrocytes that are propagated between astroglial networks through connexin gap junctions and glia release of ATP and glutamate(Araque et al., 2001; S. U. Kim & de Vellis, 2005). This intercommunication between astrocytes is dynamic and is influenced by the extent of and frequency of neurotransmitter release which is important in the modulation of synapses in both learning and memory (Perea et al., 2009).

Calcium based communication of astrocytes plays not only a large role in synaptic plasticity, but is vital to the regulation of blood flow in response to neuronal activity known as neurovascular coupling (Carmignoto & Gómez-Gonzalo, 2010; Sofroniew & Vinters, 2010). In areas of high neuronal activity, elevations in calcium in astrocytes results in release of vasoactive compounds such as nitric oxide (NO), prostaglandin E2 (PGE2), potassium (K+), and epoxygenase derivatives (EETS) at astrocytic endfeet that results in a dilation or constriction of

local vasculature (Mulligan & MacVicar, 2004; Nimmerjahn, 2009). This control of cerebral blood flow is complex and the elucidations of how astrocytes cause specific vasodilation versus vasoconstriction in response to neuronal activity is still being fully elucidated.

Astrocytes thus play very diverse and important regulators of neuronal metabolism and activity in the developed CNS; likewise, they also play an important role in the developing CNS, through neuronal guidance and synaptogenesis(Verkhratsky & Butt, 2007), and in adult neurogenesis(Doetsch, 2003). In development, boundaries created by astrocytes help the migration of axons and neuroblasts and release of thrombospondin directs synapse formation. Furthermore, tagging of formed synapses with complement protein, C1q, helps tags synapses for pruning and removal(Christopherson et al., 2005; Powell & Geller, 1999). In the adult CNS, neurogenesis within the subventricular zone of the olfactory bulb and the hippocampus is regulated by secretion of astrocytic factors such as Wnt3, interleukin-1β (IL-1β), interleukin-6, and insulin-like growth factor binding protein 6 (Parpura et al., 2012). Additionally, astrocytes themselves are believed to be the source of newly generated neurons determined by labeling based lineage tracking experiments (Doetsch, 2003). Thus neuronal generation, function, and continued survival is intimately linked and dependent on the vast and extensive physiology of their astrocytic counterparts.

Microglia

Description and Distribution

Microglia are the resident immunoeffector cells of the brain entering the CNS during embryonic development from a monocyte derived cell line (GribbinSimon, 2009; Y. S. Kim, 2005). In the adult brain microglia have very low rates of division, but their numbers can be

replenished by perivascular mononuclear phagocytes (Gehrmann, Matsumoto, Kreutzberg, 1995). They are heterogeneous through the adult brain and constitute ten to fifteen percent of all glial cells with greater numbers located within the grey matter(Verkhratsky & Butt, 2007). In particular, the highest concentrations of microglia are found within the olfactory bulb, hippocampus, and basal ganglia, with the substantia nigra holding the greatest density of microglia making up twelve percent of all cells. They exist in three different morphological states: a ramified phenotype found within the neuropil, a rod-like state in fiber tracts, and possess a macrophage/amoeboid shape in areas with an incomplete BBB (Lawson, Perry, Dri, & Gordon, 1990). Microglia are never at rest and are constantly migrating; however, these migration patterns are distinct between different cells and do not overlap (Gehrmann et al., 1995; Verkhratsky & Butt, 2007).

Functional Roles

Unlike astrocytes, microglia functions within the CNS are limited and still not fully known. As the resident immune cell, the primary role for microglia is immunosurveillance (Block & Hong, 2005; González-Scarano & Baltuch, 1999; Y. S. Kim, 2005). Microglia constantly move and sample within their individual domains, clearing up debris via their phagocytic function as they migrate(GribbinSimon, 2009; Verkhratsky & Butt, 2007). They express a variety of both neurotransmitter receptors, pattern recognition receptors (PRRs) and receptors such as P2X7 to sense alterations in brain homeostasis, presence of foreign materials, and neuronal damage (Ransohoff & Perry, 2009). Microglia represent the main class of cell involved in antigen presentation and are important in recruitment of immune cells such at T and

B lymphocytes to the sites of injury (Gehrmann et al., 1995; González-Scarano & Baltuch, 1999).

More recently, research has determined that microglia may also play integral roles in neuronal development and migration. Amoeboid microglia are implicated in synaptic remodeling and regulation of neuronal apoptosis through the release of soluble factors and phagocytic pruning of synapses in late embryonic development (Block & Hong, 2005; GribbinSimon, 2009). Furthermore, studies have shown microglia to release growth and neurotrophic factors during synaptogenesis (Nakajima & Kohsaka, 1993). As more individuals study these cells, their role in development and the adult CNS will become clearer.

Neuroinflammation

Overview

Astrocytes and microglia serve a multitude of essential functions within the CNS including integral roles in the innate immune system of the brain (Wyss-Coray & Mucke, 2002). In response to foreign or endogenous signals, both astrocytes and microglia adopt an activated phenotype resulting in the release of proinflammatory mediators (Craft, Watterson, & Van Eldik, 2005). This inflammatory system, known as neuroinflammation, is essential in normal tissue repair and in defense against foreign invasion; however, when sustained, this process can become deleterious through the release of neurotoxic factors that amplify underlying disease (Glass, Saijo, Winner, Marchetto, & Gage, 2010; Lee Mosley et al., 2006; Tansey, McCoy, & Frank-Cannon, 2007).

In normal circumstances, the neuroinflammatory reaction is self-sustaining and has mechanisms in place to limit the extent of activation as the process is neither discriminatory or

specific (Glass et al., 2010; Wyss-Coray & Mucke, 2002). For sustained inflammation to occur there must be failure of self-resolution mechanisms or the presence of endogenous or environmental factors that are perceived as a threat. There are a variety of factors known to elicit activation of both microglia and astrocytes including products released by injured neurons such as glutamate(Kaushal & Schlichter, 2008), ATP(Di Virgilio, Ceruti, Bramanti, & Abbracchio, 2009) and matrix metalloproteinase-3(Y. S. Kim, 2005)cytokines including interferon gamma (IFNγ), interleukin-1β (IL-1β), and interleukin-6 (IL-6); adhesion molecules; growth factors, blood derived factors; ionic imbalances; activation of complement, products from viruses and bacteria; and presence of reactive oxygen species (Gehrmann et al., 1995; Sofroniew & Vinters, 2010; Wyss-Coray & Mucke, 2002). Furthermore, new evidence suggests that both microglia and astrocytes express endogenous pattern recognition receptors (PRRs) that respond to a variety of damage-associated molecular patterns (DAMPs) that results in inflammation in a sterile environment and may act as important inducers of inflammation in disease pathology(Glass et al., 2010). These PRRs become activated in response to signals released by necrotic neurons or other pathologic products produced during disease including oxidized proteins and lipids(Husemann, Loike, Anankov, Febbraio, & Silverstein, 2002), messenger ribonucleic acid (mRNA), fibronectin, hyaluronic acid, heat shock proteins, amyloid-beta, neuromelanin, and alpha-synuclein (Block & Hong, 2005; Gensel, Kigerl, Mandrekar-Colucci, Gaudet, & Popovich, 2012; W. W. Zhang et al., 2005). The production of these products is further increased by the activating glia leading to a feed-forward loops and continued cycle of inflammation which leads to a release of neurotoxic mediators and tissue injury.

Activated glia release a plethora of factors including cytokines, chemokines, reactive oxygen species (ROS), and nitric oxide (NO) that have shown to be toxic to neurons (González-

Scarano & Baltuch, 1999; Y. S. Kim, 2005; Verkhratsky & Butt, 2007). Cytokines such as tumor necrosis factor alpha (TNFα) and interleukin-6 are often upregulated early and have shown to directly lead to neuronal apoptosis and amplify inflammation through recruitment of both innate and adaptive immune cells (Gensel et al., 2012; González-Scarano & Baltuch, 1999). Released reactive oxygen products are extensible tied to causing lipid peroxidation, mitochondrial dysfunction and subsequent energy failure and apoptosis, protein modifications, and DNA damage in both neurons and glial cells(Lee Mosley et al., 2006) The formation of peroxynitrite, a by-product of superoxide and NO, is thought to be a major contributor to neuronal induced cell death through nitration and nitrosylation of tyrosine and serine residues of proteins leading to impairment of normal cellular functions (McCarty, 2006). Inhibition or deletion of many of these pathways have shown to be neuroprotective, but often the neuroprotection achieved is dependent on the timing of inhibition as often early down-regulation of inflammation has actually worsened neuronal injury(Frank-Cannon, Alto, McAlpine, & Tansey, 2009). Due to the complicated nature of neuroinflammation and the vast majority of implicated factors, systematic and thorough understanding is vital to understanding the implications that may come from targeting this pathway.

Role of Astrocytes

Astrocyte activation is a biological reaction that is documented in most CNS diseases, as measured by upregulation of GFAP expression and alterations in astrocyte morphology, and is an important early indicator of neuropathology (O'Callaghan & Sriram, 2005; Parpura et al., 2012). Neuroinflammatory activation of astrocytes can be neuroprotective through isolation of damage, glutathione production, BBB repair, and release of neurotrophic factors such as neural growth

factor and glial derived growth factor (Block & Hong, 2005; Kuno et al., 2006; Sofroniew & Vinters, 2010); however, astrogliosis can also be neurotoxic and promote disease progression. Detrimental consequences of astrogliosis include inhibition of axonal regeneration (Block & Hong, 2005; J. Silver & Miller, 2004), exacerbation of inflammation via cytokine production (Brambilla, 2005; Brambilla et al., 2009), production of reactive oxygen and nitrogen species (Carbone, Popichak, Moreno, Safe, & Tjalkens, 2008; Hamby, Hewett, & Hewett, 2006; X. X. Liu, Sullivan, Madl, Legare, & Tjalkens, 2006), and excess glutamate release (Takano, Oberheim, Cotrina, & Nedergaard, 2009). Additionally, chronic inflammatory stimulation of astrocytes reduces glial capacity to generate and release neurotrophic mediators and execute normal physiological functions (Parpura et al., 2012).

The regulation of astrocyte activation is under the control of many factors including cytokines IL6, IFNγ, tumor necrosis factor-alpha (TNFα), toll-like receptor activators, neurotransmitters, ATP, reactive oxygen species, hypoxia, glucose deprivation, ammonia, and protein aggregates (Parpura et al., 2012; Sofroniew & Vinters, 2010). These activators are often by-products of already injured neurons or factors released by activated microglia which indicate that astrocyte activation is often later in disease progression (Hirsch & Hunot, 2009). However, astrogliosis is often less transitory than microgliosis and is believed to be important in amplifying the inflammatory process thereby inducing greater damage (Saijo et al., 2009). Moreover, *in vitro* studies have shown that isolated human astrocytes and not microglia are the major source of NO induced neurotoxicity indicating they may be more significant in neuroinflammatory induced neuronal death in humans than have been indicated in rodent models (S. C. Lee, Liu, Dickson, Brosnan, & Berman, 1993).

Role of Microglia

As the resident immune cells, microglia are the effectors of the innate immune response within the CNS with activation occurring early in disease often prior to overt neuropathology (Gehrmann et al., 1995; Hirsch & Hunot, 2009). Under physiological conditions, microglia exist in a resting, ramified state releasing both anti-inflammatory and neurotrophic factors while surveying their domains (Streit, 2002). However, in the presence of viral or bacterial products(Glass et al., 2010), ATP, changes in ion or neurotransmitter homeostasis(Mastroeni et al., 2009), cytokines such as IFNγ and interleukin 4(Gehrmann et al., 1995), colony stimulating factors (CSFs)(S. U. Kim & de Vellis, 2005) and a list of other pathological products, microglia transform into an activated phenotype, proliferate, and migrate to the site of injury (Block & Hong, 2005; Verkhratsky & Butt, 2007). Activation occurs in two stages. The first stage microglia adopt a rod-like shape and increase expression of major histocompatibility complex two (MHCII) and other inflammatory molecules. In the second stage, microglia morph into an amoeboid cell capable of phagocytosis (Gehrmann et al., 1995; S. U. Kim & de Vellis, 2005).

Once activated, microglia can be both beneficial and deleterious in disease as they release both pro and anti-inflammatory factors (Block & Hong, 2005). Determining whether microglia neuroinflammatory responses will be helpful or toxic is often predicted by adoption of either the M1 known as "classical activation" or M2, the "alternative activation," phenotype (David & Kroner, 2011). The M1 phenotype is primarily inflammatory with microglia upregulating MHCII, CD86, CD32, and CD16 with the production of TNFα, IL-1β, and IL-6. The M2 phenotype, on the other hand, is more involved in tissue repair with increased expression of arginase 1 and CD206 and release of brain derived neurotrophic factor (BDNF), insulin-like growth factor-1 (IGF-1) and interleukin 10 (IL10) (Kigerl et al., 2009).

The classical activated or M1 microglia are known to elicit neuronal death and perpetuate inflammation through release of a variety of cytotoxic substances such as NO, superoxide anion, cytokines, glutamate, prostaglandins, and aspartate (Gehrmann et al., 1995; Nakajima & Kohsaka, 1993). They appear to be the major initial sensors of foreign or endogenous signals, secreting inflammatory mediators such as TNFα and IL-1β that can act on astrocytes to induce secondary inflammatory responses (Saijo et al., 2009). Furthermore, prevention of microglia activation via pharmacological or genetically often protects against neuroinflammatory pathology thus placing them as important regulators of inflammatory mechanism in neurodegenerative diseases (Block & Hong, 2005; Cho et al., 2008).

Involvement of NFκB Signaling

Glial inflammatory activation is regulated by several different pathways including mitogen-activated protein kinases (MAPK), activator protein-1 (AP-1), Janus Kinase (JAK)/signal transducer and activator of transcription (STAT), and interferon regulator factor families (Glass et al., 2010; Verkhratsky & Butt, 2007); nevertheless, the nuclear factor kappa B (NFκB) appears to be the primary pathway involved in the activation of proinflammatory genes (Karin, 2005). Deletion of NFκB is detrimental to the ability of the immune system to initiate immunoprotective responses. Mice deficient in this pathway often succumb to opportunistic infections (Alcamo et al., 2001). Deletion of this pathway in specific glial cells within the CNS has shown to be very neuroprotective with better recovery after spinal cord injury(Brambilla, 2005), decreased pathology in mouse models of multiple sclerosis(van Loo et al., 2006), and decreased seizure induced neuronal death in kainic acid model of seizure (Cho et al., 2008).

NFκB represents a family of transcription factors that are regulated by inhibitory κB's (IκB). Upon signal activation, IκBs are phosphorylated by IκB kinase complex (IKK) marking them for polyubiquination and ultimately degradation by the 26s proteasome thus freeing the transcription factors, located as dimers within the cytosol, to translocate into the nucleus (DiDonato, Hayakawa, Rothwarf, Zandi, & Karin, 1997). The IKK complex consists of three different proteins including the two catalytic units IKKα/IKK1 and IKKβ/IKK2 and the regulatory subunit IKKγ. These two catalytic subunits mark the division of the two NFκB activation pathways known as the classical pathway and the alternative pathway. The classical NFκB pathway involves the dimers p50 and p65/RelA and is activated by the action of IKKβ/IKK2 of the IKK complex. This pathway is primarily involved in immunoregulation controlling innate immune responses and survival of immune cells3. The alternative pathway is primarily involved in the development of secondary lymphoid organs and requires only IKKα/IKK1 and results in the processing of p100 (Bonizzi & Karin, 2004; Karin, 1999; Li, Omori, Labuda, Karin, & Rickert, 2003). Deletion of IKKβ/IKK2 and not IKKα/IKK1 recapitulates similar mouse phenotypes as RelA knockout mice with almost complete inhibition of inflammatory responses and thus represents a major target in modulating glia neuroinflammatory activation(Alcamo et al., 2001).

Neuroinflammatory Involvement in Disease

The activation of microglia and astrocytes is one of the universal components of neuroinflammation and is implicated in the progression of neurodegeneration in ischemia, seizure, Alzheimer's disease, multiple sclerosis, amyotrophic lateral sclerosis, and Parkinson's disease (PD) (Block & Hong, 2005; Glass et al., 2010; Hirsch & Hunot, 2009; Lee Mosley et al.,

2006; Vezzani, Aronica, Mazarati, & Pittman, 2011). Since the first descriptions of activated glia in neurodegenerative disease almost 20 years ago, there have been an increasing number of nervous system pathologies describing activated glia. This research has revealed that although induction of inflammation may occur in a disease-specific manner, there is evidence of shared mechanisms for the sensing and transduction (Glass et al., 2010). Research aimed at elucidating neuroinflammatory pathogenesis and developing targeting strategies is quickly expanding due to increasing indications of the importance of this mechanism in the progression, and possibly initiation, of many neuropathologies.

Seizure

Seizure is an event where there is spontaneous synchronization of neuronal activity whereby a set or subset of neurons undergoes continual and uncontrollable electrical burst of activity and when this occurs chronically, the condition is termed epilepsy. Epilepsy, caused by both genetic and acquired factors, affects 50 million people worldwide; however, sixty percent of epileptic cases are idiopathic (Ngugi et al., 2011). The events that lead to epileptogenesis are only partially defined and a large fraction of individuals with epilepsy are either refractory to current treatments or experience important side effects (Rogawski & Löscher, 2004). Post-mortem examination of patients with intractable epilepsy has consistently identified the presence of astrogliosis and microgliosis (Najjar, Pearlman, Miller, & Devinsky, 2011), stimulating intense research focused on the involvement of glial inflammation in the etiopathogenesis of this disease (Araque et al., 2001).

The link between neuroinflammation and epilepsy is supported by both clinical and experimental evidence. Infection and gliomas have long been identified as an important trigger

for secondary or symptomatic epilepsy and a polymorphism in IL-1β is an important cause of genetic based seizures (Foresti, Arisi, & Shapiro, 2011; Losi, Cammarota, & Carmignoto, 2012). Activated astrocytes and microglia are commonly identified near or around seizure foci in many forms of epilepsy(Sofroniew & Vinters, 2010) and in temporal lobe epilepsy (TLE), removal of astrogliotic tissue in the hippocampus is an important treatment in patients with intractable forms of the disease(Alarcón & Valentín, 2010). Additionally, studies examining the cerebral spinal fluid (CSF) in patients with both non-inflammatory and immune based epilepsies often demonstrated increased levels of inflammatory cytokines such as IL-6, TNFα, and IL-1β (Aronica & Crino, 2011). Experimental seizure models have further supported glial involvement by revealing that neuroinflammatory activation of glia often proceeds seizure activity(Vezzani et al., 2011) and if specifically induced, can lead to alterations in synaptic physiology increasing hyperexcitability of local neurons(Ortinski et al., 2010).

Proposed mechanisms for glia involvement in pathophysiology of seizures include both loss of function and inflammatory modulation of neuronal excitability. Non-inflammatory based alterations include water dysregulation, alterations in potassium homeostasis, and perturbations in glutamate/GABA metabolism caused by changes in astrocytes as animals deficient in proteins important in these pathways is sufficient enough to cause or potentiate seizures (Devinsky, Vezzani, Najjar, De Lanerolle, & Rogawski, 2013; D. J. Lee, Hsu, Seldin, Arellano, & Binder, 2012a). Inflammatory mediated pathways include enhancement of glutamatergic activation and potentiation of n-methyl-d-aspartate (NMDA) induced currents (González-Scarano & Baltuch, 1999), increased release of gliotransmitters, and inhibition of astrocyte functions(Brown, 2007; Foresti et al., 2011; Kaushal & Schlichter, 2008; Vezzani et al., 2011). Implicated molecules include pro-inflammatory cytokines, nitric oxide, and arachadonic acid(González-Scarano &

Baltuch, 1999; Kovacs et al., 2009). Even with several implicated mechanisms, the most consistent alteration in both inflammatory and non-inflammatory pathways is the effects seen in glutamate/glutamine and GABA metabolism with human and rodent models revealing high levels of glutamate and low levels of GABA stemming from loss of GS and glutamate transporters in astrocytes (Coulter & Eid, 2012). This results in both increased excitatory stimulation, decreased inhibitory transmission, and facilitates a pathological condition where astrocytes actually increase glutamate release thereby affecting thousands of synapses (Araque et al., 2001; Verkhratsky & Butt, 2007). Heightened research into neuroinflammatory involvement in seizure has only begun to realize the extent and importance of glial mechanisms in this disease and understand the potential therapeutic implications of this research.

Parkinson's Disease

Parkinson's disease (PD) is a chronic and progressive neurodegenerative disease that affects 1.5% of the global population over the age of 65 and represents the most common movement disorder(Meissner et al., 2011). The most notable symptoms include bradykinesia, resting tremors, rigidity, and postural instability caused by loss of dopaminergic neurons in the nigrostriatal pathway resulting in concomitant loss of dopamine in the striatum which can often be alleviated by replacement dopamine therapy (Chaudhuri & Schapira, 2009). Other non-motor symptoms include insomnia, depression, dementia, and autonomic failure which are often unaddressed by current treatments (Jankovic, 2008). Familial forms of PD are linked to mutations in the PARK family of genes, LRRK2, DJ-1, SNCA, and PINK-1 (Gasser, 2009); however, 95% of all PD cases are idiopathic and are most likely caused by a complex interaction

between genetic susceptibility and environmental exposure to pesticides, pollutants, and heavy metals (Glass et al., 2010).

Several mechanisms are implicated in the etiology of sporadic PD including glutamatergic toxicity, misfolding of α-synuclein and tau, decreased production of neurotrophic factors, exposure to environmental and infectious insults, mitochondrial dysfunction, oxidative stress, and neuroinflammation (Glass et al., 2010; Meissner et al., 2011). In particular, recent research has primarily focused on the involvement and interaction of protein misfolding, oxidative stress, and neuroinflammation due to evidence in experimental models linking these pathways in the induction, progression, and facilitation of neuronal loss (Hirsch & Hunot, 2009; Lee Mosley et al., 2006; Lema Tomé et al., 2012). Activated microglia and astrocytes are fundamental to the pathophysiology of these mechanisms as they are the primary sources of inflammatory and oxidative factors and can both be activated by and induce production of misfolded proteins (S.-J. Lee, 2008).

Inflammation is now considered a pathological hallmark of PD as astrogliosis and microgliosis is consistently revealed in examination of *post-mortem* tissues as well as elevations in cytokines in patient CSFs (Block & Hong, 2005; Nagatsu & Sawada, 2005). Furthermore, infusion of the bacterial product lipopolysaccharide, a potent inducer of inflammation, in rodent brains is known to lead to specific loss of nigral dopamine neurons after initiation of glial activation in a manner that recapitulates the slow, progressive nature of PD(Block & Hong, 2005). Experimental models of PD using the toxin 1-methyl-4-phenyl-1,2,3,6-tetrahydropyridine (MPTP) have shown massive amounts of glial activation prior to and around neuron loss(Hirsch & Hunot, 2009; J. A. Miller et al., 2011; Saijo et al., 2009; Sugama et al., 2003). Release of glial inflammatory factors such as NO and TNFα are highly implicated in

causing the progressive loss of neurons as suppression of inducible nitric oxide (NOS2) or deletion of TNFα receptors protect mice from MPTP induced neurodegeneration (Gao et al., 2011; McCarty, 2006; Sriram, 2006). The products released from glial damaged neurons such as neuromelanin and α-synuclein can further induce gliosis creating a loop of interdependent neuronal loss and sustained glial activation(Wyss-Coray & Mucke, 2002). Intense research elucidating the mechanisms and interactions between neuroinflammation in PD pathogenesis are increasing as scientist strive to find better and more effective ways to treat this disease.

Manganism

Manganese (Mn) neurotoxicity, or Manganism, is a parkinsonian disease caused by excessive exposure to the trace mineral manganese and is marked by motor deficits such as gait disturbances, facial masking, hypo and dysphonia, dystonia, and action and postural tremor (Guilarte, 2010; Perl & Olanow, 2007). These parkinson-like manifestations are due to the neuropathological changes including neuronal loss, atrophy and gliosis within the globus pallidus (GP), substantia nigra pars reticulata (SNpr) and striatum (ST) of exposed individuals (M. ASCHNER & Aschner, 1991; A. Sigel, Sigel, & Sigel, 2007). Traditional exposures to high levels of Mn occur occupationally in welders, miners, and steel workers(Hua & Huang, 1991); however, the neurological consequences of environmental exposure to low levels of Mn through ingestion of crops with residues of the Mn-containing pesticide Maneb (Santamaria, 2008) and well water with high concentrations of Mn(Woolf, Wright, & Amarasiriwardena, 2002) in under scrutiny as an important route for non-occupational based exposure. In particular, the there is increased concern with chronic Mn exposure in children due to their lower ability to clear Mn (Collipp, Chen, & Maitinsky, 1983) higher levels of iron deficiency, which has shown to elevate

brain Mn levels (J. ASCHNER & ASCHNER, 2005) and more efficient oral uptake of Mn(Neal & Guilarte, 2012). Recent epidemiological evidence has observed cognitive deficits in children exposed to high levels of Mn in drinking water (Horacio Riojas-Rodríguez, 2010; Y. Kim et al., 2009; Menezes-Filho, Novaes, Moreira, Sarcinelli, & Mergler, 2011) highlighting the need for future studies addressing the long term consequences of these exposures.

The mechanisms of how Mn exposure leads to specific neurodegenerative changes in the basal ganglia of exposed humans and animals are poorly understood. Elevated levels of Mn are routinely documented in the basal ganglia of exposed humans and animals(Olanow, 2004) and experimental evidence has shown that Mn can be directly neurotoxic through inhibition of mitochondrial respiration leading to energy failure and oxidative stress (S. Zhang, Zhou, & Fu, 2003) and through excitotoxicity(Centonze, 2001). Other mechanisms such as oxidative stress, glial toxicity, and neuroinflammation are being researched due to the observation of continued progression of disease despite discontinued exposure in human cases and rodent studies (J. ASCHNER & ASCHNER, 2005; Filipov & Dodd, 2011; A. Sigel et al., 2007).

The involvement of glia in Mn-induced neurotoxicity has only received attention within the last 20 years as an potential mechanism in Manganism (Filipov & Dodd, 2011). Although activated astrocytes and microglia were often noted in *post mortem* evaluation of Mn patients (Perl & Olanow, 2007), few studies examined the importance of this glial activation. This was most likely due to the ability of Mn to be directly neurotoxic through inhibition of mitochondrial respiration and induction of oxidative stress (S. Zhang et al., 2003) and the current focus on acute, high level exposures. A study in 1998 by (Spranger et al., 1998)radically altered perceptions of glia involvement in this disease showing that more modest levels of Mn exposures required the presence of glia to be neurotoxic. Other studies have now built upon these initial

findings revealing that Mn can exacerbate LPS and cytokine induced activation of both microglia and astrocytes resulting in increased levels of TNFα, IL-1β, ROS, and NOS2 expression (Barhoumi, Faske, Liu, & Tjalkens, 2004; C.-J. Chen et al., 2006; Filipov, Seegal, & Lawrence, 2005; Moreno, Streifel, Sullivan, Hanneman, & Tjalkens, 2011; Moreno, Sullivan, Carbone, Hanneman, & Tjalkens, 2008). Increased levels of the aforementioned inflammatory genes has also be measured in both rodent (Moreno, Streifel, Sullivan, Legare, & Tjalkens, 2009a; Zhao et al., 2008)and non-human primate (Verina, Kiihl, Schneider, & Guilarte, 2011)studies with deletion or inhibition of these pathways showing neuroprotection (Streifel, Moreno, Hanneman, Legare, & Tjalkens, 2012; P. Zhang et al., 2009; Zhao et al., 2008).

Despite the heightened focus on glial mechanisms in Manganism, there are still many unanswered questions about relevancy and mechanisms due to the limited number of *in vivo* studies and the inability of Mn to be a very potent glia activator alone (Filipov & Dodd, 2011). Like many other CNS diseases, there exist two ideological camps, microglia versus astrocytes, with few studies examining relative glial contributions or glial crosstalk. With limited treatments available for this disease and indications that elevated Mn exposures in children can lead to adverse neurological affects, there is a need for a more systematic and comprehensive look at glial involvement and the potential importance of this response in chronic exposures.

Summary

Studies in the last several decades have demonstrated the importance of astrocytes and microglia to neuronal development, homeostasis, and survival greatly redefining the role of these cells from inert structural components to important cells in brain physiology and pathology. More specifically, the importance of astrocytes and microglia to neuronal survival has received

increased attention, as these two glial types are the most often altered during disease states and are now known to be fundamental components of the innate immune system of the brain. Inflammatory activation of glia, or neuroinflammation, is a classic and conserved marker of neuropathology and is implicated in the progression, and possibly initiation, of several CNS disorders including seizure, Parkinson's disease, and Manganism. Yet, much of the above information on neuroinflammation has been gleaned from rodent modeling with few studies utilizing translational or environmental relevant models to examine these important mechanisms. Furthermore, because glial activation can also serve either neuroprotective or neurotoxic functions, there exists a need to better understand the timeline and pathways of glial activation with a more extensive focus on the relative contributions of different glial types and the dynamics of glial-to-glial signaling. By examining specific glial derived mechanisms in several neurodegenerative diseases, we hope to better understand the implications of neuroinflammation on CNS disease pathology and discover potential targets for future research.

CHAPTER 2

EVIDENCE OF NEUROINFLAMAMTION IN CALIFORNIA SEA LIONS EXPOSED TO DOMIC ACID

Summary

California sea lions (CSLs) exposed to the marine biotoxin domoic acid (DA) develop an acute or chronic toxicosis marked by neurological dysfunction and seizures that is often refractory to current treatments. Experimental seizure studies have shown glial activation and the resultant oxidative and inflammatory mediator release to play a significant role in generation of seizures through perturbing glutamate-glutamine cycling, but the involvement of these pathways in DA toxicosis is unknown. Sections from archived hippocampi from 7 control and 13 CSLs diagnosed with DA toxicosis were immunofluorescently stained for markers of gliosis and oxidative/nitrative stress and changes in glutamine synthetase (GS) and compared to pathological changes observed in hematoxylin and eosin stained sections. Quantitative counts revealed increasing loss of microtubule associated protein-2 positive neurons with elevations in 4-hydroxynonenal based on chronicity of exposure while the number of activated glia expressing nitric oxide synthase 2 and tumor necrosis factor-α followed a pattern based on pathological severity. There were no significant changes in the amount of GS positive cells, but there was substantial upregulation of 3-nitrotyrosine in GS expressing cells and in neurons especially in chronic DA animals. These changes were most consistently seen in the dentate gyrus and in the cornu ammonis (CA) sectors CA3, CA4, and CA1; however, CA2 and subiculum were also often affected. The results of this study indicate that gliosis and resultant changes in GS are possibly important mechanisms in DA induced seizure and combinatorial therapy aimed at limiting these changes could be effective in treating animals.

Introduction

Exposure to the marine biotoxin domoic acid (DA) during harmful algal blooms results in a syndrome known as domoic acid toxicosis marked by reproductive failure, cardiotoxicity, and most prominently neurological dysfunction.(Goldstein et al., 2009; E. M. D. Gulland et al., 2002; Scholin et al., 2000; Zabka et al., 2009) The California sea lion (CSL) is the most commonly affected marine species, with hundreds of animals stranding and/or dying each year, and act as sentinels of the disease.(Bossart, 2011) Clinical signs in animals exposed to DA include head weaving, ataxia, depression, and abnormal scratching; however, the most common and morbid clinical sign is the development of persistent seizures. (Scholin et al., 2000; Silvagni, Lowenstine, Spraker, Lipscomb, & Gulland, 2005) Symptomatic treatment of seizing animals includes diazepam and lorezepam with long-term control using phenobarbitone; yet despite these treatments, more than half of animals admitted for treatment have progression of neurological symptoms resulting in *status epilepticus* leading to death or euthanasia. (Goldstein et al., 2007; E. M. D. Gulland et al., 2002) The lack of successful treatment and the increased number of sea lions diagnosed each year highlights the need for better approaches to treat this condition.

DA acts as an excitotoxin binding to kainate/alpha-amino-3-hydroxy-5-methyl-4-isoxaxole-propionic acid (AMPA) glutamate receptors causing activation of neurons, which leads to seizurogenic excitations and neuronal injury in hippocampal and limbic structures.(Dakshinamurti, Sharma, Sundaram, & Watanabe, 1993; Sutherland, Hoesing, & Whishaw, 1990) Two syndromes are now recognized, an acute toxicosis and a chronic epileptic syndrome, similar to human temporal lobe epilepsy (TLE) that develops months after a bloom has occurred. In addition, a significant percentage of animals diagnosed with acute toxicosis often progress to the chronic syndrome while in treatment or restrand as their condition

worsens.(Goldstein et al., 2007) Direct toxicity and/or seizure-induced neuronal death is therefore insufficient to explain the progressive lesion that is seen within the hippocampus of exposed CSLs as disease advances even in the absence of continued exposure to DA or when seizure is prevented using anti-epileptics.

The current limitations in successful treatments for DA induced seizures is not unique as 1/3 of human patients have retractable epilepsy.(Eid, Williamson, Lee, Petroff, & De Lanerolle, 2008; Waldbaum & Patel, 2010) Most modern anti-epileptics only treat neuronal excitability but do not address other pathophysiological events that lead to a progressive increase in seizure events. Studies in rodent seizure models and human TLE have consistently identified changes in the glutamate-glutamine cycle with elevations in extracellular glutamate and decreased synthesis of gamma-aminobutyric acid (GABA) shown prior to and around seizure foci.(Cavus et al., 2005; De Lanerolle & Lee, 2005; Ortinski et al., 2010) These changes are thought to be a consequence of decreased astrocytic glutamine synthetase (GS) expression and activity(EID et al., 2004; Ong, Leong, Garey, Reynolds, & Liang, 1996; O. Petroff, Errante, Rothman, & Kim, 2002) caused by high levels of reactive oxygen/nitrogen species and inflammatory factors that adversely affect GS.(Bidmon et al., 2008; Görg et al., 2007; Seifert & Steinhäuser, 2011)

Activated glia are the primary source of pro-inflammatory and pro-oxidant factors(Vezzani et al., 2011) and can be seen prior to recurrent seizures in experimental models of seizure(Losi et al., 2012; Scallet, Schmued, & Johannessen, 2005) and in human patients with TLE.(Aronica & Crino, 2011) Furthermore, blockade of glial activation or expression of neuroinflammatory factors such as nitric oxide synthase 2 (NOS2) and interleukin-1 Beta (IL-1β) have shown to protect against neuronal loss and prevent or reduce the magnitude/frequency of seizures.(Ananth, Gopalakrishnakone, & Kaur, 2003; Cho et al., 2008; Chuang et al., 2010;

Foresti et al., 2011) These data collectively support a role for neuroinflammation in epileptogenesis; however, the mechanisms by which activated glia contribute to the etiology of DA toxicosis is not well understood.

In the current study, we investigated the role of glutamate-glutamine changes and gliosis in acute and chronic DA-exposed CSLs postulating that the extent of neuronal injury would correlate with loss of GS and activation of both astrocytes and microglia. Immunofluorescent and immunohistochemical examination revealed significant upregulation of astrocytes and microglia expressing NOS2 and tumor necrosis factor alpha (TNF-α) in mildly and severely lesioned animals that correlated with the severity of DA-induced lesions. Additionally, 4-hydroxynonenal (4-HNE) and 3-nitrotyrosine (3NT) were elevated in neurons and GS-expressing cells, respectively. These results indicate that neuroinflammation and resultant oxidative stress may play an important role in DA toxicosis and may present new targets for therapy.

Materials and Methods

Source and Selection of Animals

This study utilized archived formalin-fixed, paraffin-embedded sea lion tissues collected by the Marine Mammal Center (MMC) in Sausalito, CA from animals that died or were humanely euthanized during veterinary care between 2000 and 2011 (table I) and sent to Colorado State University Diagnostic center as diagnostic samples. Animals were classified as DA intoxicated based on positive neurological symptoms recorded in the clinical histories and/or presence of DA consistent pathological lesions.(Scholin et al., 2000; Silvagni et al., 2005) Control animals died or were euthanized for unrelated causes and lacked any clinical symptomology or histopathology typical of DA exposure. When available, cases were further classified based on levels of DA measured in urine by direct competitive DA enzyme-linked immunosorbent assay (ELISA) or feces by high-performance liquid chromatography.(Goldstein et al., 2007)

DA cases were further subdivided based on chronicity of exposure (acute vs. chronic) and severity of lesion (normal, moderate, severe). Acute cases were animals that stranded during or near a bloom in clusters, had clinical signs of ataxia, head weaving, and seizures, and had hippocampal necrosis.(Goldstein et al., 2007; E. M. D. Gulland et al., 2002; Scholin et al., 2000) Chronic CSLs were animals that stranded alone, had intermittent seizures at least two weeks apart, abnormal behaviors, and had chronic pathologic changes such as hippocampal atrophy and gliosis.(Goldstein et al., 2007) Severity of DA induced lesions was determined by evaluation of hematoxylin and eosin stained sections by board certified veterinary pathologists for extent of neuronal loss in the hippocampus.

Immunofluorescence

Representative paraffin-embedded 10 μm coronal sections from the hippocampus were immunolabeled with microtubule associated protein-2 (MAP-2) to assess neuronal loss, glutamine synthetase (GS) and 3-Nitrotyrosine (3-NT) to assess expression and nitrosylation of GS, and glial fibrillary acidic protein (GFAP) or ionized binding adaptor protein-1 (IBA-1) in combination with NOS2 or TNFα to assess gliosis. Briefly, sections were deparaffinized in xylene and graded ethanol followed by antigen retrieval by boiling sections in 0.01M sodium citrate buffer (pH 8.5). Sections were blocked in 2% donkey serum (Sigma; St Louis, MO) in a 0.2% Triton-X solution made in 0.05M Tris Buffered Saline (Tris A; pH 7.6). Sections were incubated overnight at 4 degrees Celsius in the primary antibodies MAP-2 (Abcam; Cambridge, MA), GS (1:250; Chemicon, Temecular, CA) and 3-NT (1:100; Millipore, Billerica, MA), or GFAP (1:250: Cell Signaling, Danvers, MA) or IBA-1 (1:250; Novus Biologicals, Littleton, CO) in combination with TNFα (1:100; Abcam, Cambridge, MA) or NOS2 (1:100, BD Biosciences, San Jose, CA). After rising in Tris A, sections were incubated for 3 hours at room temperature in Alexafluor-488, Alexafluor-555, or Alexafluor-647 conjugated secondary antibodies (1:500; Invitrogen, Carlsbad, CA). To confirm specificity of staining, primary only, secondary only, and substitution of rabbit or mouse sera for primary antibodies were performed (data not shown). Sections were mounted in media containing 4′,6-diamidino-2-phenylindole dihydrochloride (DAPI) to detect cell nuclei and coverslipped. Completed sections were stored at 4 degrees Celsius until imaging.

Fluorescence images were captured using 20x or 40x air plan apochromatic objectives on a Zeiss Axiovert 200M inverted fluorescence microscope (Carl Zeiss, Inc., Thornwood, NY) equipped with a Hammatsu ORCA-ER-cooled charge-coupled device camera (Hammamatsu

Photonics, Hamamatsu City, Japan). Boundaries of specific areas of the hippocampus including the dentate gyrus (DG), subiculum (Sub), and areas 1, 2, 3, and 4 of the cornu ammonis (CA), were determined by low magnification (10x) montage imaging. Two randomly acquired images from within the boundaries of specific areas of the hippocampus were quantified utilizing Slidebook software (Intelligent Imaging Innovations Inc., Denver, CO). Prior to quantification, cases were assigned a number between 1 and 20 by using Microsoft Excel random number generator to allow for blinded measurements.

Assessment of neuronal loss, GS expression, and gliosis was determined by cell counts. Number of positive cells, defined as expressing the protein of interest and having a DAPI positive nucleus, were averaged per region and summed for the entire hippocampus. 3-NT levels per GS positive cell were calculated by determining the sum intensity of 3-NT in areas co-localized with GS divided by the number of GS positive cells in that field.

Immunohistochemistry

Representative paraffin-embedded 10 μm coronal sections from the hippocampus were labeled with 4-hydroxynonenal (4-HNE) to assess oxidative stress. Tissue sections were prepared for immunohistochemical staining as described above. Sections were incubated overnight at 4 degrees Celsius in a polyclonal rabbit 4-HNE antibody (1:500), kindly provided by Dr. Dennis Petersen, University of Colorado Denver, and then developed using horseradish peroxidase-conjugated secondary antibodies and diaminobenzidine reagents from the Vectastain ABC Kit (Vector Labs, Burlingame, CA) as described previously.(X. X. Liu et al., 2006; Moreno, Streifel, Sullivan, Legare, & Tjalkens, 2009a) Sections were then counterstained with hematoxylin and dehydrated in graded ethanol then xylene and coverslipped. Amount of 4-HNE

was assessed for each animal by examining whole hippocampi montages obtained on low magnification (10x).

Statistical Analyses

Comparison of means was performed using a one-way analysis of variance using a Tukey-Kramer *post hoc* analysis test with Prism software (Graphpad Inc., San Diego, CA). For all analyses, a $p < 0.10$ was considered significant to preserve power with limited number of cases. All data is presented as mean ± SEM while a unique letter represents statistically significant groups.

Results

Clinical and Histopathological Findings

Pertinent clinical and histologic findings of the CSL cases in this study are summarized in Table II and segregated based on chronicity of exposure. Clinical signs of neurological dysfunction were consistent with previous reports and included seizures, head bobbing, tremors, lethargy, and blindness.(Goldstein et al., 2007; E. M. D. Gulland et al., 2002; Scholin et al., 2000) The occurrence of seizures was the most consistent clinical sign and was observed after capture in the Marine Mammal Center in all 5 acute cases and 6 out of 7 chronic cases. Emaciation was also a common finding in many of the DA-exposed animals. Except for lethargy observed in one control CSL, no neurobehavioral signs associated with DA intoxication were observed in control cases.

Histopathology and severity of the DA lesion in the hippocampus were variable in both acute and chronic cases. Two acute cases lacked any significant histologic changes in the hippocampus while the remaining 3 acute cases had observed neuronal necrosis and dropout that ranged in severity from mild to severe (Fig. 1B). Hippocampal atrophy, spongiosis, and gliosis were also variably observed in acute animals. Chronic CSLs all showed signs of histologic changes with neuronal loss observed in all animals. The severity of the lesion ranged from mild to severe and neuronal necrosis and hippocampal atrophy were a consistent finding in many of the cases (Fig. 1C). Hippocampal edema, spongiosis, and lymphocytic cuffing were less commonly seen. No changes in the hippocampus were noted in any of the control cases (Fig. 1a).

Neuronal Injury and Oxidative Stress

The extent of neuronal loss and injury was determined by counting the number of MAP-2 positive neurons in the DG, CA4, CA3, CA2, CA1, and subiculum of DA intoxicated animals in comparison to control cases. Representative photomicrographs are shown in Figures 1D – 1F, depicting the pattern of MAP-2 immunolabeling of neurons in the hippocampus between control, acute DA, and chronic DA animals. The loss of MAP-2 positive neurons occurred in an increasing trend based on chronicity of exposure with significant loss seen in chronic cases at the total hippocampal level (Fig 1J) and in the DG and CA1 (Fig. 1K). Acute DA cases showed a trend of MAP2 neuronal loss at the total hippocampal level and in the DG with significant loss of immunolabeling occurring in the CA2 region. The CA3, CA1, and subiculum areas also showed significant loss of MAP-2 positive neurons in animals with lesions classified as severe (data not shown).

Production of reactive oxygen species (ROS) and the resultant oxidative stress have been shown to be essential mechanisms in DA caused excitotoxic cell death(Dakshinamurti et al., 1993) and is a potential mechanism in seizure induced neuronal loss.(Devi, Manocha, & Vohora, 2008; Waldbaum & Patel, 2010) To explore the role of oxidative stress in DA toxicosis, we labeled hippocampal sections from control and DA-exposed animals with 4-HNE, an indicator of lipid peroxidation. 4-HNE staining also followed a pattern based on chronicity with the most intense staining appearing in CSLs classified as chronic. High levels of immunoreactivity appeared in neurons of the CA3, CA4, and DG, classified in order of higher intensity, and with weaker intensity in the CA1 and subiculum in chronic CSLs (Fig. 1I). Acute cases (Fig. 1H) showed occasional 4-HNE positive neurons in the DG, CA4, and CA3 with very low 4-HNE detected in the CA2, CA1, and subiculum regions. Few of the control cases (Fig. 1G), especially

in the DG, CA4, and CA3 regions, had very weak 4-HNE detectable neurons while the other areas lacked any observable staining. 4-HNE immunoreactivity did not appear to correlate with the severity of lesioning as many animals with minimal hippocampal histopathology had high levels of 4-HNE staining while other animals classified as severe had low detectable 4-HNE reactivity.

Loss and Changes in Glutamine Synthetase

The number of GS expressing cells was similarly examined by counting the number of GS+ cells in control versus DA-exposed CSLs by immunofluorescence (Fig. 2). In control animals (Fig. 2A), GS positive cells showed characteristic glial morphology with about 50% of GS+ cells co-labeling with the astrocytic marker GFAP. The pattern of GS labeling appeared similar in acute DA animals (Fig. 2B); however, in 2/7 chronic DA cases, both glial and neuronal type cells were found expressing GS in primarily CA2, CA1, and subiculum. Neuronal expression of GS was confirmed by co-localizing the GS+ cells with the neuronal marker MAP-2 (not shown). Quantitative counts revealed a significant decrease in GS reactive cells only in the DG of chronic cases (Fig. 2E) while total levels remained unchanged (Fig. 2D). When GS levels were examined by severity of DA induced lesion, animals with mild lesions had significant decreases in GS expression, but severe cases were not different from controls (not shown).

The extent at which GS activity may be impaired due to nitration was assessed by co-immunofluorescence of GS with the nitration marker 3-NT. Hippocampi of control animals showed low overall 3-NT reactivity and low GS nitration (Fig. 2F) as measured by total immunofluorescence intensity per GS positive cell. Animals classified as DA acute showed increased levels of GS nitration (Fig. 2G); however, only DA chronic CSLs (Fig. 2H) had

significant increases over control animals at the whole hippocampus level (Fig. 2I) and in the DG and CA4 regions (Fig. 2J). The amount of nitrated GS also appeared to increase based on severity, but was not significant (not shown). In both acute and chronic cases, 3-NT positive neurons were also identified especially in the CA3, CA4, and CA1 regions. Protein nitration in neurons was again more intense in chronic than acute or control animals.

Astrocytosis and Microgliosis

With significant indications of oxidative and nitrative stress, we investigated the presence of reactive glia expressing the proto-typical neuroinflammatory markers TNF-α and NOS2 in the hippocampus and subiculum of DA-exposed CSLs. Activation of both astrocytes (Figs 3-4) and microglia (Figs. 5-6) correlated more significantly with the severity of the lesion present than with classification of chronicity (except in the DG, CA4, and CA3 regions). Animals with no significant pathology (classified as normal) showed limited numbers of GFAP (Fig 3A) or IBA-1 positive cells (Fig. 5A). Astrocytes present in these animals showed characteristic fibrous morphology typical of a resting phenotype while astrocytes in mild (Fig. 3B) and severely (Fig. 3C) lesioned animals had a thickened and hyperplastic appearance. Quantitative counts revealed significant increases in the number of GFAP positive cells over the entire hippocampus (Fig. 4A) as well as in the DG, CA3, and CA1 in only severely lesioned CSLs (Fig. 4B). Expression of NOS2 in astrocytes increased significantly in animals with mild lesions especially in CA3, CA1, and subiculum (Fig. 4D-E) while the number of TNF-α positive astrocytes was highest in CSLs with severe lesions with significant changes seen in the DG, CA4, and CA3 regions (Fig. 4F-G). Representative images from the CA3 region showing astrocytic expression of NOS2 and TNF-α for normal, mild, and severely lesioned animals are shown in figures 3D-I. Si

The degree of microgliosis was assessed in a similar manner and revealed a pattern of activation also based on severity of DA-induced histopathology as evidenced in representative figures shown in Figure 5. Microglia were present in very low numbers in CSLs with normal (Fig. 5A) and mild histopathogy (Fig. 5B) while microglia numbers significantly elevated in animals with severe lesions (Fig. 5C). Microglia present in severe animals had an obvious morphological change to a reactive phenotype with increased numbers of rod and amoeboid type microglia present. Unlike the graded increase in the number of GFAP positive cells, quantitative counts of IBA-1 positive glia demonstrated that only CSLs with severe lesions had any demonstrable increase in the number of microglia. This increase was significant in all areas of the hippocampus (Fig. 6A-B). A similar trend was seen when evaluating the number of microglia expressing NOS2 (Fig. 6C-D) or TNF-α (Fig. 6E-F) as represented by images from the CA3 region (Fig. 5D-I).

Discussion

Since the first mass stranding event in 1998, the number of sea lions diagnosed with domoic acid toxicosis has steadily risen(Goldstein et al., 2007); yet, despite increasing commonality, little is known about the pathogenesis and current treatment regiments are largely ineffective.(Ramsdell, 2010) The objective of the current study was to investigate potential mechanisms in the development of seizures in DA-exposed CSLs proposing that alterations in glutamate-glutamine cycling through neuroinflammatory activation of glia would correlate significantly with severity of disease. To examine this hypothesis, we used immunohistochemical and Immunofluorescent evaluation of archived brain tissue from California sea lions classified clinically into control, DA acute, or DA chronic. The characteristics of the cases (Table I) matched previous epidemiological findings(Bargu, Silver, Goldstein, Roberts, & Gulland, 2010; Goldstein et al., 2007) with acute animals consisting of adult females while chronic cases included both adult and younger animals of both sexes. All DA animals utilized had a known seizure event within their clinical histories and the cases ranged across several different bloom events. Furthermore, measurement of DA in urine or feces revealed high levels of DA in acute cases, consistent with recent exposure, while the chronic cases had low or no detectable levels of DA. However, DA measurements revealed that two of the control cases also had significant levels of DA within their tissues even in the absence of any clinical or pathological signs. Due to the relevant abundance of even low levels of DA in the environment, finding control animals without any known exposure is difficult and thus other measures must be utilized in classifying animals.

The most commonly affected region of the brain in DA toxicity is the hippocampal formation with neuronal loss and unspecified gliosis occurring most prominently in the CA3,

CA4, CA1, and dentate gyrus (DG)(Goldstein et al., 2007; Silvagni et al., 2005), areas of the brain involved in learning, memory, and spatial navigation. Pathological examination of the CSL cases in this study revealed similar results with the most consistent pathological changes in all parameters seen in the DG and CA3 regions. Involvement of the CA1 was variable while the CA2 region was more involved than has been previously reported. Discrepancies in the pathology from past publications could be from use of other indicators of pathology than just traditional H&E staining. Specifically, MAP-2 fluorescence has been shown to be a sensitive indicator of neuronal injury with loss of antigenicity seen prior to neuronal loss.(Huh, Raghupathi, Laurer, Helfaer, & Saatman, 2003) Although a significant trend was not seen when comparing MAP-2 loss with the classification of lesion severity, there was a measurable difference based on chronicity (Fig 1J-K) potentially indicating that even without a more substantial lesion, chronic animals neurons are more severely stressed.

To further pursue mechanisms of neuronal injury, we measured levels of 4-HNE as an indirect measure of oxidative stress. Experimental seizure models have shown excessive reactive oxygen species (ROS) production and increased nitric oxide (NO) and peroxynitrite ($ONOO^-$) generation at time points preceding neuronal death in susceptible brain regions that is alleviated through the use of antioxidants such as N-tert-butyl-alpha-phenylnitrone (PBN) and melatonin. (Waldbaum & Patel, 2010) Neurons in all areas of the hippocampus in DA exposed CSLs showed elevated 4-HNE immunoreactivity with more extensive staining seen in chronic versus acute CSLs (Fig 1G-H). The amount of staining did not correlate with the extent of neuronal loss in the animal, which may indicate that oxidative stress may be more relevant in terms of epileptogenesis than explicit neuronal loss. The role of oxidative stress in DA toxicity in

CSLs was more extensively studied in (Madl et al., 2013), but overall indicate a presence of oxidative stress in both acute and chronic DA toxicosis.

Glutamate synthetase is a key enzyme in the glutamate-glutamine cycle and is sensitive to presence of reactive oxygen and nitrogen species resulting in reduced activity and expression within astrocytes leading to elevations in extracellular glutamate.(Bidmon et al., 2008; Castegna et al., 2011; Görg et al., 2007; O. Petroff et al., 2002) Specific impairment of GS using the inhibitor methionine sulfoximine (MSO) leads to spontaneous seizures in rodents(Wang, Zaveri, Lee, & Eid, 2009) and inhibition has shown to be detrimental to glutamate cycling as well as GABA synthesis(Ortinski et al., 2010) thus indicating that GS may play a very important role in epileptogenesis. Loss of GS is a very consistent finding in patients with TLE(EID et al., 2004) and we hypothesized similar results would be found in CSLs. However, Immunofluorescent staining for GS in DA intoxicated sea lions was not altered to a great extent except in the DG of chronic animals (Fig 2) and interestingly there was neuronal expression of GS in several chronic cases especially in the CA2, CA1, and subiculum areas. More importantly, there was significant elevation in the amount of nitration of GS, as assessed by co-immunofluorescence of 3NT and GS, that was predictive based on chronicity of exposure (Fig 2F-J) that most likely indicates reduced GS activity. Because GS activity could not be directly assessed, use of fresh sea lion tissue to perform GS activity assay would be needed to verify the loss of activity that is more often seen in KA models of seizure than actual loss of GS immunoreactivity(Bidmon et al., 2008; Ong et al., 1996). Additionally, by counting the number of GS positive cells without taking into account the loss of total area of expression with individual astrocytes as reported previously(Bidmon et al., 2008; Ortinski et al., 2010), we may be underestimating the true extent of GS changes.

Inflammation and the activation of astrocytes and glia is the most common biological marker upregulated during epileptogenesis in humans with TLE.(Losi et al., 2012; Vezzani et al., 2011)'(Aronica, Ravizza, Zurolo, & Vezzani, 2012) Glia are the primary source of NO and inflammatory factors such as IL-1β and TNF-α which have been shown to inhibit GS and glutamate receptor expression in astrocytes leading to impaired glutamate clearance. (Ananth et al., 2003; Gras, Porcheray, Samah, & Leone, 2006; Losi et al., 2012) Moreover, glia are known targets for DA toxicity undergoing vacuolation and necrosis in models of toxicity(Pulido, 2008) and direct application of DA on cultured astrocytes can dose dependently decrease glutamate uptake and lead to release of inflammatory factors by both astrocytes and microglia(Gill, Hou, Ghane, & Pulido, 2008; Pulido, 2008). In this study, we saw substantial amounts of neuroinflammatory activation of both astrocytes (Fig. 3) and microglia (Fig. 5) as assessed by co-immunofluorescent study that was dependent on the severity of lesion. Interestingly, astrocytic activation observed a greater trend with severity being upregulated in mildly lesioned and chronically lesioned animals (Fig. 4) while microglia were only active in very damage hippocampi but within a greater expanse of the hippocampus and subiculum (Fig. 6). However, microglia activation followed a better, but not significant trend based on chronicity indicating that microgliosis may be more important in epileptogenic changes in CSLs while astrocytosis may be more closely associated with neuronal injury. This could fit with other models of epilepsy where specific inhibition of microglia using pharmacological and genetic ablation shows protection against seizure and overall reduced gliosis(Cho et al., 2008; Foresti et al., 2011) and other neurodegenerative models indicate microglia to be a important regulator of astrocyte activation(Glass et al., 2010).

Astrocytes and microglia activated in DA exposed CSLs upregulated both NOS2 and TNF-α; however, this increased expression was more correlated with severity while the nitration of GS and neurons was more observable based on chronicity of exposure. The discord between these two observations could be a result of a limited number of animals examined and use of tissue from animals whose disease warranted euthanasia. Additionally, although inducible NOS (NOS2) is most often implicated in the source of large levels of NO and specific inhibition using aminoguanadine can protect against seizures(Rehni, Singh, Kalra, & Singh, 2009), these findings are not consistent and other studies show that neuronal NOS (nNOS) may also play important roles in epileptogenesis(Kovacs et al., 2009). A more thorough examination of NOS expression is therefore needed in future studies.

Examination of glia involvement in DA toxicity in CSLs has been limited to only passive descriptions of gliosis. (Goldstein et al., 2007; E. M. D. Gulland et al., 2002; Silvagni et al., 2005) Few studies have begun to examine the exact pathogenic mechanisms of DA induced seizuregenesis and with current treatment failures (40-60% of animals), novel approaches to treat this condition are desperately needed as the number of animals affected increases each year. The results of this study indicate that gliosis and resultant changes in glutamine synthetase are possibly important mechanisms in DA induced seizure and neuronal loss and combinatorial therapy aimed at limiting these changes could be effective in treating animals. Future studies aimed at more causative exploration with a focus on treatment needed. California sea lions act as sentinels of the disease, but are not the only affected species with reports of intoxication occurring in dolphins, gray whales, northern seals, otters, and marine birds such as the brown pelican. (F. Gulland, 2000; la Riva et al., 2009) Thus findings pertinent to sea lion health could

be beneficial in treatment of other species including humans due to the similarities of the chronic disease to human TLE.

CHAPTER 2

TABLES AND FIGURES

TABLE 2.1

STUDY POPULATION CHARACTERISTICS

	Control CSLs	DA Exposed CSLs	
		Acute	Chronic
Number	8	5	7[a]
Date of Capture			
2000	1	-	-
2007	-	-	1
2009	2	4	-
2010	3	1	5
2011	2	-	1
Sex			
Male	2	-	-
Female	6	5	7
Age			
Sub-Adult	7	-	3
Adult	1	5	4
DA Levels			
No. Positive/No. Tested	2/3	5[b]/5	1/5
Fecal Concentration (ng/g)	8.8-28.4	4.3-4388	3.9

[a] 5 of the 7 CSLs classified as chronic DA exposed were previously stranded
[b] 1 acute DA CSL was BDL for fecal DA but was positive in other samples

TABLE 2.2

SUMMARY OF CLINICAL AND HISTOLOGIC FINIDNGS

	Control CSLs	DA Exposed CSLs	
		Acute	Chronic
Clinical Findings			
Seizures	-	5	6
Tremors	-	2	1
Head Bobbing	-	2	-
Blind	-	2	2
Lethargy	1	2	6
Emaciation	-	3	3
Histopathologic Findings	8	2	-
No significant findings	-	2	5
Hippocampal Atrophy	-	2	4
Spongiosis	-	3	6
Neuronal Necrosis	-	3	7
Neuronal Loss	-	1	1
Gliosis			
Severity of Lesion			
Normal	8	2	-
Mild/Moderate	-	1	4
Severe	-	2	3

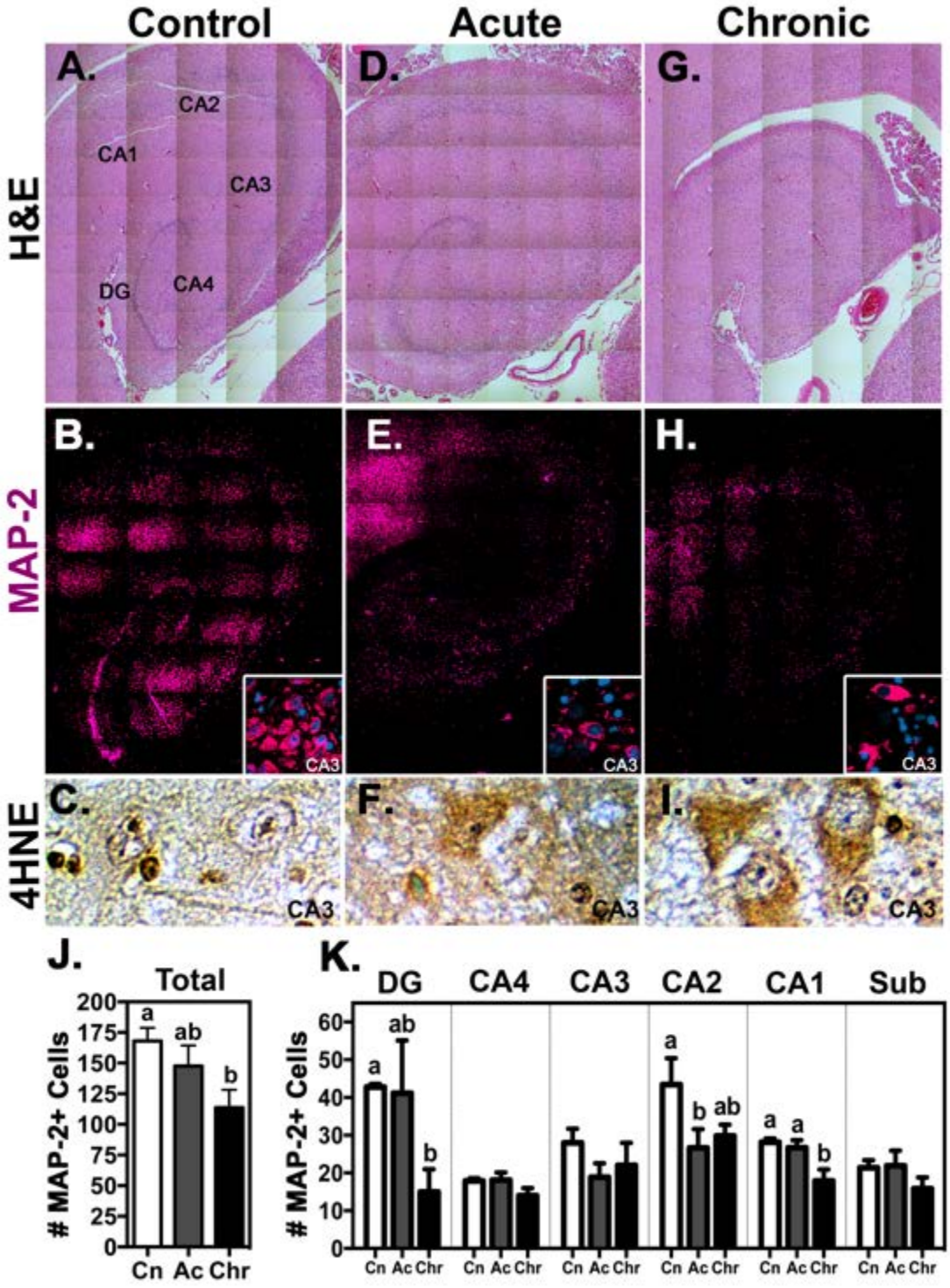
Control
Acute
Chronic
H&E
MAP-2
4HNE
A.
D.
G.
B.
E.
H.
C.
F.
I.
CA1
CA2
CA3
CA4
DG
CA3
J.
Total
MAP-2+ Cells
Cn Ac Chr
K.
DG
CA4
CA3
CA2
CA1
Sub
MAP-2+ Cells
Cn Ac Chr

Figure 2.1. Neuronal Histology. Hippocampi of DA exposed sea lions have graded neuronal loss and increased lipid peroxidation that correlates to chronicity of exposure. (Left column; panels A, B, C) Hippocampus, control adult female ID 28532, normal histology. (A) Architecture of a control hippocampus designating areas of the dentate gyrus = DG, cornu ammonis = CA regions 1, 2, 3, and 4; HE (B) Pattern of MAP2 immunolabeling in a representative montage with a 40x inset of the CA3 region. (C) Neurons in the CA3 region of control animals lack 4-HNE immunolabeling. (Middle column; panels D, E, F) Hippocampus, acute DA adult female ID 28549, mild histology. (D) Acutely exposed CSLs show mild atrophy and loss of cells in CA4, CA3, and CA1; HE. (E) Loss of MAP2 immunolabeling is evident throughout the entire hippocampus with a representative 40x image of the CA3 region (F). Few neurons in are positive for 4HNE as shown in a representative 40x image from the CA3 region. (Right column; panels G, H, I) Hippocampus, chronic DA adult female ID 60602, severe histology. (G) Chronically exposed CSLs show severe atrophy and loss of cells; HE. (H) Loss of MAP2 immunolabeling reveals only few positive neurons within the hippocampus with a representative 40x image of the CA3 region (I). Many neurons in are positive for 4HNE as shown in a representative 40x image from the CA3 region. Quantitative counts of total summation (J) and average number (K) of MAP2+ neurons in control = Cn, acute DA = Ac, and chronic DA = Chr animals. Different letters denote significant difference between groups ($p < 0.1$).

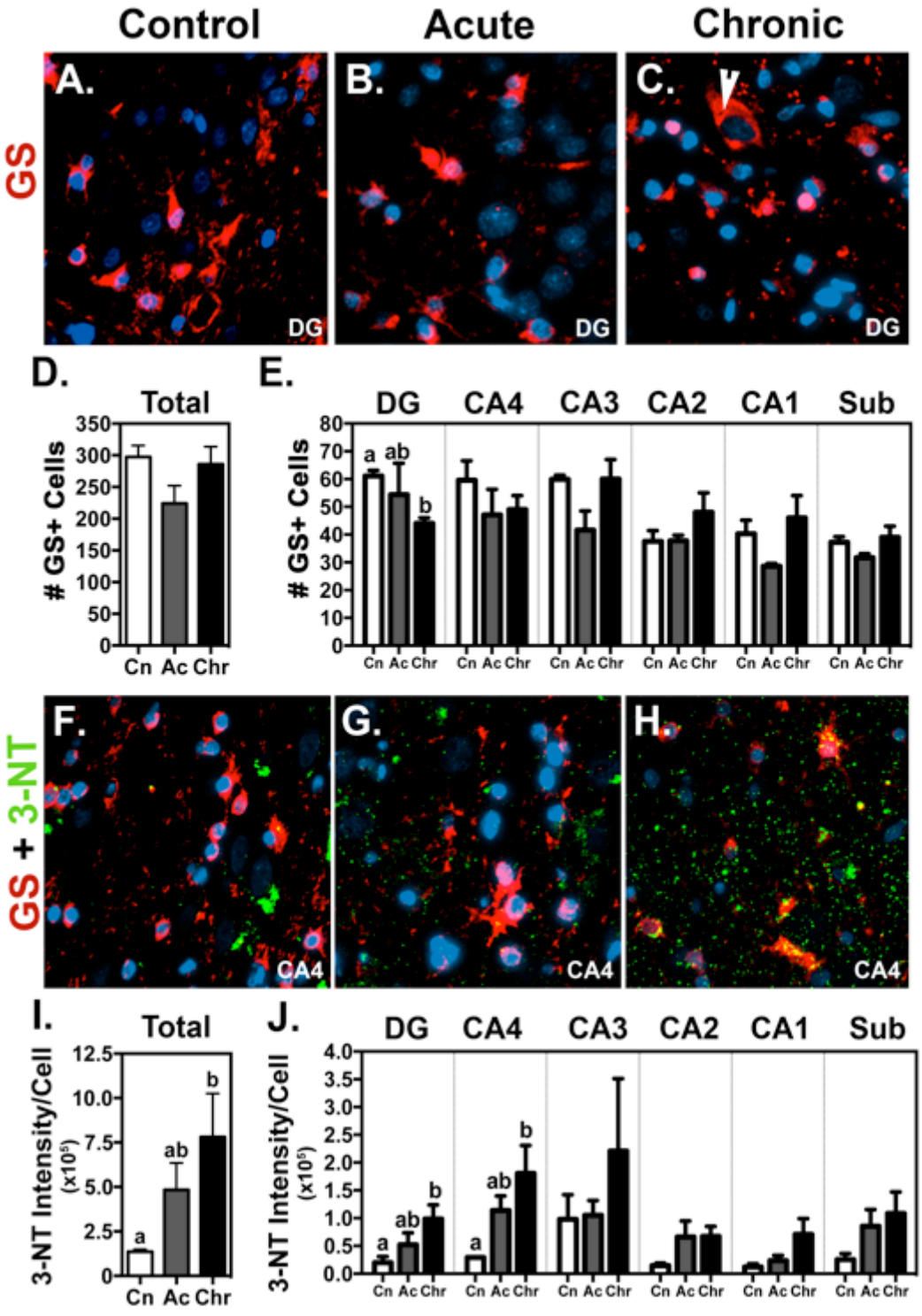
Control
Acute
Chronic
GS
A.
B.
C.
DG
D.
Total
GS+ Cells
Cn Ac Chr
E.
DG CA4 CA3 CA2 CA1 Sub
GS + 3-NT
F.
G.
H.
CA4
I.
Total
3-NT Intensity/Cell (x10⁵)
J.
DG CA4 CA3 CA2 CA1 Sub

Figure 2.2. Alterations in Glutamine Synthetase. DA exposed sea lions have progressive alterations in glutamine synthetase that is predicted by chronicity of exposure. (A) Dentate Gyrus, control adult female ID 28532, normal histology. Normal GS immunolabeling stains cell bodies and astrocytic processes. (B) Dentate Gyrus, acute DA adult female ID 44345, normal histology. Acutely exposed animals have slight loss of GS immunolabeling. (C) Dentate Gyrus, chronic DA adult female ID 60602, severe histology. Number of GS+ cells is decreased with expression primarily only seen in cell bodies and sometimes within neurons (arrow). Quantitative counts of total summation (D) and average number (E) of GS+ cells within the dentate gyrus = DG and cornu ammonis = CA regions 1-4 in control = Cn, acute DA = Ac, and chronic DA = Chr animals. Different letters denote significant difference between groups ($p < 0.1$). (F) CA4 control adult female ID 28532, normal histology. GS+ cells, red, lack 3-NT immunolabeling, green. (G) CA4, acute DA adult female ID 44345, normal histology. Acutely exposed animals have some 3-NT, green, and GS, red, colocalization. (H) Dentate Gyrus, chronic DA adult female ID 60602, severe histology. GS+ cells, red, have large increases in 3-NT, green. Quantitative analysis of 3-NT intensity over the total hippocampus (I) and individual regions (J) in control, acute DA, and chronic DA sea lions. Different letters denote significant difference between groups ($p < 0.1$).

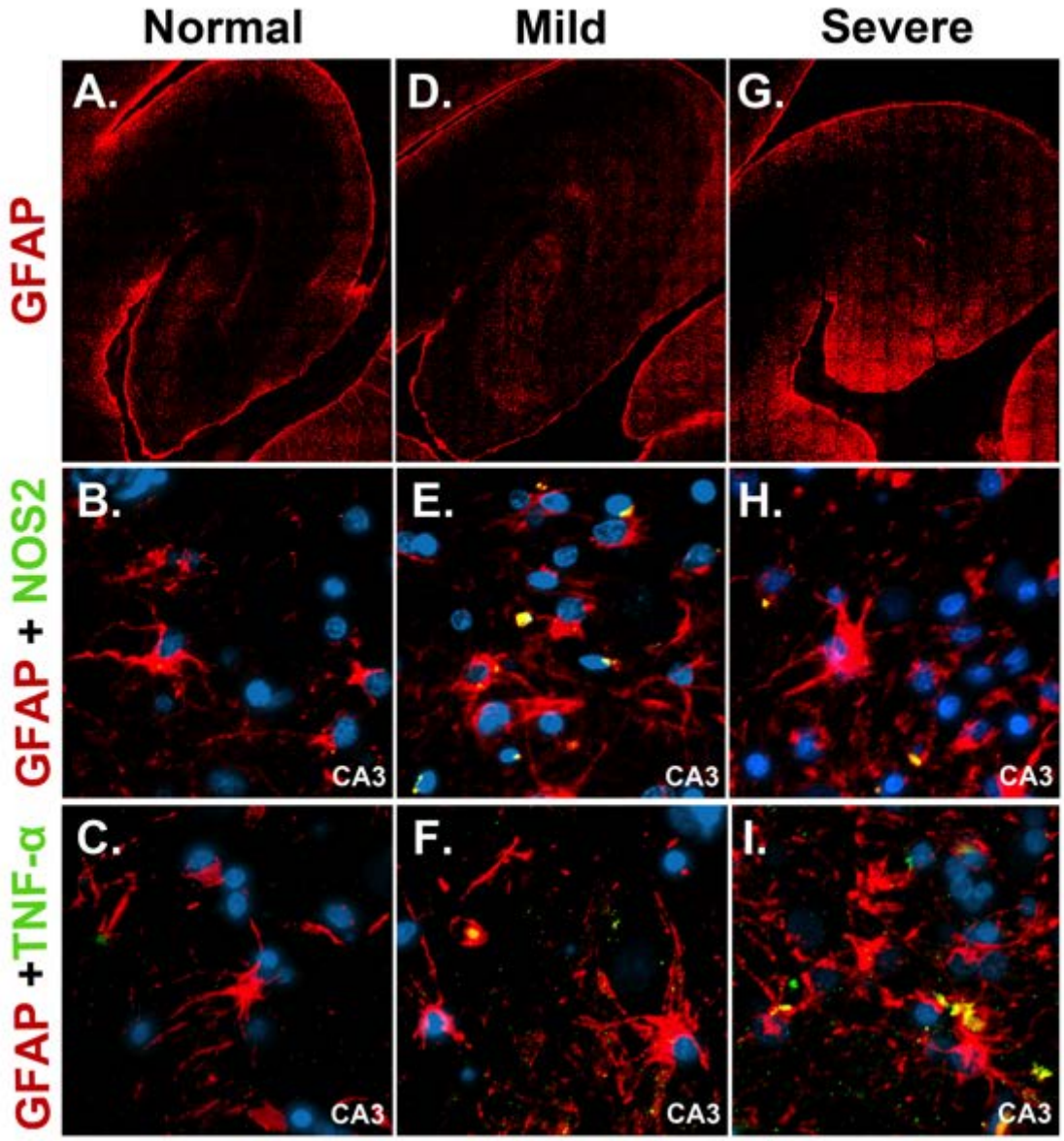

Figure 2.3. Activation of Astrocytes. (Left column; panels A, B, C) Hippocampus, control adult female ID 28532, normal histology. (A) Pattern of GFAP immunolabeling in a CSL hippocampus without any pathology. (B) Representative 40x image of the CA3 shows GFAP+ astrocytes in red with normal morphology and no visible NOS2 expression, green. (C). Representative 40x image of the CA3 shows no TNF, green, expression in GFAP+ astrocytes, red. (Middle column; panels D, E, F) Hippocampus, chronic DA adult female ID 79075, mild

histology. (D) The number of GFAP+ astrocytes is slightly elevated in CSL hippocampi with mild lesions. (E) Representative 40x image of the CA3 reveals hypertrophied astrocytes expressing GFAP, red, with increased expression of NOS2, green (F) Representative 40x image of the CA3 shows few GFAP+ astrocytes, red, expressing TNF, green. (Right column; panels G, H, I) Hippocampus, acute DA adult female ID 28534, severe histology. (G) The number of GFAP+ astrocytes is significantly elevated in CSL hippocampi with severe lesions. (E) Representative 40x image of the CA3 reveals hypertrophied GFAP+ astrocytes, red, with increased expression of NOS2, green (F) Representative 40x image of the CA3 shows many GFAP+ astrocytes, red, expressing TNF, green.

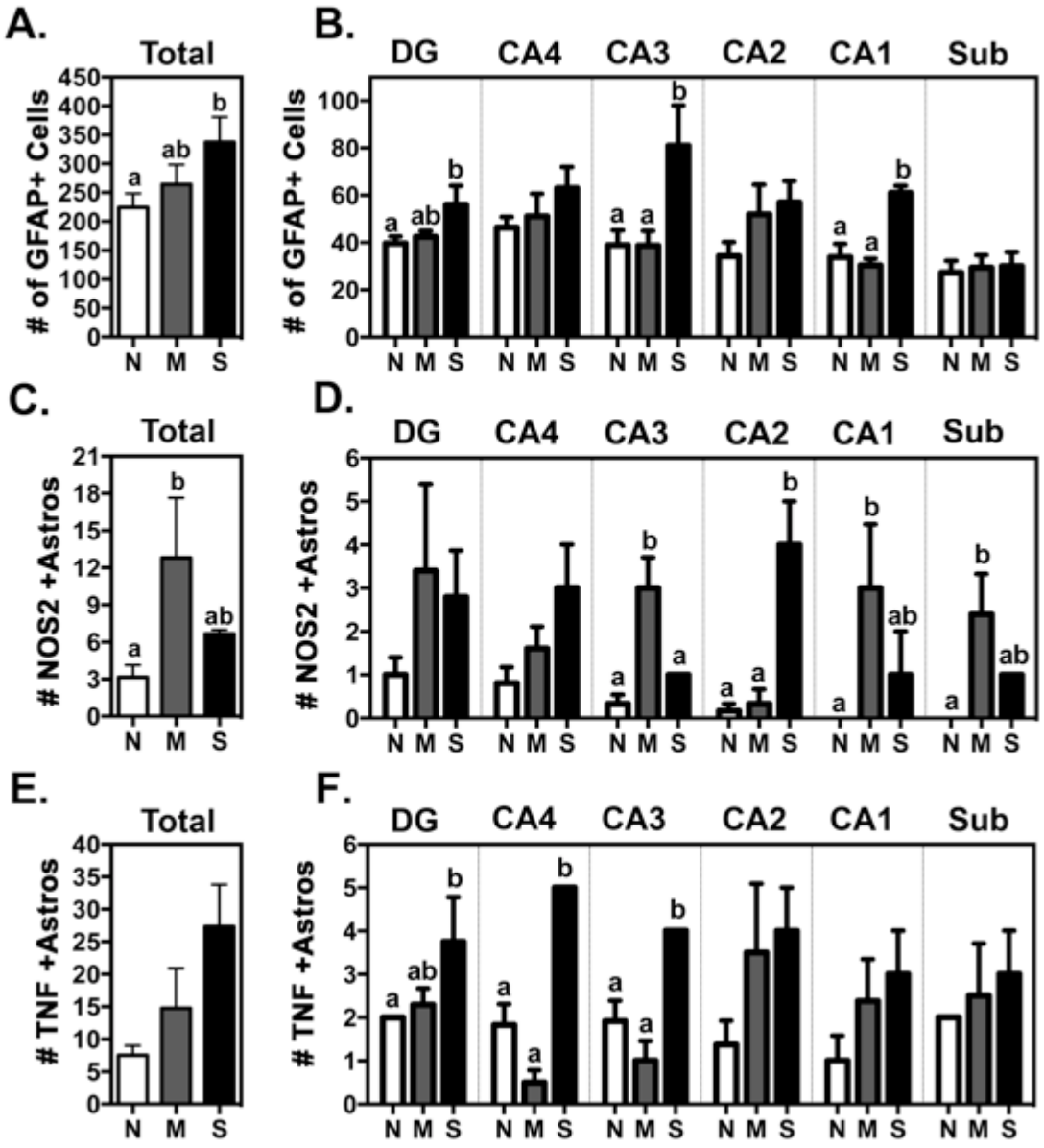

Figure 2.4. Quantification of Astrocytosis. Quantitative counts reveal that the degree of activated astrocytes expressing TNFα and NOS2 correlates with the severity of DA induced neuronal loss. Sum of the total number of GFAP+ cells (A), NOS2+ astrocytes (C) and TNF+ astrocytes (E) present in the hippocampi of animals classified as normal = N, mildly lesioned = M, and severely lesioned = S. The average number of GFAP+ cells (B), NOS2+ astrocytes (D),

and TNF+ astrocytes (F) found in the dentate gyrus (DG) and regions 4, 3, 2, and 1 of the cornu ammonis (CA) of normal, mildly lesioned, and severely lesioned animals. Different letters denote significant difference between groups ($p < 0.1$).

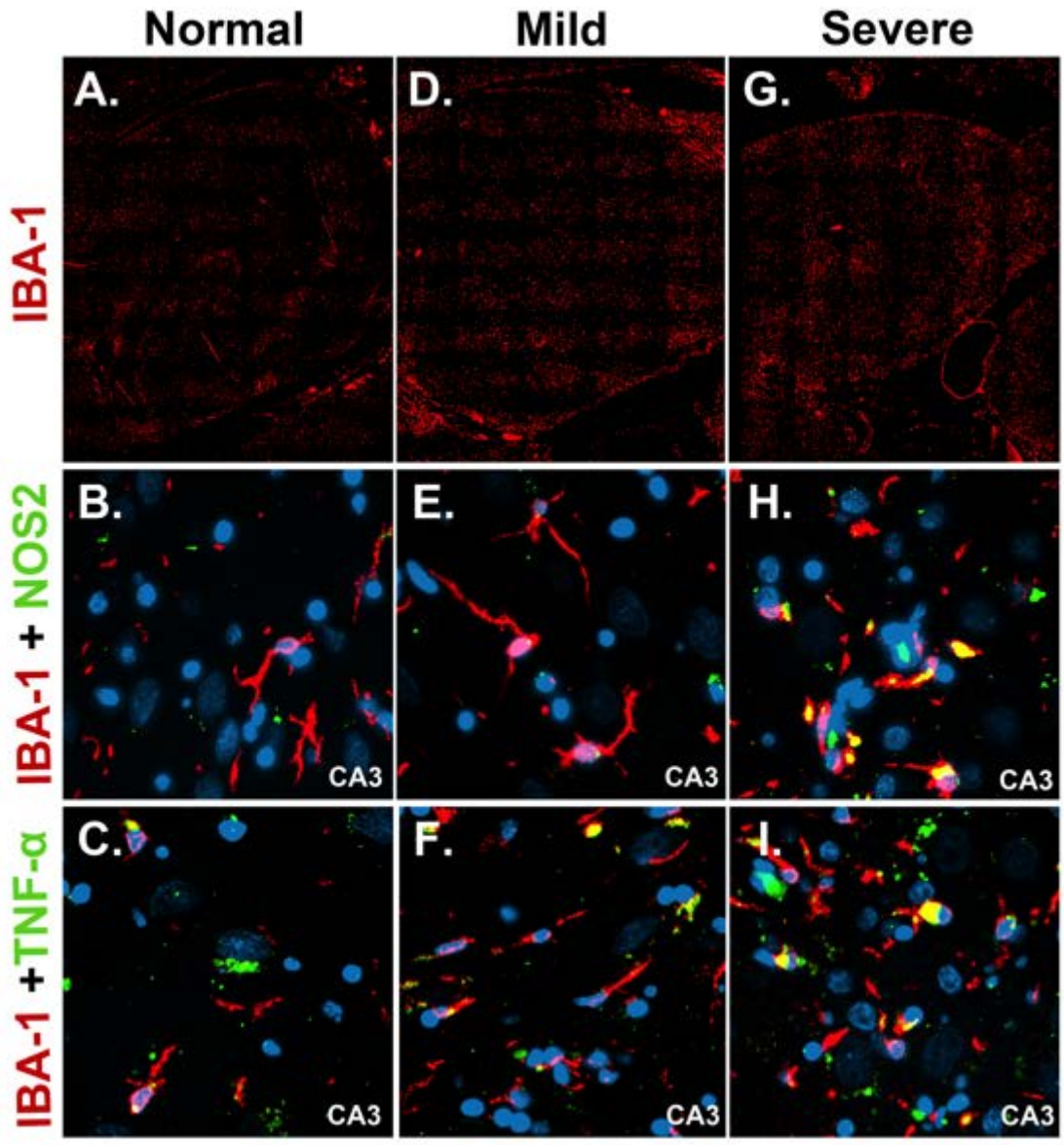

Figure 2.5. Activation of Microgliosis. (Left column; panels A, B, C) Hippocampus, control adult male ID 37540, normal histology. (A) Pattern of IBA1 immunolabeling in a CSL hippocampus without any pathology. (B) Representative 40x image of the CA3 shows IBA1+ microglia in red with normal morphology and no visible NOS2 expression, green. (C). Representative 40x image of the CA3 shows no TNF, green, expression in IBA1+ microglia, red.

(Middle column; panels D, E, F) Hippocampus, acute DA adult female ID 48125, mild histology. (D) The number of IBA1+ microglia is slightly elevated in CSL hippocampi with mild lesions. (E) Representative 40x image of the CA3 reveals hypertrophied microglia expressing IBA1, red, with increased expression of NOS2, green (F) Representative 40x image of the CA3 shows few IBA1+ microglia, red, expressing TNF, green. (Right column; panels G, H, I) Hippocampus, acute DA adult female ID 60602, severe histology. (G) The number of IBA1+ microglia is significantly elevated in CSL hippocampi with severe lesions. (E) Representative 40x image of the CA3 reveals hypertrophied IBA1+ microglia, red, with increased expression of NOS2, green (F) Representative 40x image of the CA3 shows many IBA1+ microglia, red, expressing TNF, green.

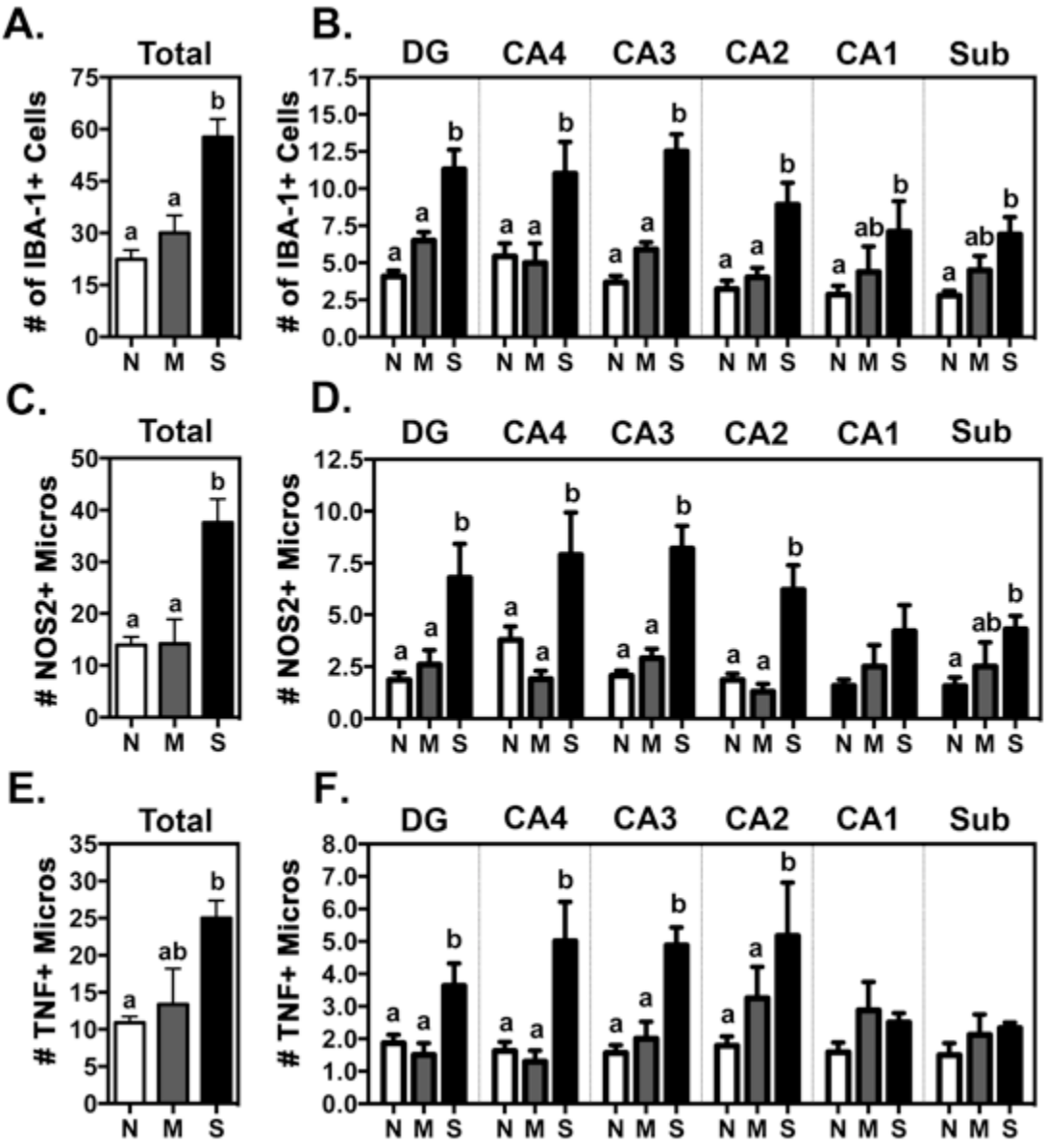

Figure 2.6. Quantification of Microgliosis. Quantitative counts reveal that the degree of activated microglia expressing TNFα and NOS2 correlates with the severity of DA induced neuronal loss. Sum of the total number of IBA1+ cells (A), NOS2+ microglia (C) and TNF+ microglia (E) present in the hippocampi of animals classified as normal = N, mildly lesioned =

M, and severely lesioned = S. The average number of IBA1+ cells (B), NOS2+ microglia (D), and TNF+ microglia (F) found in the dentate gyrus (DG) and regions 4, 3, 2, and 1 of the cornu ammonis (CA) of normal, mildly lesioned, and severely lesioned animals. Different letters denote significant difference between groups ($p < 0.1$).

CHAPTER 3

GENETIC SUPRRESION OF ASTROCYTE IKKβ/NF-κB IN A MOUSE MODEL OF PARKINSON'S DISEASE

Summary

Neuroinflammatory activation of glia is considered a pathological hallmark of Parkinson's disease (PD) and is implicated as in important mechanism in the progression of many diseases of the central nervous system. Human and experimental PD studies have often revealed activation of both microglia and astrocytes; however, the relative contributions of these cell types to disease is unknown and often debated. Previous studies in our lab have shown NFκB to be upregulated in astrocytes prior to overt pathology in a chemical model of PD and as a major regulator of glial inflammation. We sought to ascertain the importance of this pathway in PD through generation of an astrocyte specific conditional knockout (*hGFAP-Cre/Ikkβ*$^{F/F}$) in which *Ikkβ* is specifically deleted in astrocytes. Measurements of *Ikkβ* expression at genomic and protein levels revealed a 70% deletion rate of *Ikkβ* specific to astrocytes, as compared to littermate controls (*Ikkβ*$^{F/F}$). Use of this mouse in a subacute, progressive model of PD through exposure to 1-methyl-4-phenyl-1,2,36,-tetrahydropyridine and probenecid revealed significant protection of these mice to both direct and progressive loss of dopaminergic neurons. *hGFAP-Cre/Ikkβ*$^{F/F}$ mice were also protected against MPTP induced loss in motor activity, but did not alter reductions in striatal catacholamines. Current data suggests we were successful in specifically deleting *Ikkβ* within astrocytes and that neuroprotection upon deletion of this pathway in astrocytes indicates that this pathway is a significant contributor to both the initiation and potentiation of nigral pathology.

Introduction

The activation of glia is implicated in the progression of neuronal injury and loss in several neurodegenerative diseases including Parkinson's disease (PD) through the upregulation and release of pro-inflammatory and pro-oxidant factors that exert neurotoxic effects on surrounding neurons (Glass et al., 2010; Hirsch & Hunot, 2009). In PD, neuroinflammation is considered a pathological hallmark of the disease as examination of tissues from human patients and rodents in experimental models consistently show presence of astrogliosis and microgliosis in lesioned areas(Damier, Hirsch, Zhang, Agid, & Javoy-Agid, 1993; Nagatsu & Sawada, 2005; Ouchi, Yagi, Yokokura, & Sakamoto, 2009). Furthermore, several lines of evidence point to these reactive glia being important participants in disease pathology as upregulation of glia expressing factors such as tumor necrosis factor alpha (TNFα) and inducible nitric oxide synthase 2 (NOS2) are documented prior to overt pathology(Hirsch & Hunot, 2009; J. A. Miller et al., 2011; Saijo et al., 2009; Sugama et al., 2003) and when down-regulated with specific genetic and pharmacologic models, help protect against neurodegeneration (Dehmer, Heneka, Sastre, Dichgans, & Schulz, 2003; Dehmer, Lindenau, Haid, Dichgans, & Schulz, 2000; McCarty, 2006; Mondal et al., 2012). Both microglial activation and astrocyte activation have been cited as the primary culprits in the disease (P. C. Chen et al., 2009; McCarty, 2006); however, glial responses can often also be neuroprotective(Frank-Cannon et al., 2009) and the current modeling systems are often too generalized to determine the exact contributions of these glial subtypes to disease.

The most widely utilized model of PD is the 1-methyl-4-phenyl-1,2,3,6-tetrahydropyridine (MPTP) neurotoxicant model of PD. Since its accidental discovery in the 1980's, it has become the most invaluable model of PD as primates, and to some extent rodents, exhibit classical neuropathological and neurobehavioral deficits when exposed to this neurotoxicant; a better

recapitulation than any other currently available toxicant or genetic model of this disease. The specificity of this model relies in the specificity of MPTP to the dopaminergic system of the basal ganglia(Bové & Perier, 2012). This specificity is achieved because MPTP is lipophilic and can easily cross the blood-brain barrier, being taken up into astrocytes and converted to its active toxic metabolite 1-methyl-4-phenylpyridinium (MPP+). This active metabolite when released by astrocytes, is taken only into dopamine producing neurons through interaction with the dopamine transporter and induces neuronal death through inhibition of complex I of mitochondrial respiration resulting in ATP depletion and oxidative stress. Due to the extensive knowledge of this toxicant model, utilization in combination with genetic manipulation is the next progressive step in examining glial responses in this disease(Tieu, 2011).

The classical nuclear factor kappa B (NFκB) pathway involving activation of inhibitory kappa alpha kinase beta (IKKβ) and translocation of p65/p50 dimers is the primary pathway involved in the activation of inflammatory pathways (Bonizzi & Karin, 2004; Karin, 1999; 2005) and has been shown to be a critical pathway for glial production of inflammatory mediators (Glass et al., 2010). NFκB is thought to play an important role in PD as upregulation of NFκB is noted in both neurons(Hunot et al., 1997) and glia in brains of patients with PD (Ghosh et al., 2007) and in experimental models (Saijo et al., 2009). Recent reports have shown that targeting global NFκB to be protective in chemical models of PD(Dehmer et al., 2003; Ghosh et al., 2007; Mondal et al., 2012; Saijo et al., 2009); yet, these studies do not ascertain the specific cellular mechanisms of this protection as both glial and neuronal expression of NFκB can be neurotoxic (Grilli & Memo, 1999; Herrmann et al., 2005).

Studies in our laboratory utilizing a transgenic mouse expressing green fluorescent protein under the control of NFκB reported activation of the NFκB pathway in astrocytes prior to overt

loss of nigral neurons (J. A. Miller et al., 2011). Recent rodent models in multiple sclerosis and spinal cord injury have shown that specific deletion of the NFκB pathway to be neuroprotective (Brambilla, 2005; Brambilla et al., 2009; van Loo et al., 2006). The implications of astrocyte NFκB signaling in PD is unknown; however, due to protection seen in other models, we hypothesized that elimination of astrocyte neuroinflammatory activation through NFκB would also show neuroprotection in a PD model. As the phosphorylation of the IκB inhibitor complex by IKKβ is an important regulation step in the classical inflammatory pathway of NFκB(Karin, 1999), we sought to test this hypothesis by utilizing Cre-loxp technology to delete IKKβ in only astrocytes of the brain.

Materials and Methods

Animals and Genotyping

Astrocyte specific *Ikkβ*-deficient mice (*hGFAP-Cre/Ikkβ*$^{F/F}$) were generated by breeding *Ikkβ*-floxed mice ((Li et al., 2003); C57Bl/6 background; provided by Dr. Michael Karin at University of California San Diego) with *hGFAP*-Cre transgenic mice ((Zhuo et al., 2001); FVB-Tg(GFAP-CRE)25Mes/J; FVB background; Jackson Laboratories, Bar Harbor, ME) expressing Cre under the control of the human GFAP promoter (Fig 1). Littermates lacking *hGFAP-Cre* (known as *Ikkβ*$^{F/F}$) were utilized as controls and mice from fourth generation breeding were used in both expression and treatment studies. PCR genotyping on ear tags was performed using the primers

5'-GTC ATT TCC ACA GCC CTG TGA-3' and 5'-CCT TGT CCT ATA GAA GCA CAA C-3', which amplify both the *Ikkβ*$^{+}$ (220-bp) and *Ikkβ*^{F} (310-bp) alleles and primers 5'-ACT CCT TCA TAA AGC CCT CG-3' and 5'-ATC ACT CGT TGC ATC GAC CG-3', which amplifies the *hGFAP-Cre* allele (190-bp). Animals were housed in microisolater cages (2-3 animals per cage), kept on a 12-h light/dark cycle, and had access to both chow and water *ad libitum*. All procedures were performed in accordance with National Institutes of Health guidelines for the care and use of laboratory animals and with approval by the Institutional Animal Care and Use Committee (IACUC) of Colorado State University.

Primary Glial and Neuronal Cultures

Mixed glial cultures from whole brain (excluding cerebellum and brain stem) of postnatal day 1 (neonatal) and 3-month old (adult) *hGFAP-Cre/Ikkβ*$^{F/F}$ (n = 3) and *Ikkβ*$^{F/F}$ (n = 4) mice were isolated using a modification of a previously described method (M. ASCHNER &

Kimelberg, 1991; Carbone et al., 2008; Moreno et al., 2008). Briefly, mice were euthanized by decapitation under isofluorane anesthesia and whole brains were rapidly dissected out and placed into ice-cold minimum essential medium with L-glutamine (MEM; Gibco). Meninges were removed and tissues completely digested with Dispase (1.5U/ml) with each animal extracted separately. Dissociated cells from individual animals were plated onto 100-mm tissue culture plates and kept in MEM supplemented with 10% heat-inactivated FBS (Sigma) and penicillin (0.002 mg/ml), streptomycin (0.002 mg/ml), and neomycin (0.001 mg/ml) antibiotic mixture (PSN). Media was changed every 4-5 days and cells were maintained at 37°C and 5% CO2 in humidified chambers until confluency was reached (~14-18 days). Microglia were purified from astrocytes via column-free magnetic separation using the EasySep mouse CD11b positive selection kit (Stemcell technologies, Vancouver, Canada) according to manufacturer instructions and as outlined in (R. R. Gordon et al., 2011) Positively selected microglia and negatively selected astrocytes were determined to be 97% and 99% pure (data not shown).

Primary striatal neurons were extracted in a similar fashion as the mixed glial cultures except performed in neurobasal medium. Primary neuronal cultures were seeded onto poly(L-lysine)-coated 22mm glass coverslips at 4 x 105 cells/well and maintained in neurobasal media supplemented with 2mM L-glutamine, a B27 supplement, and PSN antibiotic mixture. Neuronal culture media was changed every 2 days with purity ascertained via cell morphology and immunolabeling with the neuron specific marker MAP2 (Fig. 3).

Evaluation of Genomic Deletion of Ikkβ$^{F/F}$ via real time PCR

Genomic DNA was isolated from purified neonatal and adult astrocyte cultures utilizing a DNeasy kit (QIAGEN, Valencia, CA) with purity and concentration confirmed using a Nanodrop

ND-1000 spectrophotometer (NanoDrop Technologies, Wilmington, DE). 100 ng of DNA was mixed with Sybrgreen and primers (10μM) 5'-AAG ATG GGC AAA CTG TGA TGT G-3' and 5'-CAT ACA GGC ATC CTG CAG AAC A-3' to amplify the *Ikkβ*^{F} allele or 5'-ATG GCC TTG CAT GAG GAT ACA CCA-3' and 5'-GAG TCT CAG TCT TCA ACT CCC TGT-3' or the *Nos2* promoter as a control. Percent expression of *Ikkβ*^{F} in astrocytes from *hGFAP-Cre/Ikkβ*$^{F/F}$ mice was determined based on comparison of *Ikkβ*^{F} signal in astrocytes from *Ikkβ*$^{F/F}$ littermate controls, defined at 100%, after normalization to *Nos2* promoter signal. For these experiments, three or four mice per genotype were used for analysis.

Western Blotting for IKKβ

Protein from purified neonatal astrocyte cultures from *hGFAP-Cre/Ikkβ*$^{F/F}$ and *Ikkβ*$^{F/F}$ mice were lysed using a RIPA lysis buffer supplemented with complete protease inhibitor (Roche, Indianapolis, IN). Protein was quantified using a BCA Assay (Pierce, Rockford, IL) and 50μg of protein was separated using a 10% SDS polyacrylamide gel electrophoresis followed by a wet transfer to a polyvinylidene fluoride membrane (Pall Corporation, Pensacola, FL). Membranes were blocked in 5% nonfat dry milk in Tris-Buffered saline containing 0.2% Tween 20 then incubated with primary rabbit anti-IKKβ (1:500; Cell Signaling, Danvers, MA) overnight followed by incubation in horseradish peroxidase-conjugated secondary antibody (1:5000, Santa Cruz, Dallas, TX) for one hour. Chemiluminescent detection was performed and analyzed using the ChemiDoc XRX imaging system and Quantity One software (Bio-Rad, Hercules, CA). Membranes were reprobed with β-actin as a control with all analysis normalized to β-actin signal.

Immunofluorescence detection of IKKβ

Purified astrocytes, microglia, and neurons from *hGFAP-Cre/Ikkβ*$^{F/F}$ and *Ikkβ*$^{F/F}$ mice were plated at 1 x 10^4 cells on 22mm poly-D-lysine coated glass coverslips and allowed to adhere for 48 hours. Cells were fixed using methanol, washed in PBS, and then blocked in 1% Bovine Serum Albumin (w/v) in PBS for one hour. Cells were incubated overnight at 4°C in primary antibodies for IKKβ (1:50; Imgenex, San Diego, CA) and for cell specific markers GFAP (1:500; Sigma, St. Louis, MO), ionized binding adaptor protein-1 (IBA1; 1:250; Wako, Osaka, Japan), or microtubule associated protein-2 (MAP2; 1:100; Abcam, Cambridge, MA). After rinsing in PBS, cells were incubated in for one hour at room temperature in AlexaFluor-488 (IKKβ) and AlexaFluor-647 (cell markers) conjugated secondary antibodies (1:500; Invitrogen, Carlsbad, CA) and then mounted in medium containing 4′,6-diamidino-2-phenylindole dihydrochloride (DAPI) to detect cell nuclei. Images were acquired using a 40x air plan apochromatic objectives on a Zeiss Axiovert 200M inverted fluorescence microscope (Carl Zeiss, Inc., Thornwood, NY) equipped with a Hammatsu ORCA-ER-cooled charge-coupled device camera (Hammamatsu Photonics, Hamamatsu City, Japan). Mean fluorescence intensity of IKKβ, reported with subtraction of mean background fluorescence, was determined by utilizing Slidebook software (Intelligent Imaging Innovations Inc., Denver, CO) with 15 individual fields examined per animal with at least 3 animals utilized per genotype.

In vivo assessment of IKKβ was performed on free-floating 40μm brain sections obtained from the substantia nigra of *hGFAP-Cre/Ikkβ*$^{F/F}$ and *Ikkβ*$^{F/F}$ mice (procedure detailed below) using primary antibodies for IKKβ (1:50; Imgenex) and MAP2 (1:100; Abcam) and Alexafluor-488 and Alexa-fluor-647 conjugated secondary antibodies (1:500; Invitrogen). Sections were mounted in medium containing DAPI and representative images were captured using a 40x air

plan apochromatic objective on a Zeiss Axiovert 200M inverted fluorescence microscope (Carl Zeiss, Inc., Thornwood, NY).

MPTP Treatment Regiment

hGFAP-Cre/Ikkβ$^{F/F}$ and *Ikkβ*$^{F/F}$ male and female littermates aged to 20 weeks were divided to best pair siblings and sex between treatment groups and then exposed to a subacute PD lesioning model utilizing 1-methyl-4-phenyl-1,2,3,6-tetrahydropyridine/probenecid (MPTPp) as described previously (De Miranda et al., 2013; J. A. Miller et al., 2011). In brief, mice were injected every other day with probenecid (250 mg/kg i.p. prepared in 5% sodium bicarbonate; Sigma) and with saline or MPTP (20 mg/kg s.c. prepared in saline as free base, Sigma) for 7 days receiving a total of 4 injections. Mice were euthanized under deep isofluorane anesthesia at either 7 days (MPTPp7d) or 14 days (MPTPp14d) after their initial injection.

Locomotor Assessment

Open field activity parameters were assessed using the Versamax behavior chambers with an infrared beam grid detection array (Accuscan Instruments, Inc., Columbus , OH). Mice were monitored for 10 minutes under low ambient light in the presence of white noise. Animals were pre-conditioned one day prior to their first treatment and then assessed at day 0 (first day of treatment) to establish baseline, day 7, and day 14. Several behavioral parameters were collected and analyzed using Versadat Software (Accuscan Instruments, Inc.) including total distance traveled, number of movements, time spent moving, time spent in the margin, and the # of rearing movements. These parameters have been previously shown to assess basal ganglia function ((X. X. Liu et al., 2006; J. A. Miller et al., 2011; Moreno, Yeomans, Streifel, Brattin,

Taylor, & Tjalkens, 2009b; Streifel et al., 2012)) and were normalized to % expression of baseline.

HPLC Analysis of Striatal Dopamine and Metabolites

Mice terminated at day 7 and day 14 were placed under deep isofluorane anesthesia and quickly decapitated followed by rapid removal of the striatum using a brain matrix block for reference. The tissue was flash frozen in liquid nitrogen and stored at -80°C until analysis. Samples were coded for unbiased analysis and sent to the Neurochemistry Core Laboratory at Vanderbilt University's Center for Molecular Neuroscience Research (Nashville, TN). High Performance Liquid Chromatography with electrochemical detection was used to determine the concentrations of dopamine and dopamine-related metabolites 3,4-dihydroxyphenylacetic acid (DOPAC), and homovanillic acid (HVA) in the striatum of control and MPTPp treated mice as detailed in (Perez & Palmiter, 2005).

Tissue Processing and Sectioning

At day 7 and 14, mice were euthanized and tissues obtained as reported previously (J. A. Miller et al., 2011). Briefly, animals were terminated under isofluorane anesthesia and transcardially perfused with 20 mM cacodylate-phosphate buffered saline (cPBS) containing 10U/ml heparin, followed by 4% paraformaldehyde in cPBS. Brains were carefully removed from the skull and placed within 4% formaldehyde in cPBS overnight then cryoprotected in 15% sucrose (w/v cPBS) then 30% sucrose (w/v cPBS). Brains were stored in 30% sucrose at 4°C until sectioning. Coronal 40μm sections through the entire length of the striatum and substantia nigra were collected using a freezing sliding microtome (Microm HM450; Thermoscientific,

Waltham, MA). Sections were stored free floating at -20°C in cryoprotectant (30% w/v sucrose, 30% v/v ethylene glycol; 0.05M phosphate buffer) until staining.

Stereological Counts of Tyrosine Hydroxylase (TH) Positive Neurons

Stereological assessment of TH-positive dopaminergic neurons within the substantia nigra pars compacta (SNpc) was performed as detailed in (De Miranda et al., 2013; J. A. Miller et al., 2011). In brief, free floating serial sections were obtained by systematic sampling of every third tissue from sections encompassing the entire length of the SNpc and immunolabeled using primary rabbit anti-TH antibody (1:500 overnight, Chemicon, Temecula, CA) and AlexaFluor-555 conjugated secondary antibody (1:500 for 3 hours; Invitrogen). Slides were mounted in DAPI containing medium, coverslipped, and stored at 4°C until imaging.

Slides were imaged using a 40x air apochromatic objective on a Zeiss Axiovert 200M inverted fluorescence microscope (Carl Zeiss) with stereological counts of TH-positive cells performed using Slidebook software (Intelligent Imaging Innovations). The boundary of the SNpc was determined using 10x magnification montaging and numbers of TH-positive cells determined via assessment of uniform (40x) randomly placed counting frames (100µm x 100µm) using an optical dissector of 30µm with 5µm upper and lower guard zones. Representative montage images were generated for each treatment group with use of a 20x objective and displayed using inverted monochrome.

Statistical Analyses

All statistical analysis was performed using Prism software (version 6.0; Graphpad Software, Inc., San Diego, CA) with a Student's *t* test utilized for comparison of two means,

whereas a two-way analysis of variance (ANOVA) followed by a Tukey-Kramer multiple comparison *post-hoc* test was used for comparison of three or more means. Independent variables for two-way ANOVA were defined as genotype (*hGFAP-Cre/Ikkβ*$^{F/F}$ versus *Ikkβ*$^{F/F}$) and treatment (saline versus MPTPp). Statistical significance was defined at a p value less than 0.05 and indicated by *, #, or by assignment of a unique letter.

Results

Conditional deletion of Ikkβ in Astrocytes

To study the role of neuroinflammatory activation of astrocytes in the onset and progression of PD, we generated a mouse with a conditional deletion of IKKβ, an essential kinase involved in the initiation of inflammation through the NFkβ pathway(Bonizzi & Karin, 2004). This was accomplished through breeding *Ikkβ*-floxed mice(Li et al., 2003) with *hGFAP-Cre* transgenic mice expressing Cre under the control of the human GFAP promoter(Zhuo et al., 2001). As shown in Fig. 1, three generations of pairing were required to generate mice that had both the *hGFAP-Cre* allele and were homozygous for floxed-*Ikkβ* (*hGFAP-Cre/Ikkβ*$^{F/F}$) and thus for all experiments littermates homozygous for floxed-*Ikkβ*, but lacking *hGFAP-Cre*, known as *Ikkβ*$^{F/F}$, were utilized as controls. Confirmation of genotype for presence of *hGFAP-Cre* (Fig. 2A) and *Ikkβ*^{F} (Fig. 2B) was achieved through PCR on ear tags in adults and tail biopsies from neonatal mice.

To test the efficiency of Cre induced recombination in the brain, we cultured primary astrocytes from *hGFAP-Cre/Ikkβ*$^{F/F}$ and *Ikkβ*$^{F/F}$ mice and measured the deletion of *Ikkβ* at the genomic level utilizing real time-PCR. Cultured astrocytes from *hGFAP-Cre/Ikkβ*$^{F/F}$ neonates showed 71% deletion rate of *Ikkβ* (Fig. 2C) at the genomic level that corresponded to roughly a 70% loss of IKKβ protein measured by western blotting (Fig. 2D-E) and immunofluorescently (Fig. 3A-B). To ensure that the rate of deletion was similar in adult animals, we harvested astrocytes directly from 20-week old adult mice and analyzed genomic levels of *Ikkβ*. Albeit slightly lower than neonates, astrocytes from adult mice showed a similar level of *Ikkβ* deficiency with a calculated deletion rate around a 65% (Fig. 2C).

The use of *hGFAP-Cre* mice to target specific deletion in astrocytes has shown conflicting

results with studies reporting non-targeted recombination events in neurons(Casper & McCarthy, 2006; Malatesta et al., 2003; Zhuo et al., 2001). To ensure specificity of our conditional knockout, we probed for expression of IKKβ via immunofluorescence in microglia (Fig 3C-D) and neurons (Fig. 3E cultured from *hGFAP-Cre/Ikkβ*$^{F/F}$ and *Ikkβ*$^{F/F}$ neonates. Both neurons and microglia from *hGFAP-Cre/Ikkβ*$^{F/F}$ mice showed no detectable loss of IKKβ immunolabeling in comparison to cells obtained from *Ikkβ*$^{F/F}$ littermates. This is in sharp contrast to the large decrease in IKKβ fluorescence seen in astrocytes from the same animals (Fig. 3A). Furthermore, IKKβ appeared intact in neurons of the SNpc in adult *hGFAP-Cre/Ikkβ*$^{F/F}$ mice (Fig. 3F) with frequency and intensity of levels of IKKβ mirroring *Ikkβ*$^{F/F}$ littermates (Fig. 3G). These data indicate a significant and specific reduction of IKKβ in *hGFAP-Cre/Ikkβ*$^{F/F}$ to astroglial cells within the brain of both neonatal and adult mice.

Differences in MPTPp induced locomotor changes

Based on confirmed specificity of the conditional deletion of IKKβ to astrocytes, mice were subjugated to a subacute MPTPp dosing regiment to determine the importance of astrocytic NFκB expression to loss of nigral neurons in a chemical model of PD. The effects of MPTPp on neurobehavioral function in *hGFAP-Cre/Ikkβ*$^{F/F}$ versus *Ikkβ*$^{F/F}$ mice were determined by open-field activity measurements (Fig 4). In comparison to baseline measurements recorded at day 0, only *Ikkβ*$^{F/F}$ mice exposed to MPTPp had significant depression of spontaneous locomoter activity observed at day 7 post-treatment compared with their saline controls, whereas MPTPp treated *hGFAP-Cre/Ikkβ*$^{F/F}$ mice displayed no changes in locomotion. Significant reductions were observed for total distance traveled (Fig 4A), as assessed by two-way ANOVA, with treatment having significant effects on the total distance traveled that was dependent on the

genotype of the mouse. *Post-hoc* analysis revealed that decrease in total distance moved in MPTPp *Ikkβ*$^{F/F}$ mice was statistically different from their saline counterparts and MPTPp treated *hGFAP-Cre/Ikkβ*$^{F/F}$. Additionally, significant reductions were seen in the total time spent moving at day 7 (Fig. 4C), but not for the number of movements (Fig. 4B), or time spent in margin (Fig. 4D). The number of rearing movements (Fig. 4E) appeared to be reduced in both MPTPp treated genotypes that were significant based on treatment; however, *post-hoc* analysis did not reveal any statistical differences between groups.

The protection of *hGFAP-Cre/Ikkβ*$^{F/F}$ mice from MPTPp neurobehavioral depression was not preserved when assessed at day 14. Although only *Ikkβ*$^{F/F}$ mice had statistically significant reductions in total distance and moving time in comparison to their saline controls, two-way ANOVA revealed a significant effect of treatment on behavior that was not dependent on the genotype of the mouse and *post-hoc* analysis revealed no differences in the behavioral scores of *hGFAP-Cre/Ikkβ*$^{F/F}$ and *Ikkβ*$^{F/F}$ mice MPTPp treated mice.

Determination of MPTPp induced changes in striatal catacholamines

Due to observed MPTPp induced effects on behavior, striatal levels of dopamine (DA) and its metabolites DOPAC and HVA were measured from *hGFAP-Cre/Ikkβ*$^{F/F}$ and *Ikkβ*$^{F/F}$ mice via HPLC. Levels of dopamine were significantly decreased at day 7 in both *hGFAP-Cre/Ikkβ*$^{F/F}$ and *Ikkβ*$^{F/F}$ mice, with continued, but not further reduction, at day 14 (Fig. 5A). There were no significant differences between dopamine losses between genotypes; however, MPTPp exposed *hGFAP-Cre/Ikkβ*$^{F/F}$ trended toward higher recovery at 14 days than their littermate counterparts. Similar patterns were observed for the dopamine metabolites DOPAC (Fig. 5B) and HVA (Fig. 5C). Measurements of the DOPAC to DA ratio were unchanged by treatment and were not

different between genotypes (Fig. 5D). However, the HVA to DA ratio, an indicator of dopamine turnover, was significantly increased in *hGFAP-Cre/Ikkβ*$^{F/F}$ MPTPp exposed mice at day 7 as compared to their saline controls, but not MPTPp exposed littermates (Fig. 5E). This change in DA turnover in *hGFAP-Cre/Ikkβ*$^{F/F}$ mice declined at 14 days post-treatment while *Ikkβ*$^{F/F}$ MPTPp exposed mice HVA/DA ratio was statistically elevated. Although these elevations of the HVA/DA ratio were not significant between genotypes, they do indicate that DA metabolism is being affected differently in *hGFAP-Cre/Ikkβ*$^{F/F}$ than *Ikkβ*$^{F/F}$ mice exposed to MPTPp.

Assessment of Neuroprotectiveness of Astrocyte-specific Ikkβ deletion

To determine the extent of MPTPp induced dopamine neurodegeneration, systematic stereological counts of the SNpc were performed as reported in Fig. 6. Stereologic counts indicated that *Ikkβ*$^{F/F}$ mice treated with MPTPp had marked reductions in the number of TH positive cells at day 7 as compared to saline treated mice (Fig 6B). Number of TH positive cells continued to trend downward between 7-14 days, even after cessation of MPTPp treatment resulting in greater than 50% loss of TH positive cells by day 14. *hGFAP-Cre/Ikkβ*$^{F/F}$ mice appeared to be protected from both direct lesioning affects of MPTPp treatment as well as from progressive loss of TH-positive neurons from day 7-14. Levels of TH positive cells in *hGFAP-Cre/Ikkβ*$^{F/F}$ mice slightly decreased over the treatment course, but were not statistically different from saline levels. Analysis by two-way ANOVA revealed a substantial effect of MPTPp treatment on SNpc levels of TH positive neurons that differed depending on genotype with the most marked and statistically significant difference observed during the progressive lesioning phase at days 7-14.

Discussion

To address the role of inflammatory activated astrocytes in PD, we generated an astrocyte specific *Ikkβ* conditional knockout mouse (*hGFAP-Cre/Ikkβ*$^{F/F}$) postulating that deletion of astrocytic *Ikkβ* would protect mice against progressive neuronal loss when treated with MPTP/probenecid. To assess the extent and specificity of loss, the rate of *Ikkβ* deletion was measured in primary astrocytes from adult and neonatal mouse and compared to astrocytes cultured from littermate controls (*Ikkβ*$^{F/F}$). The genomic frequency of recombination in both neonatal and adult astrocytes was ~ 70% (Fig. 2C) that correlated at the protein level assessed by both western blotting and immunofluorescence (Fig. 2D; Fig. 3A-B). A total deletion of *Ikkβ*$^{F/F}$ was never observed; however, incomplete elimination is a common problem in the use of Cre/loxp systems credited to problems in epigenetic modification in Cre expression (Kaufman et al., 2008). Other conditional Cre/loxp systems often see even lower amounts of recombinatorial success, when reported, with frequency rates of 40% shown for a PolB conditional T-cell knockout(Sauer, 1998), 36% in a microglial specific *Ikkβ* knockout(Cho et al., 2008), and only 30 to 70% seen when a tetracycline inducible *hGFAP-Cre* mouse is utilized (Casper, Jones, & McCarthy, 2007; Chow, Zhang, & Baker, 2008). Other factors that may have influenced the frequency of deletion could be from the presence of low levels of microglia contamination, studies from our laboratory often show only 97% astrocyte purity in culture (Carbone et al., 2008), or result from incomplete mediated deletion whereby cells that retained at least one functional *Ikkβ* were strongly selected for. This has been seen in conditional knockout of *Ikkβ* in B-lymphocytes where cells that underwent Cre mediated deletion of both *Ikkβ* alleles had higher turnover rates and a higher rate of apoptosis(Li et al., 2003).

Even though the rate of Cre-mediated deletion of *Ikkβ* in astrocytes was not 100%, deletion

was found to be specific to astrocytes with no apparent loss measured in cultured microglia or neurons (Fig. 3). Furthermore, this preservation of *Ikkβ* was confirmed *in vivo* revealing that MAP2 positive neurons of the SNpc retained *Ikkβ* (Fig 3F-G). *In vivo* expression of *Ikkβ* was not detectable in astrocytes of microglia in adult mice even in $Ikk\beta^{F/F}$ littermates (data not shown). Other studies have cited the same inability to specifically probe for glial *Ikkβ* in tissue(Cho et al., 2008)and are most likely due to low constitutive expression as it is now thought that NFκB expression in glia is inducible(B. Kaltschmidt & Kaltschmidt, 2009). Taken together, these data argue that we were successful in creating a conditional astrocyte specific *Ikkβ* mouse and that *hGFAP-Cre/*$Ikk\beta^{F/F}$ mice will be a useful tool in elucidating the *in vivo* contribution of astrocyte neuroinflammation.

The inhibition of NFκB has shown to be neuroprotective in both rodent and non-human primate models of PD (Dehmer et al., 2003; Ghosh et al., 2007; Mondal et al., 2012); however, these models employ the use of broad pharmacological inhibition of NFκB and neurons versus specific glial effects cannot be differentiated. Circumstantial evidence in cultured cells has provided some evidence that astrocyte specific NFκB activation is important in MPTP induced neuronal death (Carbone et al., 2008; J. A. Miller et al., 2011), but whether this translates *in vivo* is unknown. In this regard, our study using *hGFAP-Cre/*$Ikk\beta^{F/F}$ mice clearly demonstrates an important role of NFκB/Ikk*β* mediated astrocyte inflammation in PD.

hGFAP-Cre/$Ikk\beta^{F/F}$ mice were subjugated to a subacute dosing regiment of MPTP and probenecid to differentiate the importance of astrocyte inflammation in both direct and progressive neuronal lesioning. This dosing regimen spanning over 14 days has been previously published in our lab and shown to produce more modest and progressive lesioning with MPTP that better capitulates the slow, continuous loss of neurons seen in PD patients (De Miranda et al.,

2013). *hGFAP-Cre/Ikkβ*$^{F/F}$ mice exposed to this model showed significant protection from both direct neurotoxicant induced SN dopaminergic neuronal loss as well as from progressive inflammatory loss (Fig. 6). This indicates that astrocyte NFκB driven neuroinflammation is playing a vital role in not only progressive neuronal degeneration, but also in the initiation of MPTP neurotoxicity. This is in coordination with epidemiological and experimental evidence where use of anti-inflammatories prior to lesion induction have shown to be neuroprotective (Sastre, 2010; Sugama et al., 2003), but is in contrast to a recent study published by (Oeckl, Lattke, Wirth, Baumann, & Ferger, 2012) where overexpression of astrocyte *Ikkβ* did not alter sensitivity to MPTP. However, this study employed an acute MPTP dosing regiment and only measured pathology within days of dosing. Therefore, the lack of protection is more likely due to ineffectiveness in preserving against direct MPTP neurotoxicity with the long-term implications of increased astrocyte activation on progression unresolved.

In accordance with the observed preservation of dopaminergic neurons, measure of neurobehavioral parameters in MPTPp exposed mice indicated significant protection of *hGFAP-Cre/Ikkβ*$^{F/F}$ mice from reductions in locomotion (Fig. 4). This difference from littermate controls was most evident at day 7 of the treatment course for total distance traveled and total moving time. This difference, however, was only temporary as by day 14 of treatment *hGFAP-Cre/Ikkβ*$^{F/F}$ mice treated with MPTPp showed observable downward trends in both aforementioned parameters while treated *Ikkβ*$^{F/F}$ mice showed partial recovery. The reversible nature of MPTP affects on hypokinesia is often observed after cessation of MPTP treatments (J. A. Miller et al., 2011), but other studies utilizing broad inhibition of in both rodents(Ghosh et al., 2007) and non-human primates (Mondal et al., 2012) showed better protection against changes in neurobehavior than measured in this study. These differences show that microglial and neuronal

expression of NFκB remain unaltered in this model and thus may have important influences on MPTPp induced alterations in locomotion.

The observed differences in neurobehavioral parameters between *Ikkβ*$^{F/F}$ and *hGFAP-Cre/Ikkβ*$^{F/F}$ mice were not explainable by alterations in striatal catacholamines. Measurements of DA, DOPAC, and HVA were sharply reduced in striatal tissue in both *Ikkβ*$^{F/F}$ and *hGFAP-Cre/Ikkβ*$^{F/F}$ mice at both day 7 and day 14 even in the face of improved neurobehavior measures (Fig. 5). The only discernable difference was seen in the HVA/DA ratio, which was elevated in hGFAP-Cre/IkkβF/F mice at day 7, and *Ikkβ*$^{F/F}$ at day 14 indicating differences in DA metabolism that may account for improvements in neurobehavior. Other MPTP models have shown similar disconnects between neurochemistry and neurobehavioral parameters (Dehmer et al., 2003; J. A. Miller et al., 2011; Mondal et al., 2012) and most likely reflects the insensitivity of catacholamines measurements to reflect subtle changes in brain environment and the ability of other systems to compensate for the changes in dopamine(Przedborski et al., 2000).

The above data demonstrates that we were successful in generating a mouse with an astrocyte specific deficiency in NFκB. Utilization of this animal in a chemical model of PD showed that elimination of neuroinflammatory activation of astrocytes via NFκB to be protective to nigral neurons indicating that this pathway to be significant contributor to both the initiation and potentiation of nigral pathology. The mechanisms by which astrocyte specific NFκB suppression leads to neuroprotection in this model warrants further investigation as NFκB has shown to be an important regulator of many pro-inflammatory genes in glia including NOS2, cyclooxygenase, tumor necrosis factor alpha (TNFα) and a plethora of other cytokines(B. Kaltschmidt & Kaltschmidt, 2009). However, even without mechanistic details, this mouse study definitively indicates a toxic role of astrocyte induced neuroinflammation in

neurodegeneration and that development of therapeutics to alter this response may show potential benefits in PD and other neurodegenerative models.

CHAPTER 3

FIGURES

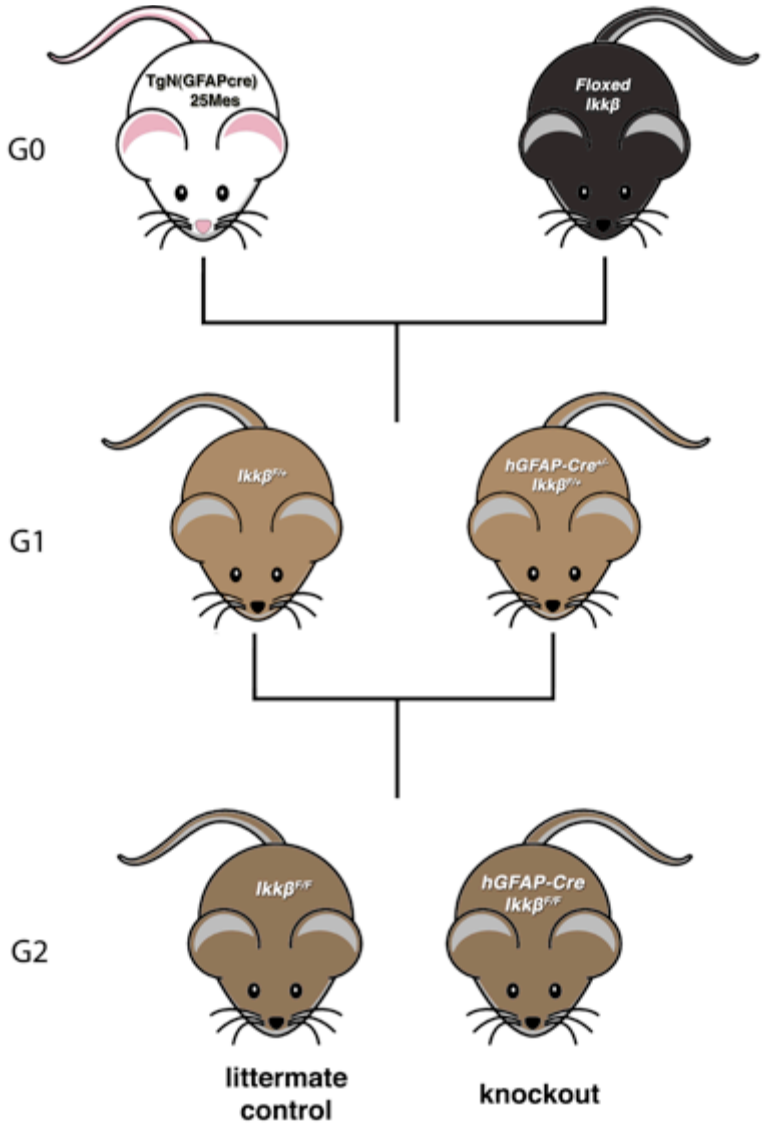

Figure 3.1. Breeding strategy for generation of a conditional *hGFAP-Cre/Ikkβ*$^{F/F}$ mouse. Conditional deletion of *Ikkβ* in astrocytes was achieved through breeding *Ikkβ*-floxed mice on a C57Bl/6 background with *hGFAP*-Cre transgenic mice on an FVB background until homozygozity of the floxed-*Ikkβ* allele was achieved. Two generations (G) of sister-brother pairings were required to produce *hGFAP-Cre/Ikkβ*$^{F/F}$ *and Ikkβ*$^{F/F}$ littermates.

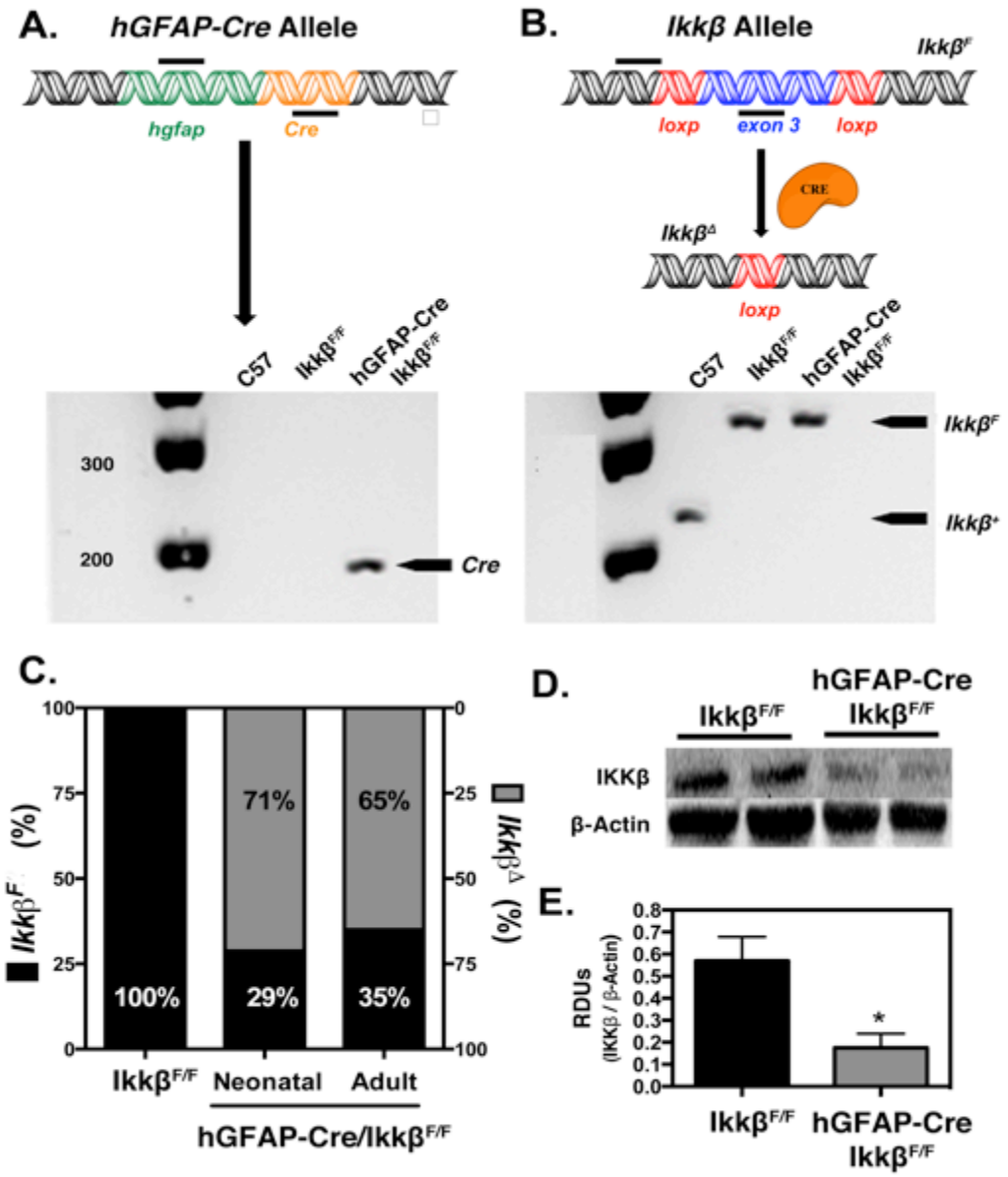

Figure 3.2. Extent of *Ikkβ* deletion in astrocytes cultured from *hGFAP-Cre/Ikkβ*$^{F/F}$ mice. (**A** and **B**) Ear tags from *hGFAP-Cre/Ikkβ*$^{F/F}$ *and Ikkβ*$^{F/F}$ littermates were genotyped via PCR for presence of *hGFAP-Cre* allele (**A**) and presence for floxed (F) or wild type (+) *Ikkβ* allele (**B**). Genotyping of a C57/Bl6/J mouse is provided for reference. (**C**) Genomic DNA from primary astrocytes cultured from neonatal (day 1) and adult (20-week) *hGFAP-Cre/Ikkβ*$^{F/F}$ *and Ikkβ*$^{F/F}$ mice was analyzed via real time-PCR to assess the rate of *Ikkβ* deletion. Percentages of floxed

Ikkβ^{F} and deleted *Ikkβ*$^{\Delta}$ are shown in black and gray, respectively. (**D**) Protein isolated from *hGFAP-Cre/Ikkβ*$^{F/F}$ *and Ikkβ*$^{F/F}$ neonatal astrocyte cultured was analyzed for amount of IKKβ (upper panel) and quantified using densitometric analysis (**E**) with normalization to levels of β-Actin probed on the same blot (lower panel). Data are presented as mean ± SEM. (Student *t*-test; * $p < 0.05$).

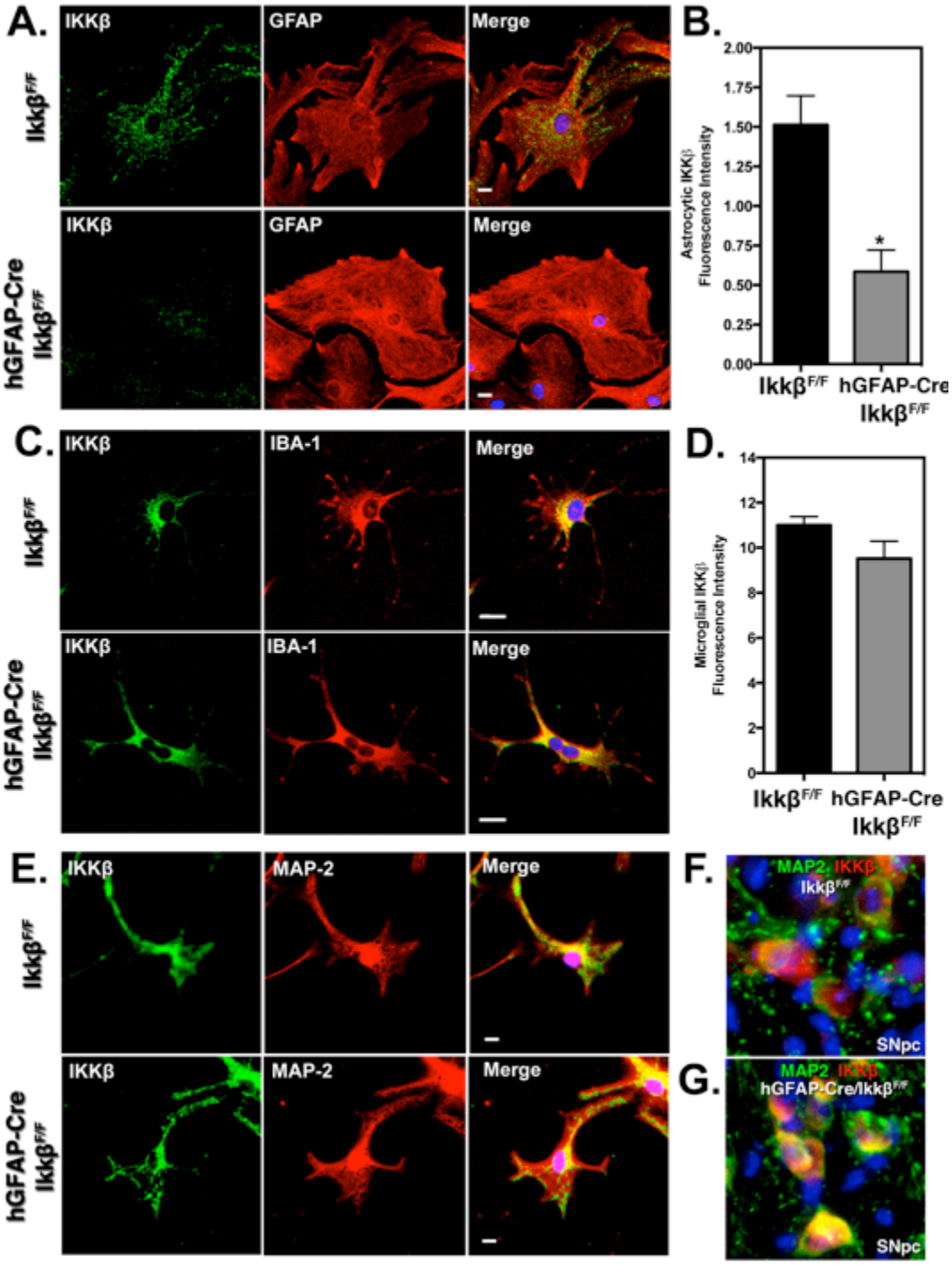

Figure 3.3. *Ikkβ* directed deletion occurs specifically in astrocytes in *hGFAP-Cre/Ikkβ*$^{F/F}$ mice. (**A-E)** Cell specific IKKβ expression in astrocytes, microglia, and astrocytes cultured from *hGFAP-Cre/Ikkβ*$^{F/F}$ and *Ikkβ*$^{F/F}$ neonatal mice. Cells were immunolabeled for IKKβ (green), cell

specific markers (red) for astrocytes (GFAP; **A**), microglia (IBA1; **C**), or neurons (MAP2, **E**) and counterstained with DAPI (blue) to visualize cell nuclei. Scale bar = 10μm. The mean IKKβ fluorescence intensity (with background subtraction) between *hGFAP-Cre/Ikkβ*$^{F/F}$(black bars) and *Ikkβ*$^{F/F}$(gray bars) was measured in astrocytes (**B**) and microglia (**D**). Data are presented as mean ± SEM. (Student *t*-test; * $p < 0.05$). (**F-G**) Representative 40x images of colocalization of MAP2+ neurons (green) and IKKβ (red) in the SNpc of adult *Ikkβ*$^{F/F}$ (**F**) and *hGFAP-Cre/Ikkβ*$^{F/F}$(**G**) mice. Blue = DAPI.

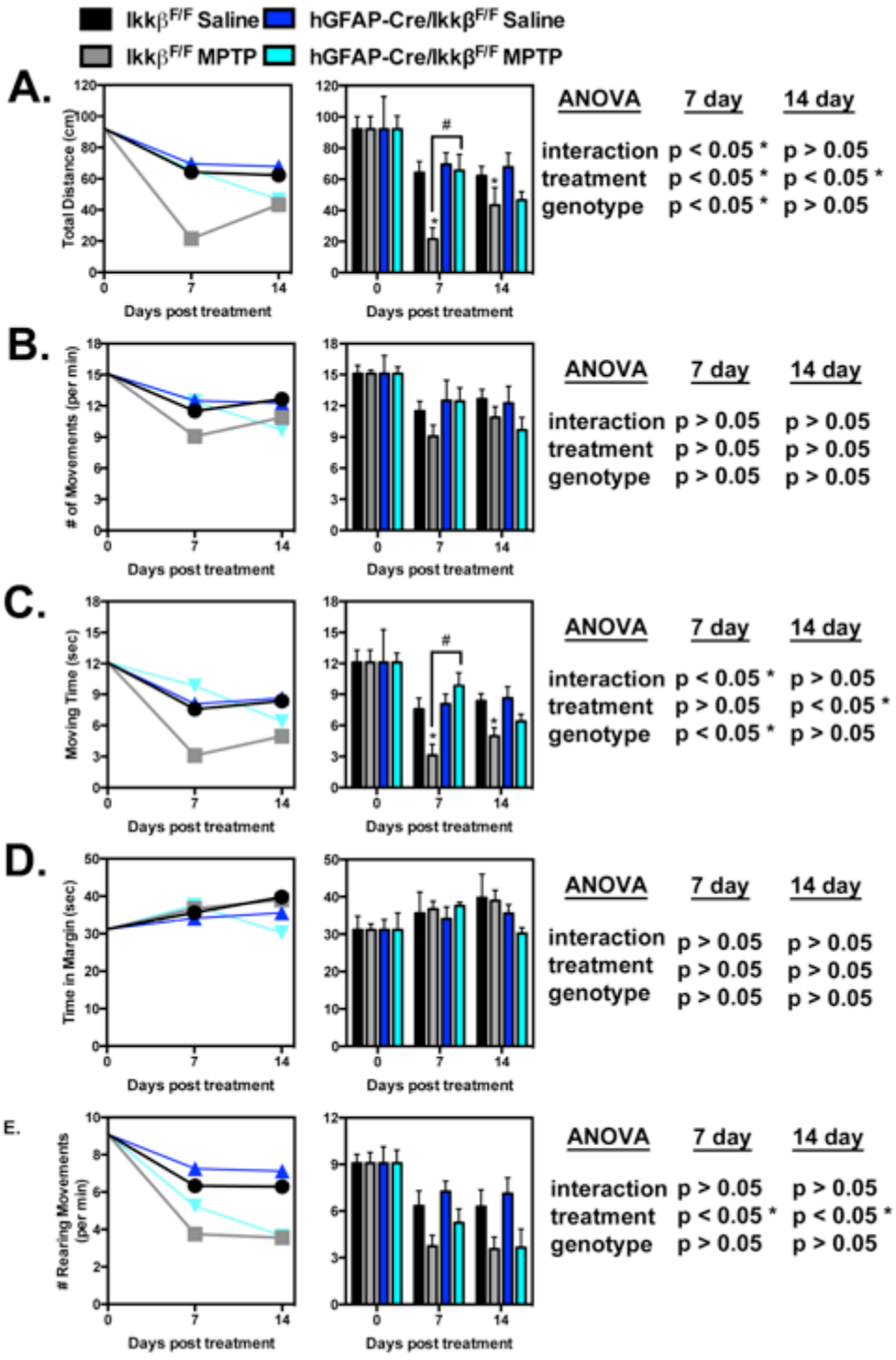
Ikkβ F/F Saline
hGFAP-Cre/Ikkβ F/F Saline
Ikkβ F/F MPTP
hGFAP-Cre/Ikkβ F/F MPTP
A.
Total Distance (cm)
Days post treatment
ANOVA 7 day 14 day
interaction p < 0.05 * p > 0.05
treatment p < 0.05 * p < 0.05 *
genotype p < 0.05 * p > 0.05
B.
# of Movements (per min)
Days post treatment
ANOVA 7 day 14 day
interaction p > 0.05 p > 0.05
treatment p > 0.05 p > 0.05
genotype p > 0.05 p > 0.05
C.
Moving Time (sec)
Days post treatment
ANOVA 7 day 14 day
interaction p < 0.05 * p > 0.05
treatment p > 0.05 p < 0.05 *
genotype p < 0.05 * p > 0.05
D.
Time in Margin (sec)
Days post treatment
ANOVA 7 day 14 day
interaction p > 0.05 p > 0.05
treatment p > 0.05 p > 0.05
genotype p > 0.05 p > 0.05
E.
Rearing Movements (per min)
Days post treatment
ANOVA 7 day 14 day
interaction p > 0.05 p > 0.05
treatment p < 0.05 * p < 0.05 *
genotype p > 0.05 p > 0.05

Figure 3.4. *hGFAP-Cre/Ikkβ*$^{F/F}$ mice are protected from early MPTP/probenecid-induced effects on neurobehavior. Changes in open field activity were monitored in *Ikkβ*$^{F/F}$ and *hGFAP-Cre/Ikkβ*$^{F/F}$ mice treated in a subacute MPTP/probenecid model at days 0, 7, and 14. Changes in total distance moved (**A**), number of total movements (**B**), time spent moving (**C**), time in margin (**D**), and number of rearing movements (**E**) are expressed over time (left graph) and between groups (right graph) and represented as the average percent of baseline (day 0) ± SEM. Data was analyzed by two-way ANOVA with Tukey-Kramer *post hoc* test with independent variables of treatment (saline vs. MPTPp) and genotype (*Ikkβ*$^{F/F}$ vs. *hGFAP-Cre/Ikkβ*$^{F/F}$). Results of analysis are presented to the right (* $p < 0.05$ vs. saline; # $p < 0.05$ vs. MPTPp treated *Ikkβ*$^{F/F}$).

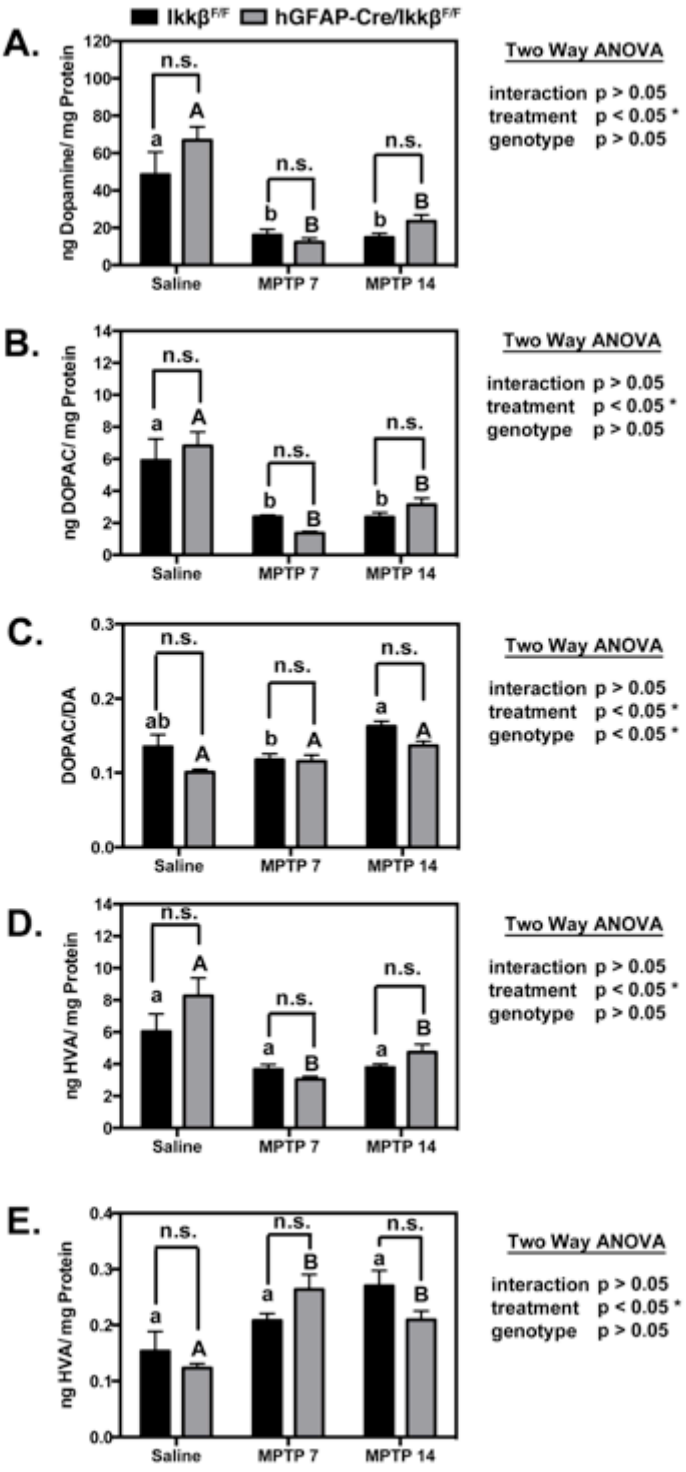
Ikkβ F/F
hGFAP-Cre/Ikkβ F/F
A.
ng Dopamine/ mg Protein
n.s.
a
A
n.s.
b
B
n.s.
b
B
Saline
MPTP 7
MPTP 14
Two Way ANOVA
interaction p > 0.05
treatment p < 0.05 *
genotype p > 0.05
B.
ng DOPAC/ mg Protein
Two Way ANOVA
interaction p > 0.05
treatment p < 0.05 *
genotype p > 0.05
C.
DOPAC/DA
ab
A
b
A
a
A
Two Way ANOVA
interaction p > 0.05
treatment p < 0.05 *
genotype p < 0.05 *
D.
ng HVA/ mg Protein
Two Way ANOVA
interaction p > 0.05
treatment p < 0.05 *
genotype p > 0.05
E.
ng HVA/ mg Protein
Two Way ANOVA
interaction p > 0.05
treatment p < 0.05 *
genotype p > 0.05

Figure 3.5. Loss of striatal DA in response to MPTP/probenecid exposure is unaltered by deletion of *Ikkβ* in astrocytes. Striatal levels of DA (**A**), its metabolites DOPAC (**B**) and HVA (**C**) were analyzed via HPLC. Furthermore, the rate of dopamine metabolism was determined by measuring the DOPAC/DA (**A**) and HVA/DA ratios (**A**). Data are presented as mean ± SEM and were analyzed by two-way ANOVA with Tukey-Kramer *post hoc* test with independent variables of treatment (saline vs. MPTPp) and genotype ($Ikk\beta^{F/F}$ vs. $hGFAP\text{-}Cre/Ikk\beta^{F/F}$). Results of analysis are presented to the right. Lower case letters denote significance between treatment groups of $Ikk\beta^{F/F}$ mice while upper case letters denote significance between treatment groups of $hGFAP\text{-}Cre/Ikk\beta^{F/F}$ mice ($p < 0.05$; n=5).

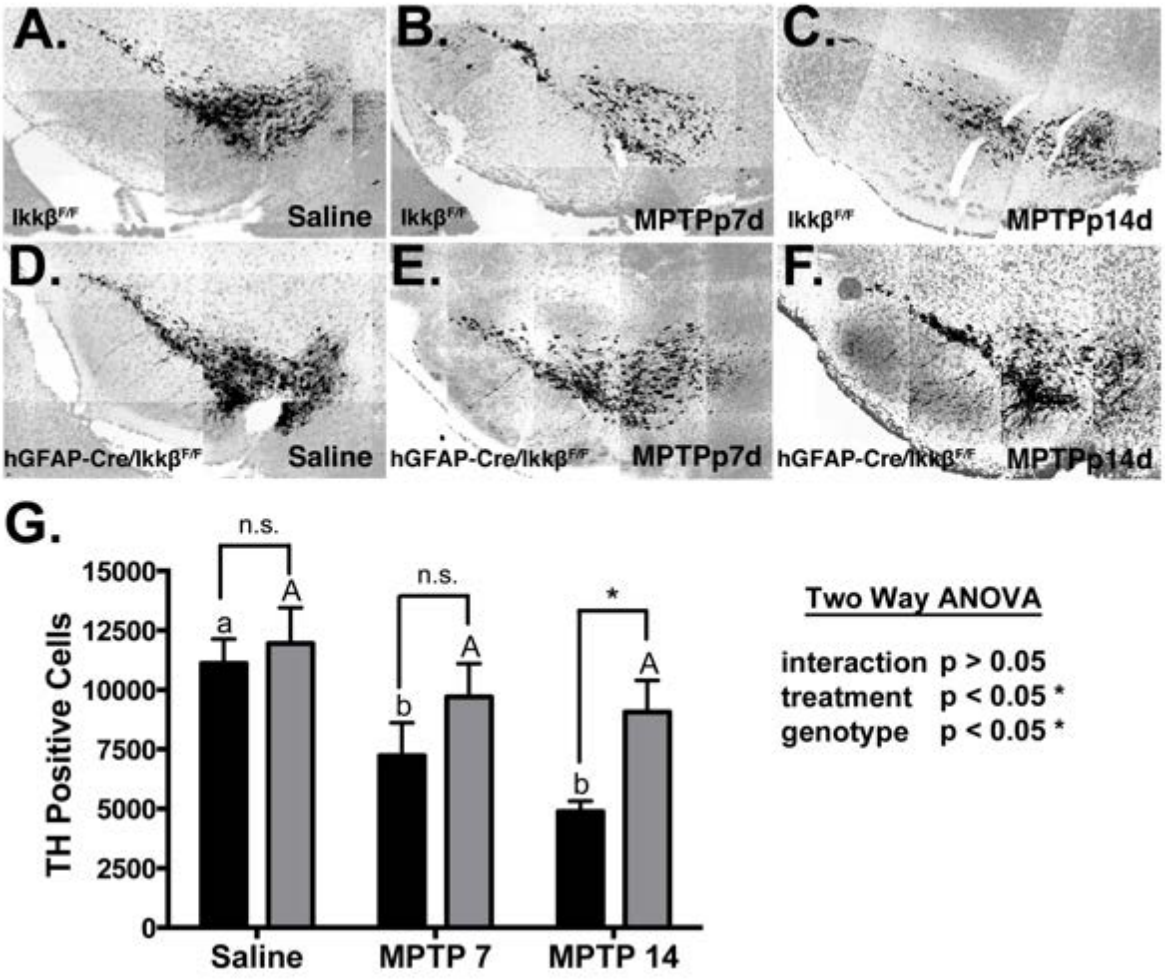

Figure 3.6. *hGFAP-Cre/Ikkβ*$^{F/F}$ mice are protected against direct and progressive loss of TH positive neurons in the SN after exposure to MPTP/probenecid. The number of tyrosine hydroxylase positive neurons in the SNpc of *Ikkβ*$^{F/F}$ and *hGFAP-Cre/Ikkβ*$^{F/F}$ mice treated in a subacute MPTP/probenecid model was assessed via immunofluorescence-based stereology at day 7 and 14. Representative montages generated from individual 20x images are presented as inverted monochromes for *Ikkβ*$^{F/F}$ mice (**A-C**) and *hGFAP-Cre/Ikkβ*$^{F/F}$ mice (**D-F**) with saline on the far left panels (**A,D**), MPTPp 7 days in the middle panels (**B,E**), and MPTPp 14 days on the far right panels (**C,F**). (**G)** Quantitative stereological counts estimating the total number of TH+

neurons presented as average number of TH+ cells ± SEM. Data was analyzed by two-way ANOVA with Tukey-Kramer *post hoc* test with independent variables of treatment (saline vs. MPTPp) and genotype (*Ikkβ*$^{F/F}$ vs. *hGFAP-Cre/Ikkβ*$^{F/F}$). Results of analysis are presented to the right. Lower case letters denote significance between treatment groups of *Ikkβ*$^{F/F}$ mice while upper case letters denote significance between treatment groups of *hGFAP-Cre/Ikkβ*$^{F/F}$ mice ($p < 0.05$; n=5).

CHAPTER 4

MANGANESE ACTIVATES MICROGLIA TO RELEASE SOLUBLE FACTORS THAT AMPLIFIES MN-INDUCED ASTROCYTE ACTIVATION

Summary

Microglia are the resident immune cells of the brain that help protect the brain from stress and infection, but chronic activation of microglia results in the production of chemokines and proinflammatory mediators such as tumor necrosis factor α (TNFα) and inducible nitric oxide synthase (NOS2). Previous studies have implicated activated microglia and astrocytes in neurodegenerative disorders of the basal ganglia such as Parkinson's disease and manganism. Recent work from our laboratory identified activated microglia expressing inducible nitric oxide 2 in the basal ganglia of mice exposed to manganese (Mn) before the appearance of activated astrocytes; however, the mechanism by which Mn activates microglia and the role of activated microglia in manganism is poorly understood. In this study we postulated that Mn directly activates microglia, resulting in increased expression of tumor necrosis factor alpha (TNFα) and other inflammatory mediators that ultimately lead to increased astrocyte activation. Primary microglia and astrocytes were isolated in mixed cultures then purified for experiments using a column-free magnetic separation method. Purity was assed via immunofluorescence staining for microglia and astrocytes using ionized calcium binding adaptor protein-1 (IBA-1) and glial fibrillary acidic protein (GFAP), respectively yielding culture purities of 97% for microglia and 99% for astrocytes. Treatment of microglia with Mn induced a dose-dependent expression of proinflammatory genes; however, there also was significant upregulation of anti-inflammatory genes indicating a mixed phenotype. Treatment of astrocytes with conditioned media from Mn-treated microglia or via co-culture with microglia caused an activated phenotype in astrocytes characterized by increased *Nos2*, *Tnfα,* and interleukin 1-Beta expression. Furthermore, a quantitative cytokine and chemokine PCR array revealed a long list of potential factors that may be involved in microglia induced astrocyte activation. Collectively,

these data indicate that Mn activates microglia in a dose-dependent manner resulting in an increased production of proinflammatory mediators that enhance activation of astrocytes suggesting a complex pattern of glial-glial interactions underlying a neuroinflammatory phenotype in this model.

Introduction

As the resident macrophage, microglia play an important role in the response of the brain to both foreign and endogenous insults; however, sustained and persistent inflammatory activation of microglia is implicated as an important mechanism in the progression of many neurodegenerative diseases including multiple sclerosis, stroke, Alzheimer's disease, and Parkinson's disease (PD; (Block & Hong, 2005; Glass et al., 2010; González-Scarano & Baltuch, 1999; Minghetti, Ajmone-Cat, De Berardinis, & De Simone, 2005). When activated, microglia transition from a resting, ramified cell to a rod-like morphology to a final phagocytic, amoeboid phenotype upregulating expression of a plethora of immunological and inflammatory genes (Gehrmann et al., 1995; S. U. Kim & de Vellis, 2005). Experimental PD models have often identified the transition of microglia from a resting to activated phenotype prior to overt neuropathology releasing factors such as tumor necrosis factor alpha (TNFα) and interleukin 1 beta (IL-1β) that can act on astrocytes to induce secondary inflammatory responses (Hirsch & Hunot, 2009; Saijo et al., 2009); yet, these important glial-glial interactions are virtually unknown in manganese neurotoxicity.

Manganism or manganese neurotoxicity is a disease caused by chronic exposure to elevated levels of the essential trace metal manganese (Mn) that results in clinical motor deficits reminiscent of PD attributed to neuropathology within the basal ganglia of affected individuals (Guilarte, 2010; Huang, 2007; Neal & Guilarte, 2012). The pathologic events that lead to neuronal loss in this disease are largely undefined especially in chronic, low level exposures; however, recent literature has shown a prominent presence of neuroinflammation with increased expression of proinflammatory genes such as *Tnfα, IL-1β* and nitric oxide synthase 2 (*Nos2*) in rodent and non-human primates treated with Mn (Verina et al., 2011; Zhao et al., 2008).

Furthermore, recent studies focused on low level exposures in juveniles has seen that early Mn exposures can result in persistent activation of astrocytes that is associated with higher levels of neuronal injury and neurobehavioral changes in adult animals (Kern & Smith, 2010; Moreno, Streifel, Sullivan, Legare, & Tjalkens, 2009a; Moreno, Yeomans, Streifel, Brattin, Taylor, & Tjalkens, 2009b). Yet, the involvement of microglia is largely understudied in these models with only a handful of studies investigating their role in Mn toxicity (Filipov et al., 2005; Verina et al., 2011; P. Zhang et al., 2009; P. Zhang, Hatter, & Liu, 2007).

Previous studies from our laboratory have indicated that astrocyte activation in Mn models requires the presence of other inflammatory mediators such as TNFα for potent astrocytic expression of *Nos2*(Moreno et al., 2008). Furthermore, studies from our lab have measured microgliosis in juvenile mice prior to astrocyte activation. This may indicate that microglia may play large roles in the initiation of neuroinflammatory mechanisms in this toxicity(Moreno, Streifel, Sullivan, Legare, & Tjalkens, 2009a). In the current study, we sought to explore if manganese could directly cause activation of microglia and if this activation could modulate Mn affects on astrocytes. We explored this model by utilizing purified primary cultures of microglia and astrocytes in a co-culture model. These studies reveal Mn to be a potent inducer of an inflammatory microglia phenotype that is essential for a full-scale astrocyte response to Mn.

Materials and Methods

Cell Culture

Mixed glial cultures from whole brain (excluding cerebellum and brain stem) were prepared from 1-day-old transgenic mice expressing an enhanced-green fluorescent (EGFP) reporter under the control of three *cis*-NFκB elements (*cis*-NFκB^{EGFP}; C57Bl6 background; (Magness et al., 2004); generously provided by Dr. Christian Jobin, University of North Carolina at Chapel Hill) using a modification of a previously described method(M. ASCHNER & Kimelberg, 1991; Carbone et al., 2008; Moreno et al., 2008). Briefly, mice were euthanized by decapitation under isofluorane anesthesia and whole brains were rapidly dissected out and placed into ice cold minimum essential medium with L-glutamine (MEM; Gibco/Invitrogen, Grand Island, NY). Meninges were removed and tissues completely digested with Dispase (1.5U/ml). Dissociated cells were plated onto 100-mm tissue culture plates and kept in MEM supplemented with 10% heat-inactivated FBS (Sigma) and penicillin (0.002 mg/ml), streptomycin (0.002 mg/ml), and neomycin (0.001 mg/ml) antibiotic mixture (PSN). Media was changed every 4-5 days and cells were maintained at 37°C and 5% CO_2 in humidified chambers until confluency was reached (~14-18 days).

Purification of Astrocytes and Microglia

Microglia were purified from astrocytes via column-free magnetic separation using the EasySep mouse CD11b positive selection kit (Stemcell technologies, Vancouver, Canada) according to manufacturer instructions and as outlined in (R. R. Gordon et al., 2011) Briefly, cells from confluent mixed glial cultures (~14-18 days old) were detached using 0.25% trypsin (Gibco). Trypsin reaction was halted using MEM complete media with remaining cells removed

using a cell lifter. Harvested cells were gently triturated and passed through a 70µm cell strainer to remove any cell aggregates, centrifuged, and resuspended at 1 x 10^8 cells/ml in the recommended media (calcium and magnesium free phosphate buffered saline containing 2% FBS and 1 mM Ethylenediaminetetraacetic acid). Cells were transferred to a 5 ml round bottom tube and were incubated at room temperature with the CD11b-Phycoerythin (PE) monoclonal antibody (50µL/mL) for 15 minutes, EasySep PE-Selection Cocktail (70µL/ml) for 15 minutes, followed by a 10 minute incubation with Dextran coated EasySep magnetic nanoparticles (50µL/ml). The cell suspension was brought up to 2.5 mL of recommended media, mixed, and placed in the EasySep purple magnet for 5 minutes. After 5 minutes, the tube was inverted and the solution of un-labeled cells was collected while labeled cells remained in the tube. The solution remaining in the tube was resuspended in another 2.5mL of recommended media and placed in the magnet. This process was repeated for a total of 5 extractions. The purified microglia in the positive fraction and purified astrocytes in the negative fraction were resuspended in complete MEM and seeded onto tissue culture plates. Purified astrocytes and microglia were utilized in experiments within a week of purification. For time course experiments, microglia were seeded onto 6-well tissue culture plates at a density of 3 x 10^5 cells/well and treated with 0.9% saline or 10, 30, or 100µM $MnCl_2$ for 2, 4, 6, 8, or 24 hours.

Immunofluorescence

Purified microglia and astrocytes obtained from magnetic separation were seeded onto serum coated 12 mm glass coverslips at a density of 1 x 10^5 cells per well and allowed to adhere for 48 hours. Cells were fixed using methanol, washed in PBS, and then blocked in 1% Bovine Serum Albumin (w/v) in PBS for one hour. Cells were incubated overnight at 4°C in primary

antibodies for ionized binding adaptor protein 1 (IBA-1; 1:50; Wako, Osaka, Japan) and glial fibrillary acidic protein (GFAP; 1:500; Sigma, St. Louis, MO). After rinsing in PBS, cells were incubated for one hour at room temperature in AlexaFluor-488 (IBA-1) and AlexaFluor-647 (GFAP) conjugated secondary antibodies (1:500; Invitrogen, Carlsbad, CA) and then mounted in medium containing 4′,6-diamidino-2-phenylindole dihydrochloride (DAPI) to detect cell nuclei. Images were acquired using a 20x or 40x air plan apochromatic objectives on a Zeiss Axiovert 200M inverted fluorescence microscope (Carl Zeiss, Inc., Thornwood, NY) equipped with a Hammatsu ORCA-ER-cooled charge-coupled device camera (Hammamatsu Photonics, Hamamatsu City, Japan). Determination of purity was performed by counting the number of IBA-1 and GFAP positive cells in at least 5 fields in at least 3 separate coverslips for every purification experiment.

Gene Expression (qRT-PCR)

RNA was isolated from microglia or astrocytes utilizing a RNeasy Minikit (Qiagen, Valencia, CA) with purity and concentration confirmed using a Nanodrop ND-1000 spectrophotometer (NanoDrop Technologies, Wilmington, DE). 250 ng of RNA (microglia) and 500 ng of RNA (astrocytes) were used as a template for reverse transcriptase reactions using the iScript Reverse Transcriptase kit (Bio-Rad, Hercules CA). Generated cDNA was mixed with Sybrgreen (Biorad, Hercules, CA) and primer pairs listed in Table I. The $2^{-\Delta\Delta}$CT method (Schmittgen & Livak, 2008) was used to determine fold expression with normalization to β-Actin expression. Microglial RNA obtained in the above manner was also utilized in a Mouse Cytokine and Chemokine RT2 Profiler PCR Array (catalog # PAMM 150Z; SA Biosciences, Frederick, MD) according to the manufacturers protocols. The amplification process and

detection were performed using an icycler (Biorad) with gene expression analyzed using the Web-Based PCR Array Data Analysis Tool using the ΔΔCt method and normalized to 5 housekeeping genes: β-actin, β-glucoronidase, hypoxanthine guanine phosphoribosyl transferase 1, heat shock protein 90 alpha, and gluyceraldehyde-3-phosphate dehydrogenase.

Microglia Conditioned Media Experiments

Microglia were seeded onto 6-well tissue culture plates at $3x10^5$ cells/well and treated with saline or 100μM $MnCl_2$ for 24 hours. Microglia conditioned Media (MCM) was pooled per treatment and centrifuged at 800xg for 10 minutes to remove detached cells. Media was placed onto astrocytes seeded in 6-well tissue culture plates at $5x10^5$ cells/well for 24 hours. As a comparison, astrocytes plated at the same density were treated with saline or 100μM $MnCl_2$ concurrent to astrocytes treated with MCM. RNA was extracted as cited above and analyzed for changes in gene expression.

Measurement of Mn in Cell Culture Media

Media samples (500μL) were collected from saline and 100μM $MnCl_2$ treated microglia at the 0 and 24 hours after treatment. Media was stored at -80°C until analyzed. Metals were complexed in the samples using hydrochloric acid then brought up to a final volume of 1 mL using Milli-Q water. Analysis was performed by inductively coupled plasma-mass spectrometry (ICP-MS) on a Perkin-Elmer Elan DRC-II instrument (Perkin Elmer, Waltham, MA) at the Center of Environmental Medicine Analytical Core at Colorado State University. Media blanks underwent the same processing to ensure low levels of Mn in complete MEM. At least 3 samples were analyzed per treatment.

Microglia-Astrocyte Co-Culture

Purified microglia were seeded onto permeable cell culture inserts (BD Biosciences, Franklin Lakes, NJ) at $3x10^5$ cells/well and astrocytes onto 6-well tissue culture plates at $5x10^5$ cells/well and allowed to adhere for 48 hours. Cell media was changed 24 hours prior to treatment. Microglia inserts were placed into 6-well culture plates seeded with astrocytes and both were treated with either saline or 100μM $MnCl_2$ concurrently for 24 hours. RNA was then isolated from astrocytes as detailed above.

Statistical Analyses

All statistical analysis was performed using Prism software (version 6.0; Graphpad Software, Inc., San Diego, CA) with a Student's *t*-test utilized for comparison of two means whereas a one-way analysis of variance (ANOVA) followed by a Tukey-Kramer multiple comparison *post-hoc* test was used for comparison of three or more means. Two-way analysis of variance (ANOVA) followed by a Tukey-Kramer multiple comparison *post-hoc* test was used for comparison of three or more means in analyzing astrocyte responses. Independent variables for two-way ANOVA were defined as treatment (saline versus Mn) and microglial presence (Mn alone vs. presence of microglia/MCM). Statistical significance was defined at a p value less than 0.05 and indicated by *, #, or by assignment of a unique letter.

Results

Purity of Separated Glia

The purity of microglia isolated via the EasySep column free immunomagnetic method was assessed by co-immunofluorescence immunolabeling for IBA-1 and GFAP. Counts of individual fields for the presence of astrocytes or microglia revealed microglial cultures to be 97% pure (Fig. 1C). Assessment of purified astrocyte cultures was determined using the same co-immunofluorescence method with purity > 98% (not shown). Representative micrographs of cultured microglia (Fig. 1A-B) indicate a the cells to possess a resting, ramified morphology.

Mn Induces an Activated, Inflammatory Phenotype in Microglia

To assess if primary microglia activate in response to the presence of manganese alone, gene expression profiling was performed on purified microglia cultures exposed to increasing doses of $MnCl_2$ (Fig. 2). Treatment of primary microglia for 24 hours to 0, 10, 30, or 100μM $MnCl_2$ resulted in dose-dependent upregulation of *Nos2, Il6, Il-1β, Tnfα,* and *caspase 1;* however, only *NOS2* was significantly upregulated from saline treated at a dose lower than 100μM $MnCl_2$. Treatment of microglia with 100μM $MnCl_2$ over time revealed that Mn time-dependently activates microglia with *NOS2* upregulated early at 8 hours of treatment while cytokine and *caspase 1* expression is not significant from control until 24 hours of treatment. Based on these results, future treatments of microglia were conducted with 100μM $MnCl_2$ for 24 hours.

Microglia are a myeloid derived cell and recent evidence suggests that they can express two different phenotypes: an inflammatory M1 phenotype and an anti-inflammatory M2 phenotype (Crain, Nikodemova, & Watters, 2013; Kigerl et al., 2009). Gene expression analysis of Mn-treated microglia for prototypical M1 markers such as cluster of differentiation *(CD)86,*

CD32, and *CD16* revealed mixed results with significant upregulation of *CD86* and down regulation of *CD32* and *CD16 (*Fig. 3A-C). Similar mixed results were seen when evaluating classical M2 genes with brain derived neurotrophic factor *(Bdnf)* and insulin like growth factor-1 *(Igf-1)* upregulated while *CD206* was significantly reduced in Mn treated microglia (Fig 3D-F).

Mn-Activated Microglia potentiate Mn-induced neuroinflammatory activation of Astrocytes

To assess the ability of Mn-activated microglia to modulate astrocyte activation kinetics, we treated astrocytes with either MCM or treated astrocytes in a co-culture system with microglia (Fig. 4). Levels of Mn in MCM were measured via ICP-MS to determine the amount of Mn uptake in microglia, but also to quantify the remaining levels of Mn in media placed on astrocytes (Fig. 4C). Measurements of media placed at time 0 on microglia revealed levels around 100μM $MnCl_2$ while at 24 hours after treatment the levels of Mn remaining in culture media was significantly reduced to 30μM $MnCl_2$. No detectable levels of Mn were measured in culture media from microglia treated with saline or in the media used for all experiments.

Assessment for upregulation of prototypical inflammatory genes in astrocytes by qRT-PCR revealed marked differences in astrocytes treated with Mn alone versus in the presence of microglial factors by either MCM or by co-culturing astrocytes with microglia (Fig. 5). Treatment of astrocytes with 100μM $MnCl_2$ resulted in a large, albeit not significant, increase in the fold expression of *Nos2*, but did not alter levels of astrocyte expression of *Tnfα* or *Il-1β*. However, treatment with MCM or co-culturing of astrocytes with microglia resulted in both potentiation of *Nos2* expression and substantial increases in astrocyte expression of *Tnfα* or *Il-1β*. Two-way ANOVA analysis revealed that the extent of astrocyte activation in response to Mn was dependent on the presence of microglia or microglial derived factors ($p < 0.05$ for treatment

and presence of microglial variables; $p < 0.05$ for interaction).

Potential Microglia Factors Involved in Astrocyte Modulation

A cytokine and chemokine array was used to explore possible genes involved in microglia potentiation of Mn responses on astrocytes (Table II). Several genes were highly upregulated including *caspase 1, chemokine ligand 12, interleukin receptor 1,* and *macrophage migration inhibitory factor* with the largest fold change seen with *caspase 1*. Other notable genes included *Tnf* and *IL-4,* classical pro and anti-inflammatory cytokines, respectively.

Discussion

Microglial activation has been cited as an early event in many neurodegenerative diseases including Alzheimer's disease and PD and is hypothesized to be a critical step in the recruitment of astrocytes and other immune cells in the inflammatory process (Kraft & Harry, 2011). Use of minocycline in experimental models of neurodegenerative disease has proven to be partially if not wholly neuroprotective when used early in treatment regiments (McCarty, 2006; Sugama et al., 2003; Tansey et al., 2007). Yet, despite the wealth of studies examining microglial mechanisms, the involvement of microglia in Manganism is understudied especially when examining the importance of microglia-astrocyte crosstalk. In this study we utilized a column free magnetic based immunopurification protocol to obtain high yields of pure microglia and astrocytes to investigate the role of microglia in manganese toxicity. We postulated that Mn could directly activate microglia and this activation would lead to potentiation of astrocyte responses. Use of conditioned media and co-culturing systems in this study overwhelming indicate that not only does Mn cause direct inflammatory activation of microglia, but also that this response is vital to the full inflammatory induction of astrocytes.

The first indications that microglia may be directly activated by Mn was in a study by (Chang & Liu, 1999) where treatment of N9 microglial cell line with a combination of Mn and lipopolysaccharide (LPS) resulted in dose dependent and metal dependent increases in nitric oxide production through upregulation of the *Nos2* gene. Since that study, only a handful of other groups have built upon those early observations with a majority of the available studies utilizing microglial cell lines due to the difficulties of culturing and obtaining enough primary microglia for study (R. R. Gordon et al., 2011). However, a recent report by (Horvath, Nutile-McMenemy, Alkaitis, & DeLeo, 2008) comparing microglial cells lines to primary cultured

microglia reveal that there are marked deviations between primaries microglia and microglial cell lines in both the amount of stimulus needed to generate an inflammatory response and in the amount of NO and cytokine production in response to a stimulus. Primary microglia in Horvath's study generated higher levels of NO, TNFα, IL-1β, and IL-6 in response to LPS stimulation than the cell lines and at lower concentrations than their BV2 counterparts indicating that primary microglia are a more sensitive indicator of inflammatory activation than transformed cell lines. These obvious differences could account for why in this study we overwhelming observed that Mn alone resulted in inflammatory activation of primary microglia (Fig. 2). Except for two studies by (Bae et al., 2006; M. Liu et al., 2009), past experiments show that without an additional inflammatory stimulus like LPS, even high concentrations of Mn is often insufficient to cause increases in NO and cytokine production in microglia(Filipov et al., 2005; P. Zhang et al., 2007). This deviation in our results from past publications is most likely a reflection of the use of primary microglia than a microglial cell line and not a factor of low LPS contamination in serum as suggested by (Filipov & Dodd, 2011) due to rigorous testing performed in our lab to ensure low endotoxin levels in purchased sera (data not shown).

The reliance of past literature on microglial cell lines stems from the high cost and low yield of microglia by traditional methods of differential adhesion and thus limited our understanding of microglial responses in Mn neurotoxicity. In this study, we were able to move past these limitations through use a column based magnetic separation method for microglia first published by (R. R. Gordon et al., 2011) that allowed us to obtain a high number of microglial cultures with a purity > 97% (Fig. 1). Use of these pure primary cultures in an Mn model revealed that microglia could be directly acted upon by manganese in a dose and time dependent manner to cause upregulation of *Nos2, TNFα*, *IL-1β*, *IL-6,* and *caspase 1* (Fig. 2). Except for

caspase 1, which was found to be highly upregulated through a cytokine array (Table II), *Nos2, Tnfα, Il-1β*, and *Il-6* have been shown to be upregulated in brains of animals exposed to Mn (Moreno, Yeomans, Streifel, Brattin, Taylor, & Tjalkens, 2009b; Verina et al., 2011; Zhao et al., 2008)and shown to be important in other neurodegenerative models to be potential sources of microglia induced astrocyte activation(Harms et al., 2011; Hwang et al., 2006; Saijo et al., 2009). Furthermore, because microglia can more potently upregulate these genes in comparison with astrocytes, they most likely represent the main source of these cytokines measured in Mn exposed animals (S. U. Kim & de Vellis, 2005; S. C. Lee et al., 1993).

In attempt to further characterize the Mn induced activation of microglia, we studied whether Mn leads to a classical (M1) versus alternative activation (M2) of primary microglia (Fig. 3) as determination of this phenotype can be predictive if microglia activation is protective or neurotoxic (Crain et al., 2013). Treatment of microglia with Mn resulted in a mixed phenotype in this study with no clear indications of either a M1 or M2 phenotype. This incomplete phenotype possibly stems from Mn being a required trace element and our study using concentrations that are only 2-5 fold above what is normally found in the brain (J. ASCHNER & ASCHNER, 2005; Bonilla, Salazar, Villasmil, & Villalobos, 1982) .

With evidence that Mn can directly cause inflammatory activation of microglia, we wanted to determine if Mn-activated microglia would release factors that could amplify astrocytic responses to Mn. Treatment of primary astrocyte cultures with MCM or co-cultured in the presence of microglia resulted in large inductions of inflammatory gene expression in astrocytes that was several fold above with treatment of astrocytes with Mn alone (Fig. 5). Microglia were required for astrocyte induction of *Tnfα* and *Il-1β* expression, as Mn alone, even at a high concentration, could not induce this expression in astrocytes. This phenotypic response

fits with previous studies from our laboratory that have shown that Mn alone is often insufficient to activate astrocytes and requires the presence of LPS or cytokines to get a large increase in expression of inflammatory genes such as *Nos2* (Moreno et al., 2008). However, this study is the first indications that activated microglia are most likely the source of co-activating factors and that this response is necessary for complete astrocyte activation in a manganese model. Additionally, measurement of Mn in MCM media revealed (Fig. 4) that the levels of Mn were 70% lower in microglia culture media after 24 hours revealing that microglia can sequester Mn and that even low levels of Mn in media in addition to microglia factors can have potentiating effects.

The source of microglia induced astrocyte activation in this model is most likely a complex array of products released by activated microglia and requires further study; however, large inductions in caspase 1, the enzyme responsible for cleaving IL-1β and interleukin 18, indicate that interleukin release may play a large role. In the few studies examining glia-glia interactions in other neurodegenerative models, cytokines such as interferon gamma, IL-6, prostaglandin E2, TNFα and IL-1β have all been indicated as possible activators of astrocytes (Hwang et al., 2006; Kuno et al., 2006; K.-W. Lee et al., 2012b; Saijo et al., 2009) as inhibition of microglia release or blockade of astrocyte receptors for these factors have proven to be effective in preventing astrocyte activation. This highlights the need for more in depth look at these interactions in these diseases as targeting these interactions in Mn toxicity and other neurodegenerative models might prove important in preventing or reducing the neuroinflammatory responses in these diseases.

CHAPTER 4

TABLES AND FIGURES

TABLE 4.1

qRT-PCR PRIMERS

Gene	Accession Number	Forward Primer (5'-3')	Reverse Primer (5'-3')	References
iNOS	NM_010927.2	TCACGCTTGGG CTTGTT	CAGGTCACTTTGGTAGGATTTG	1
TNFα	NM_013693.3	GTTGCCTGATTCTTGCTTCTG	GCCACCACTTGCTCCTAC	2
IL-1β	NM_008361.3	GCAGCAGCACATCAACAAAG	CACGGGAAAGACACAGGTAG	2
IL-6	NM_031168.1	GACAACTTTGGCATTGTGG	ATGCAGGGATGATGTTCTG	3
Caspase 1	NM_009807.2	ATGAATACAACCACTCGTACAC	ATCCTCCAGCAGCAACTTC	2
CD86	NM-019388	TTGTGTGTGTTCTGGAAACGGAG	AACTTAGAGGCTGTGTTGCTGGG	4
CD32	NM_010187.2	AATCCTGCCGTTCCTACTGATC	GTGTCACCGTGTCTTCCTTGAG	4
CD16	NM_010188.4	TTTGGACACCCAGATGTTTCAG	GTCTTCCTTGAGCACCTGGATC	4
IGF-1	NM_010512.4	AAAGCAGCCCGCTCTATCC	CTTCTGAGTCTTGGGCATGTCA	3
BDNF	NM_001048139.1	TTACCTGGATGCCGCAAACAT	TGACCCACTCGCTAATACTGTC	3
CD206	NM_008625.1	TCTTTGCCTTTCCCAGTCTCC	TGACACCCAGCGGAATTTC	4
β-Actin	NM_00793.3	GCTCTCCTATGTTGCTCTAG	CGCTCCTTGCCAATACTC	1

[1] Sequences taken from (Carbone et al. 2008).
[2] Primers designed using NCBI/Primer-BLAST
[3] Sequences obtained from PrimerBank
[4] Sequences taken from (Kigerl et al. 2009).

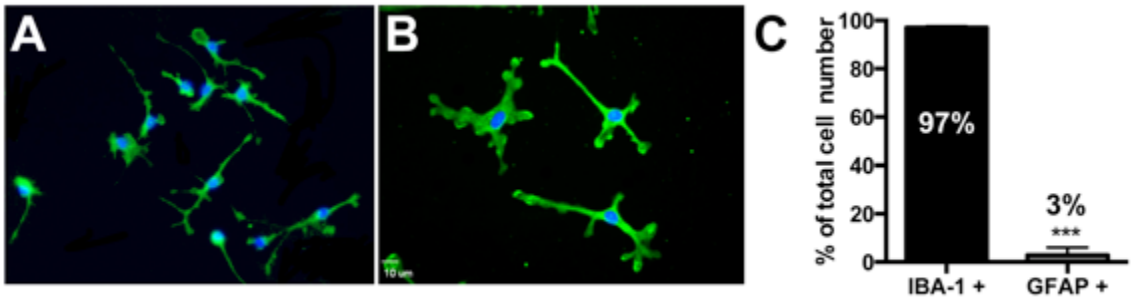

Figure 4.1. Purified microglia cultures are 97% pure. Culture purity of purified microglia cultures were assessed via immunofluorescent detection for GFAP and IBA-1 positive cells. Representative images of IBA-1 positive (green) microglial cultures at low (**A)** and high resolution (**B**) with DAPI (blue) to visualize cell nuclei. (**C**) Quantified counts of the number of IBA-1 versus GFAP positive cells in microglia cultures. Data are presented as average percent expression ± SEM (Student *t* test; *** $p < 0.0001$).

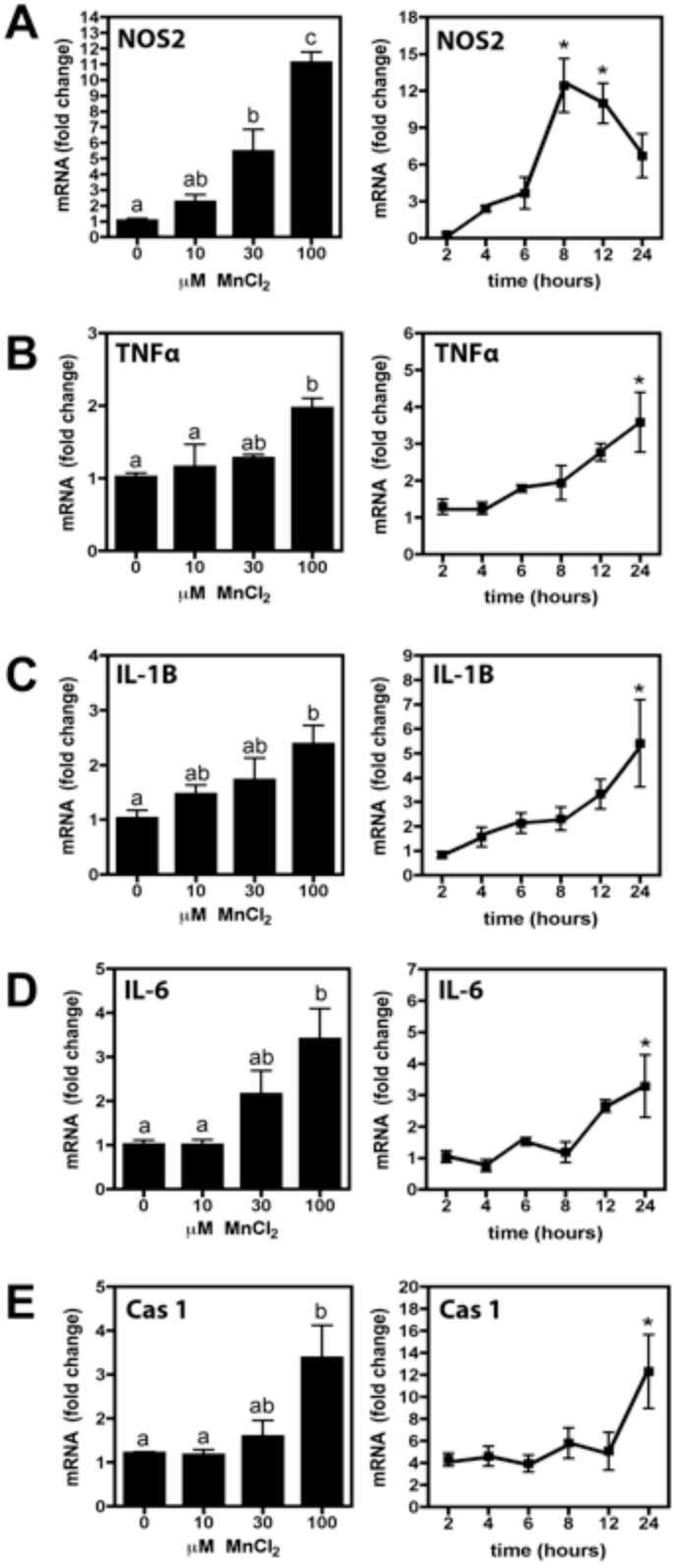
A
NOS2
mRNA (fold change)
μM MnCl2
time (hours)
B
TNFα
C
IL-1B
D
IL-6
E
Cas 1

Figure 4.2. Manganese induces a dose and time dependent increase in inflammatory gene expression in microglia. Purified primary microglia were treated with increasing doses of Mn over time to determine the dose (right panels) and time dependent (left panels) effects of Mn on *Nos2* (**A**)*, Tnfα* (**B**)*, Il-1β* (**C**)*, Il-6* (**D**)*,* and *caspase 1* (**E**) expression. Data are presented as fold change in mRNA ± SEM (one way ANOVA; different letters and * denote a $p < 0.05$).

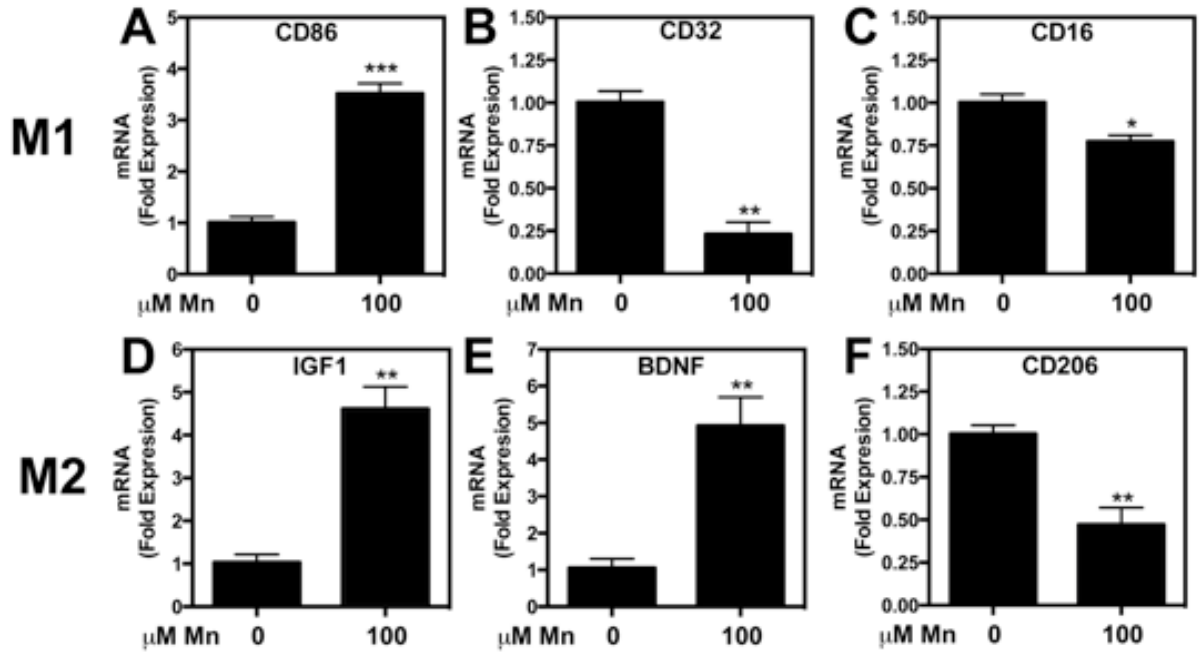

Figure 4.3. Manganese causes development of a mixed M1/M2 phenotype. The expression levels of M1 (top panels) and M2 (lower panels) genes were assessed via qRT-PCR in primary microglia treated with 100μM $MnCl_2$. M1 genes analyzed included *CD86* (**A**), *CD32* (**B**), and *CD16* (**C**). M2 genes analyzed included *Igf-1* (**D**), *Bdnf* (**E**), and *CD206* (**A**). Data are presented as the average fold change ± SEM (Student *t* test; ** $p < 0.01$, *** $p < 0.0001$).

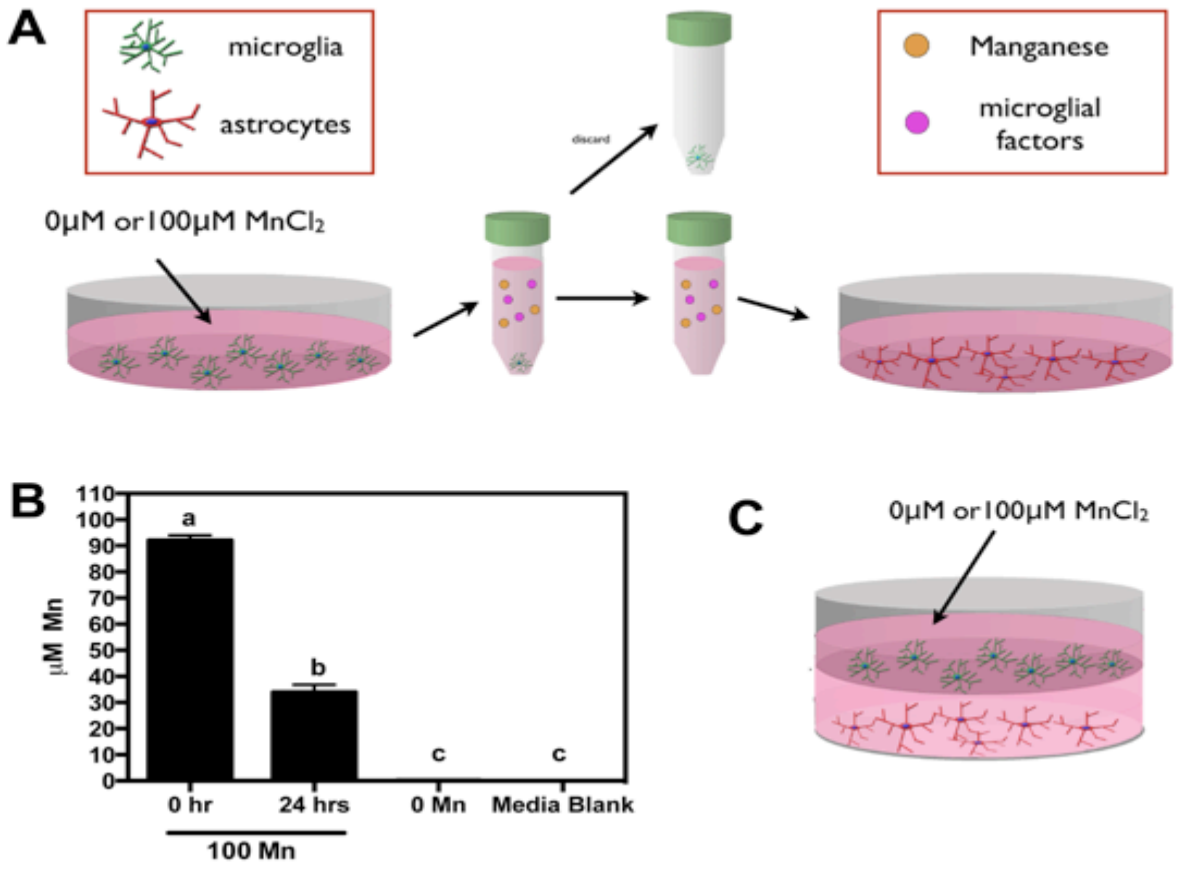

Figure 4.4. Schematics of microglia conditioned media (MCM) and co-culture experiments. (**A)** In MCM experiments, microglia were treated with either saline or 100μM $MnCl_2$ for 24 hours. Media was removed, centrifuged to remove any unattached cells, and supernatants were placed on astrocytes for 24 hours. (**B**) The levels of Mn in in MCM were measured via ICP-MS at time 0 and 24 hours post treatment. Data are presented as the average micromolar concentration of Mn ± SEM (one-way ANOVA; different letters indicate a $p < 0.05$). (**C**) In co-culture experiments, microglia seeded on permeable cell culture inserts were cultured with astrocytes plated on 6-well tissue plates and simultaneously treated with 100μM $MnCl_2$ for 24 hours.

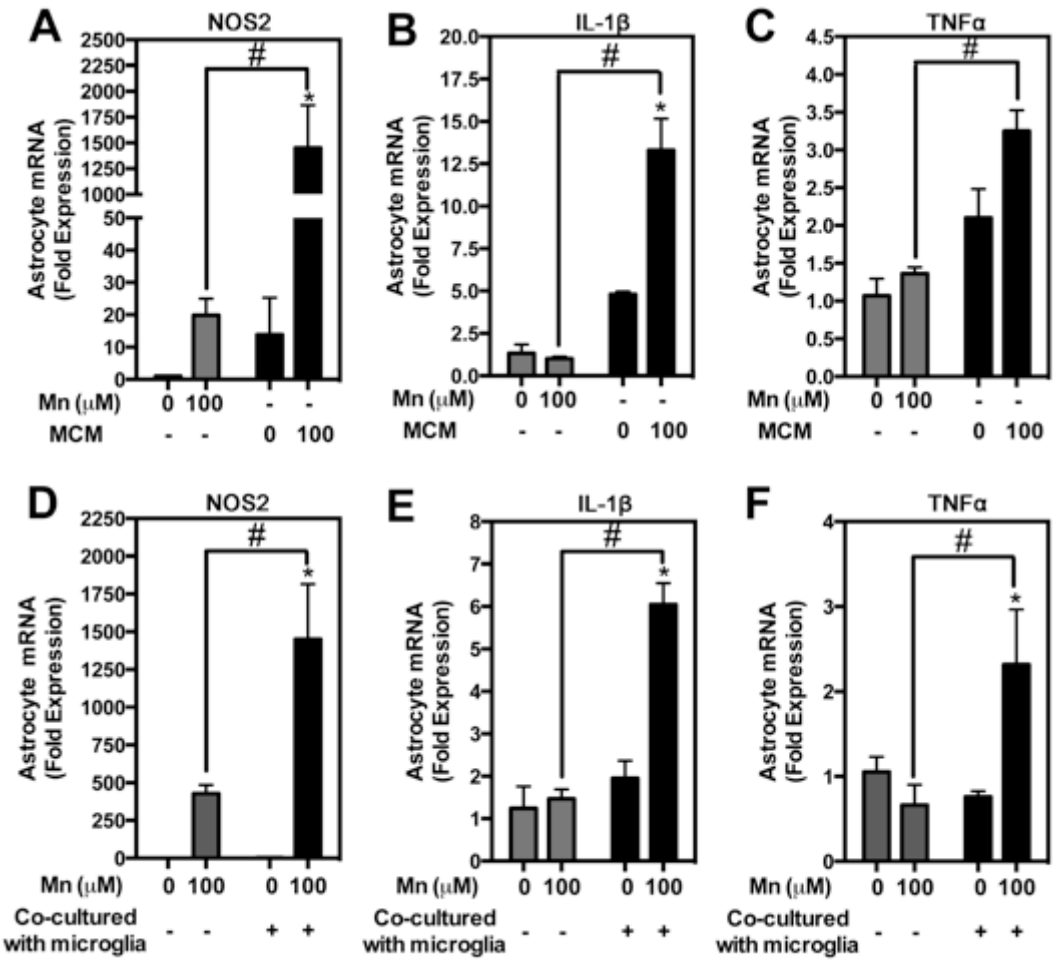

Figure 4.5. Presence of microglia or microglial derived factors are required for complete astrocyte activation. Levels of inflammatory gene expression in astrocytes treated with only saline or 100μM $MnCl_2$ versus Mn with MCM (**A-C**) or when co-cultured with microglia (**D-F**) were determined via qRT-PCR. (**A**) Astrocyte expression of *Nos2* when treated with Mn alone versus MCM. (**B**) Astrocyte expression of *Tnfα* when treated with Mn alone versus MCM. (**C**) Astrocyte expression of *Il-1β* when treated with Mn alone versus MCM. (**D**) Astrocyte expression of *Nos2* when treated with Mn alone versus when co-cultured with microglia. (**E**) Astrocyte expression of *Tnfα* when treated with Mn alone versus when co-cultured with microglia. (**F**) Astrocyte expression of *Il-1β* when treated with Mn alone versus when co-

cultured with microglia. Data are presented as the average fold change ± SEM. (Two way ANOVA with Tukey *post hoc* analysis; * $p < 0.05$ between saline and 100μM $MnCl_2$; # $p < 0.05$ versus 100μM $MnCl_2$ alone).

TABLE 4.2

CYTOKINE AND CHEMOKINE ARRAY

Gene	Control	100 µM Mn	Fold Change
Caspase 1	0.0	10.1	**1,097.5**
Chemokine ligand 5	10.4	12.1	**3.2**
Chemokine ligand 9	2.8	5.1	**4.9**
Chemokine ligand 10	7.5	10.2	**6.5**
Chemokine ligand 12	8.3	11.6	**9.8**
Chemokine receptor 4	2.8	4.3	**2.8**
Chemokine receptor 6	0.2	2.6	**5.3**
Chemokine receptor 9	1.2	2.8	**3.0**
Interleukin 4	1.9	3.2	**2.5**
Interleukin 11	4.7	6.2	**2.8**
Interleukin 15	9.7	11.5	**3.5**
Interleukin 1 receptor, type II	0.0	3.0	**8.0**
Interleukin 2 receptor, beta chain	1.4	3.1	**3.2**
Interleukin 2 receptor, gamma chain	9.3	10.6	**2.5**
Interleukin 8 receptor, beta	0.0	1.8	**3.5**
Macrophage migration inhibitory factor	13.3	16.8	**11.3**
Secreted phosphoprotein 1	16.3	18.2	**3.7**
Tumor necrosis factor	7.5	9.0	**2.8**
Toll interacting protein	8.8	10.0	**2.3**

CHAPTER 5

CONCLUSIONS

Final Conclusions

Patients with neurodegenerative diseases such as PD, Mn neurotoxicity, and chronic epilepsy have poor treatment options and often a low quality of life. Available treatments only target clinical symptoms with majority of current therapeutics unable to address the cause of pathology or prevent further progression of the disease. The experiments described herein are the first step towards elucidating the pathological role of NFκB induced neuroinflammatory activation of glia in three neurodegenerative diseases: seizures, PD and, Mn neurotoxicity. Due to the controversial role of glia in these neurodegenerative diseases and the poor understanding of disease pathogenesis, experiments that further investigate glia responses can only provide better insights into finding new and potentially better treatment paradigms for these diseases. In particular, as NFκB has proven to be a key regulator of glial inflammatory responses, understanding the role of this pathway in activated glia during disease can better predict how treatments affecting this pathway may alter disease pathology.

Studies examining the involvement of neuroinflammation in diseases of domestic animals and in wildlife are lacking with the primary dogma still considering glia involvement in these diseases to still be a passive reaction. In this study, we are the first to show evidence of significant glial activation that highly correlated to neuronal loss in sea lions exposed to domoic acid. These glial alterations were often seen in a greater expanse of the hippocampus than overt neuronal loss and often preceded pathological changes. Furthermore, significant oxidative and nitrative stress was identified in both neurons and cells expressing GS, a pathological change that has been shown in rodents to be involved in seizuregenesis. Although further investigation is required to show causality of these neuroinflammatory changes in this disease, these initial investigations have proven that neuroinflammation is playing a large role in this disease and

continued research in this model can provide invaluable insights in not only treating domoic acid exposed wildlife, but in potentially finding new therapeutic targets in human epilepsies. Translational models have proven to be a very effective research design allowing faster therapeutic development and benefits that span multiple species.

Unlike the previous model, glia involvement in PD has been extensively researched with clear evidence of neuroinflammatory presence during disease progression. However, the implications of these glial reactions in this disease are still debated, as the pathways involved have not been fully elicited. Therapeutic interventions targeting glial activation often show great promise in early phases of drug development, but often fail when progressing to phase two, highlighting again the need to better understand the pathogenesis of the disease to make better models, but to determine correct treatment targets. In these experiments, we utilized the cell-specific knockout technology to specifically examine how the NFκB pathway in astrocytes was contributing to PD pathology in MPTP treated mice. These experiments gave clear evidence that removal of this pathway in astrocytes protected against the initial lesioning as well as progressive loss of neurons in this model. These findings support that astrocyte activation involving the NFκB pathway in this disease is playing a detrimental role in neuronal survival and allows us to design more effective NFκB inhibitors for this disease. The NFκB pathway plays a complicated, but prominent role in neurodegenerative diseases, but also in many other conditions that affect older individuals including a variety of cancers and immune-mediated conditions. Global therapeutics inhibiting this pathway may have unintended consequences of promoting cancerous growth or preventing neuronal survival. We have only begun to scratch the surface with the development of this mouse and represent a great asset in further describing the involvement of NFκB induced inflammatory activation of glia in PD and in other diseases.

Astrocytes appear to play a prominent and intimate role in neurodegenerative disease; however, involvement of microglia has received increasing attention due to their faster activation kinetics and larger immunological outputs. The ability of microglia to be directly activated to a neuroinflammatory phenotype in Mn neurotoxicity is not a novel finding; however, this is the first evidence using primary cells that Mn alone, and not with a co-activating factor, can directly induce a inflammatory phenotype in this cells. Additionally, this Mn induced activation of microglia appears to be necessary for full activation of astrocytes when exposed to Mn. Glial dynamics are complex and have only begun to be explored, but investigations into these mechanisms appear key in understanding the progressive nature of neuroinflammation and in understanding how this process switches from a neuroprotective to neurotoxic role during disease.

Glial physiology and pathology in neurodegenerative diseases are complex and are understanding of the pathways has only just begun. The results in this study further add to our knowledge of these cells during neurodegenerative disease by exploring the mechanisms in three different disease models. These various models show consistently that activated astrocytes and microglia are presence and actively participating in generating inflammatory mediators that are detrimental to neuronal survival. Further study into designing pharmacological inhibition of these pathways may prove beneficial in helping to target the source of disease pathology, but also in delaying further neuronal loss in these diseases.

CHAPTER 6

LITERATURE CITED

Alarcón, G., & Valentín, A. (2010). Mesial Temporal Lobe Epilepsy with Hippocampal Sclerosis. In *Atlas of Epilepsies* (pp. 1171–1175). London: Springer London. doi:10.1007/978-1-84882-128-6_173

Alcamo, E., Mizgerd, J. P., Horwitz, B. H., Bronson, R., Beg, A. A., Scott, M., et al. (2001). Targeted mutation of TNF receptor I rescues the RelA-deficient mouse and reveals a critical role for NF-kappa B in leukocyte recruitment. *Journal of immunology (Baltimore, Md. : 1950)*, *167*(3), 1592–1600.

Ananth, C. C., Gopalakrishnakone, P. P., & Kaur, C. C. (2003). Induction of inducible nitric oxide synthase expression in activated microglia following domoic acid (DA)-induced neurotoxicity in the rat hippocampus. *Neuroscience Letters*, *338*(1), 49–52. doi:10.1016/S0304-3940(02)01351-4

Araque, A., Carmignoto, G., & Haydon, P. G. (2001). Dynamic signaling between astrocytes and neurons. *Annual review of physiology*, *63*, 795–813. doi:10.1146/annurev.physiol.63.1.795

Aronica, E., & Crino, P. B. (2011). Inflammation in epilepsy: Clinical observations. *Epilepsia*, *52*, 26–32. doi:10.1111/j.1528-1167.2011.03033.x

Aronica, E., Ravizza, T., Zurolo, E., & Vezzani, A. (2012). Astrocyte immune responses in epilepsy. (C. Steinhäuser & D. Boison, Eds.)*Glia*, *60*(8), 1258–1268. doi:10.1002/glia.22312

ASCHNER, J., & ASCHNER, M. (2005). Nutritional aspects of manganese homeostasis. *Molecular Aspects of Medicine*, *26*(4-5), 353–362. doi:10.1016/j.mam.2005.07.003

ASCHNER, M., & Aschner, J. L. (1991). Manganese neurotoxicity: cellular effects and blood-brain barrier transport. *Neuroscience & Biobehavioral Reviews*.

ASCHNER, M., & Kimelberg, H. K. (1991). The use of astrocytes in culture as model systems for evaluating neurotoxic-induced-injury. *NeuroToxicology*, *12*(3), 505–517.

Bae, J.-H., Jang, B.-C., Suh, S.-I., Ha, E., Baik, H. H., Kim, S.-S., et al. (2006). Manganese induces inducible nitric oxide synthase (iNOS) expression via activation of both MAP kinase and PI3K/Akt pathways in BV2 microglial cells. *Neuroscience Letters*, *398*(1-2), 151–154. doi:10.1016/j.neulet.2005.12.067

Bargu, S., Silver, M., Goldstein, T., Roberts, K., & Gulland, F. (2010). Complexity of domoic acid-related sea lion strandings in Monterey Bay, California: foraging patterns, climate events, and toxic blooms. *Marine Ecology Progress Series*, *418*, 213–222. doi:10.3354/meps08816

Barhoumi, R., Faske, J., Liu, X., & Tjalkens, R. B. (2004). Manganese potentiates lipopolysaccharide-induced expression of NOS2 in C6 glioma cells through mitochondrial-dependent activation of nuclear factor kappaB. *Molecular Brain Research*, *122*(2), 167–179. doi:10.1016/j.molbrainres.2003.12.009

Bidmon, H.-J., Görg, B., Palomero-Gallagher, N., Schleicher, A., Häussinger, D., Speckmann, E. J., & Zilles, K. (2008). Glutamine synthetase becomes nitrated and its activity is reduced during repetitive seizure activity in the pentylentetrazole model of epilepsy. *Epilepsia*, *49*(10), 1733–1748. doi:10.1111/j.1528-1167.2008.01642.x

Block, M. L., & Hong, J.-S. (2005). Microglia and inflammation-mediated neurodegeneration: Multiple triggers with a common mechanism. *Progress in Neurobiology*, *76*(2), 77–98. doi:10.1016/j.pneurobio.2005.06.004

Bonilla, E., Salazar, E., Villasmil, J. J., & Villalobos, R. (1982). The regional distribution of manganese in the normal human brain. *Neurochemical research*, *7*(2), 221–227.

Bonizzi, G., & Karin, M. (2004). The two NF-κB activation pathways and their role in innate and adaptive immunity. *Trends in Immunology*, *25*(6), 280–288. doi:10.1016/j.it.2004.03.008

Bossart, G. D. (2011). Marine Mammals as Sentinel Species for Oceans and Human Health. *Veterinary Pathology Online*.

Bové, J., & Perier, C. (2012). Neurotoxin-based models of Parkinson's disease. *Neuroscience*, *211*, 51–76. doi:10.1016/j.neuroscience.2011.10.057

Brambilla, R. (2005). Inhibition of astroglial nuclear factor B reduces inflammation and improves functional recovery after spinal cord injury. *Journal of Experimental Medicine*, *202*(1), 145–156. doi:10.1084/jem.20041918

Brambilla, R., Persaud, T., Hu, X., Karmally, S., Shestopalov, V. I., Dvoriantchikova, G., et al. (2009). Transgenic Inhibition of Astroglial NF- B Improves Functional Outcome in Experimental Autoimmune Encephalomyelitis by Suppressing Chronic Central Nervous System Inflammation. *The Journal of Immunology*, *182*(5), 2628–2640. doi:10.4049/jimmunol.0802954

Brown, G. C. (2007). Mechanisms of inflammatory neurodegeneration: iNOS and NADPH oxidase. *Biochemical Society transactions*, *35*(Pt 5), 1119–1121. doi:10.1042/BST0351119

Carbone, D. L., Popichak, K. A., Moreno, J. A., Safe, S., & Tjalkens, R. B. (2008). Suppression of 1-Methyl-4-phenyl-1,2,3,6-tetrahydropyridine-Induced Nitric-Oxide Synthase 2 Expression in Astrocytes by a Novel Diindolylmethane Analog Protects Striatal Neurons against Apoptosis. *Molecular Pharmacology*, *75*(1), 35–43. doi:10.1124/mol.108.050781

Carmignoto, G., & Gómez-Gonzalo, M. (2010). The contribution of astrocyte signalling to neurovascular coupling. *Brain Research Reviews*, *63*(1-2), 138–148. doi:10.1016/j.brainresrev.2009.11.007

Casper, K. B., & McCarthy, K. D. (2006). GFAP-positive progenitor cells produce neurons and oligodendrocytes throughout the CNS. *Molecular and Cellular Neuroscience*, *31*(4), 676–684. doi:10.1016/j.mcn.2005.12.006

Casper, K. B., Jones, K., & McCarthy, K. D. (2007). Characterization of astrocyte-specific conditional knockouts. *genesis*, *45*(5), 292–299. doi:10.1002/dvg.20287

Castegna, A., Palmieri, L., Spera, I., Porcelli, V., Palmieri, F., Fabis-Pedrini, M. J., et al. (2011). Oxidative stress and reduced glutamine synthetase activity in the absence of inflammation in the cortex of mice with experimental allergic encephalomyelitis. *Neuroscience*, *185*, 97–105. doi:10.1016/j.neuroscience.2011.04.041

Cavus, I., Kasoff, W. S., Cassaday, M. P., Jacob, R., Gueorguieva, R., Sherwin, R. S., et al. (2005). Extracellular metabolites in the cortex and hippocampus of epileptic patients. *Annals of Neurology*, *57*(2), 226–235. doi:10.1002/ana.20380

Centonze, D. (2001). Impaired Excitatory Transmission in the Striatum of Rats Chronically Intoxicated with Manganese. *Experimental Neurology*, *172*(2), 469–476. doi:10.1006/exnr.2001.7812

Chang, J. Y., & Liu, L. Z. (1999). Manganese potentiates nitric oxide production by microglia. *Brain research. Molecular brain research*, *68*(1-2), 22–28.

Chaudhuri, K. R., & Schapira, A. H. (2009). Non-motor symptoms of Parkinson's disease: dopaminergic pathophysiology and treatment. *The Lancet Neurology*, *8*(5), 464–474. doi:10.1016/S1474-4422(09)70068-7

Chen, C.-J., Ou, Y.-C., Lin, S.-Y., Liao, S.-L., Chen, S.-Y., & Chen, J.-H. (2006). Manganese modulates pro-inflammatory gene expression in activated glia. *Neurochemistry International*, *49*(1), 62–71. doi:10.1016/j.neuint.2005.12.020

Chen, P. C., Vargas, M. R., Pani, A. K., Smeyne, R. J., Johnson, D. A., Kan, Y. W., & Johnson, J. A. (2009). Nrf2-mediated neuroprotection in the MPTP mouse model of Parkinson's disease:

Critical role for the astrocyte. *Proceedings of the National Academy of Sciences*, *106*(8), 2933–2938. doi:10.1073/pnas.0813361106

Cho, I. H., Hong, J., Suh, E. C., Kim, J. H., Lee, H., Lee, J. E., et al. (2008). Role of microglial IKK in kainic acid-induced hippocampal neuronal cell death. *Brain*, *131*(11), 3019–3033. doi:10.1093/brain/awn230

Chow, L. M. L., Zhang, J., & Baker, S. J. (2008). Inducible Cre recombinase activity in mouse mature astrocytes and adult neural precursor cells. *Transgenic Research*, *17*(5), 919–928. doi:10.1007/s11248-008-9185-4

Christopherson, K. S., Ullian, E. M., Stokes, C. C. A., Mullowney, C. E., Hell, J. W., Agah, A., et al. (2005). Thrombospondins are astrocyte-secreted proteins that promote CNS synaptogenesis. *Cell*, *120*(3), 421–433. doi:10.1016/j.cell.2004.12.020

Chuang, Y.-C., Chen, S.-D., Lin, T.-K., Chang, W.-N., Lu, C.-H., Liou, C.-W., et al. (2010). Transcriptional upregulation of nitric oxide synthase II by nuclear factor-κB promotes apoptotic neuronal cell death in the hippocampus following experimental status epilepticus. *Journal of neuroscience research*, NA–NA. doi:10.1002/jnr.22369

Collipp, P. J., Chen, S. Y., & Maitinsky, S. (1983). Manganese in infant formulas and learning disability. *Annals of nutrition and metabolism*.

Coulter, D. A., & Eid, T. (2012). Astrocytic regulation of glutamate homeostasis in epilepsy. (C. Steinhäuser & D. Boison, Eds.)*Glia*, *60*(8), 1215–1226. doi:10.1002/glia.22341

Craft, J. M., Watterson, D. M., & Van Eldik, L. J. (2005). Neuroinflammation: a potential therapeutic target. *Expert Opinion on Therapeutic Targets*, *9*(5), 887–900. doi:10.1517/14728222.9.5.887

Crain, J. M., Nikodemova, M., & Watters, J. J. (2013). Microglia express distinct M1 and M2 phenotypic markers in the postnatal and adult central nervous system in male and female mice. *Journal of neuroscience research*, *91*(9), 1143–1151. doi:10.1002/jnr.23242

Dakshinamurti, K., Sharma, S. K., Sundaram, M., & Watanabe, T. (1993). Hippocampal changes in developing postnatal mice following intrauterine exposure to domoic acid. *The Journal of neuroscience*, *13*(10), 4486–4495.

Damier, P., Hirsch, E. C., Zhang, P., Agid, Y., & Javoy-Agid, F. (1993). Glutathione peroxidase, glial cells and Parkinson's disease. *Neuroscience*, *52*(1), 1–6.

David, S., & Kroner, A. (2011). Repertoire of microglial and macrophage responses after spinal cord injury. *Nature Reviews Neuroscience*, *12*(7), 388–399. doi:10.1038/nrn3053

De Lanerolle, N. C., & Lee, T.-S. (2005). New facets of the neuropathology and molecular profile of human temporal lobe epilepsy. *Epilepsy & Behavior*, *7*(2), 190–203. doi:10.1016/j.yebeh.2005.06.003

De Miranda, B. R., Miller, J. A., Hansen, R. J., Lunghofer, P. J., Safe, S., Gustafson, D. L., et al. (2013). Neuroprotective Efficacy and Pharmacokinetic Behavior of Novel Anti-Inflammatory Para-Phenyl Substituted Diindolylmethanes in a Mouse Model of Parkinson's Disease. *Journal of Pharmacology and Experimental Therapeutics*, *345*(1), 125–138. doi:10.1124/jpet.112.201558

Dehmer, T., Heneka, M. T., Sastre, M., Dichgans, J., & Schulz, J. B. (2003). Protection by pioglitazone in the MPTP model of Parkinson's disease correlates with IκBα induction and block of NFκB and iNOS activation. *Journal of Neurochemistry*, *88*(2), 494–501. doi:10.1046/j.1471-4159.2003.02210.x

Dehmer, T., Lindenau, J., Haid, S., Dichgans, J., & Schulz, J. B. (2000). Deficiency of inducible nitric oxide synthase protects against MPTP toxicity in vivo. *Journal of Neurochemistry*,

74(5), 2213–2216.
Devi, P. U., Manocha, A., & Vohora, D. (2008). Seizures, antiepileptics, antioxidants and oxidative stress: an insight for researchers. *Expert Opinion on Pharmacotherapy*, *9*(18), 3169–3177. doi:10.1517/14656560802568230
Devinsky, O., Vezzani, A., Najjar, S., De Lanerolle, N. C., & Rogawski, M. A. (2013). Glia and epilepsy: excitability and inflammation. *Trends in Neurosciences*, *36*(3), 174–184. doi:10.1016/j.tins.2012.11.008
Di Virgilio, F., Ceruti, S., Bramanti, P., & Abbracchio, M. P. (2009). Purinergic signalling in inflammation of the central nervous system. *Trends in Neurosciences*, *32*(2), 79–87. doi:10.1016/j.tins.2008.11.003
DiDonato, J. A., Hayakawa, M., Rothwarf, D. M., Zandi, E., & Karin, M. (1997). A cytokine-responsive IκB kinase that activates the transcription factor NF-κB. *Nature*, *388*(6642), 548–554.
Doetsch, F. (2003). The glial identity of neural stem cells. *Nature Neuroscience*, *6*(11), 1127–1134. doi:10.1038/nn1144
EID, T., THOMAS, M., SPENCER, D., RUNDENPRAN, E., LAI, J., MALTHANKAR, G., et al. (2004). Loss of glutamine synthetase in the human epileptogenic hippocampus: possible mechanism for raised extracellular glutamate in mesial temporal lobe epilepsy. *The Lancet*, *363*(9402), 28–37. doi:10.1016/S0140-6736(03)15166-5
Eid, T., Williamson, A., Lee, T.-S. W., Petroff, O. A., & De Lanerolle, N. C. (2008). Glutamate and astrocytes-Key players in human mesial temporal lobe epilepsy? *Epilepsia*, *49*, 42–52. doi:10.1111/j.1528-1167.2008.01492.x
Filipov, N. M., & Dodd, C. A. (2011). Role of glial cells in manganese neurotoxicity. *Journal of Applied Toxicology*, *32*(5), 310–317. doi:10.1002/jat.1762
Filipov, N. M., Seegal, R. F., & Lawrence, D. A. (2005). Manganese potentiates in vitro production of proinflammatory cytokines and nitric oxide by microglia through a nuclear factor kappa B-dependent mechanism. *Toxicological sciences : an official journal of the Society of Toxicology*, *84*(1), 139–148. doi:10.1093/toxsci/kfi055
Foresti, M. L., Arisi, G. M., & Shapiro, L. A. (2011). Role of glia in epilepsy-associated neuropathology, neuroinflammation and neurogenesis. *Brain Research Reviews*, *66*(1-2), 115–122. doi:10.1016/j.brainresrev.2010.09.002
Frank-Cannon, T. C., Alto, L. T., McAlpine, F. E., & Tansey, M. G. (2009). Does neuroinflammation fan the flame in neurodegenerative diseases? *Molecular Neurodegeneration*, *4*, 47. doi:10.1186/1750-1326-4-47
Gao, H. M., Zhou, H., Zhang, F., Wilson, B. C., Kam, W., & Hong, J. S. (2011). HMGB1 Acts on Microglia Mac1 to Mediate Chronic Neuroinflammation That Drives Progressive Neurodegeneration. *Journal of Neuroscience*, *31*(3), 1081–1092. doi:10.1523/JNEUROSCI.3732-10.2011
Gasser, T. (2009). Molecular pathogenesis of Parkinson disease: insights from genetic studies. *Expert reviews in molecular medicine*, *11*, e22. doi:10.1017/S1462399409001148
Gehrmann, Matsumoto, Kreutzberg. (1995). Microglia: intrinsic immuneffector cell of the brain. *Brain Research Reviews*, *20*(3), 19–19. doi:10.1016/0165-0173(94)00015-H
Gensel, J. C., Kigerl, K. A., Mandrekar-Colucci, S. S., Gaudet, A. D., & Popovich, P. G. (2012). Achieving CNS axon regeneration by manipulating convergent neuro-immune signaling. *Cell and tissue research*, *349*(1), 201–213. doi:10.1007/s00441-012-1425-5
Ghosh, A., Roy, A., Liu, X., Kordower, J. H., Mufson, E. J., Hartley, D. M., et al. (2007).

Selective inhibition of NF-κB activation prevents dopaminergic neuronal loss in a mouse model of Parkinson's disease. *Proceedings of the National Academy of Sciences of the United States of America*, *104*(47), 18754–18759.
Gill, S. S., Hou, Y., Ghane, T., & Pulido, O. M. (2008). Regional susceptibility to domoic acid in primary astrocyte cells cultured from the brain stem and hippocampus. *Marine Drugs*, *6*(1), 25–38.
Glass, C. K., Saijo, K., Winner, B., Marchetto, M. C., & Gage, F. H. (2010). Mechanisms Underlying Inflammation in Neurodegeneration. *Cell*, *140*(6), 918–934. doi:10.1016/j.cell.2010.02.016
Goldstein, T., Mazet, J. A. K., Zabka, T. S., Langlois, G., Colegrove, K. M., Silver, M., et al. (2007). Novel symptomatology and changing epidemiology of domoic acid toxicosis in California sea lions (*Zalophus californianus*): an increasing risk to marine mammal health. *Proceedings of the Royal Society B: Biological Sciences*, *275*(1632), 267–276. doi:10.1098/rspb.2007.1221
Goldstein, T., Zabka, T. S., Delong, R. L., Wheeler, E. A., Ylitalo, G., Bargu, S., et al. (2009). The role of domoic acid in abortion and premature parturition of California sea lions (Zalophus californianus) on San Miguel Island, California. *Journal of wildlife diseases*, *45*(1), 91–108.
González-Scarano, F., & Baltuch, G. (1999). Microglia as mediators of inflammatory and degenerative diseases. *Annual review of neuroscience*, *22*, 219–240. doi:10.1146/annurev.neuro.22.1.219
Gordon, R. R., Hogan, C. E. C., Neal, M. L. M., Anantharam, V. V., Kanthasamy, A. G. A., & Kanthasamy, A. A. (2011). A simple magnetic separation method for high-yield isolation of pure primary microglia. *Journal of Neuroscience Methods*, *194*(2), 287–296. doi:10.1016/j.jneumeth.2010.11.001
Görg, B., Qvartskhava, N., Voss, P., Grune, T., Häussinger, D., & Schliess, F. (2007). Reversible inhibition of mammalian glutamine synthetase by tyrosine nitration. *FEBS Letters*, *581*(1), 84–90. doi:10.1016/j.febslet.2006.11.081
Gras, G., Porcheray, F., Samah, B., & Leone, C. (2006). The glutamate-glutamine cycle as an inducible, protective face of macrophage activation. *Journal of Leukocyte Biology*, *80*(5), 1067–1075. doi:10.1189/jlb.0306153
Gribbin, Simon. (2009). 5.2 Barres Q&A NS CNS, 1–3.
Grilli, M., & Memo, M. (1999). Nuclear factor-κB/Rel proteins. *Biochemical Pharmacology*, *57*(1), 1–7. doi:10.1016/S0006-2952(98)00214-7
Guilarte, T. R. (2010). Manganese and Parkinson's Disease: A Critical Review and New Findings. *Environmental Health Perspectives*, *118*(8), 1071–1080. doi:10.1289/ehp.0901748
Gulland, E. M. D., Haulena, M., Fauquier, D., Lander, M. E., Zabka, T., Duerr, R., & Langlois, G. (2002). Domoic acid toxicity in Californian sea lions (Zalophus californianus): clinical signs, treatment and survival.
Gulland, F. (2000). Domoic acid toxicity in California sea lions (Zalophus californianus) stranded along the central California coast, May-October 1998. *NOAA Technical Memorandum NMFS-OPR-17*.
Hamby, M. E. M., Hewett, J. A. J., & Hewett, S. J. S. (2006). TGF-beta1 potentiates astrocytic nitric oxide production by expanding the population of astrocytes that express NOS-2. *Glia*, *54*(6), 566–577. doi:10.1002/glia.20411
Harms, A. S., Lee, J.-K., Nguyen, T. A., Chang, J., Ruhn, K. M., Treviño, I., & Tansey, M. G.

(2011). Regulation of microglia effector functions by tumor necrosis factor signaling. *Glia*, *60*(2), 189–202. doi:10.1002/glia.21254

Herrmann, O., Baumann, B., de Lorenzi, R., Muhammad, S., Zhang, W., Kleesiek, J., et al. (2005). IKK mediates ischemia-induced neuronal death. *Nature Medicine*, *11*(12), 1322–1329. doi:10.1038/nm1323

Hirsch, E. C., & Hunot, S. (2009). Neuroinflammation in Parkinson's disease: a target for neuroprotection? *Lancet neurology*, *8*(4), 382–397. doi:10.1016/S1474-4422(09)70062-6

Horacio Riojas-Rodríguez, R. S.-V. A. S. S. M. S. R. C. R. Y. R.-A. (2010). Intellectual Function in Mexican Children Living in a Mining Area and Environmentally Exposed to Manganese. *Environmental Health Perspectives*, *118*(10), 1465–1470. doi:10.1289/ehp.0901229

Horvath, R. J., Nutile-McMenemy, N., Alkaitis, M. S., & DeLeo, J. A. (2008). Differential migration, LPS-induced cytokine, chemokine, and NO expression in immortalized BV-2 and HAPI cell lines and primary microglial cultures. *Journal of Neurochemistry*, *107*(2), 557–569. doi:10.1111/j.1471-4159.2008.05633.x

Hua, M. S., & Huang, C. C. (1991). Chronic occupational exposure to manganese and neurobehavioral function. *Journal of clinical and experimental …*.

Huang, C.-C. (2007). Parkinsonism induced by chronic manganese intoxication--an experience in Taiwan. *Chang Gung medical journal*, *30*(5), 385–395.

Huh, J. W. J., Raghupathi, R. R., Laurer, H. L. H., Helfaer, M. A. M., & Saatman, K. E. K. (2003). Transient loss of microtubule-associated protein 2 immunoreactivity after moderate brain injury in mice. *Journal of Neurotrauma*, *20*(10), 975–984. doi:10.1089/089771503770195821

Hunot, S., Brugg, B., Ricard, D., Michel, P. P., Muriel, M.-P., Ruberg, M., et al. (1997). Nuclear translocation of NF-κB is increased in dopaminergic neurons of patients with Parkinson disease.

Husemann, J. J., Loike, J. D. J., Anankov, R. R., Febbraio, M. M., & Silverstein, S. C. S. (2002). Scavenger receptors in neurobiology and neuropathology: their role on microglia and other cells of the nervous system. *Glia*, *40*(2), 195–205. doi:10.1002/glia.10148

Hwang, S.-Y., Jung, J.-S., Kim, T.-H., Lim, S.-J., Oh, E.-S., Kim, J.-Y., et al. (2006). Ionizing radiation induces astrocyte gliosis through microglia activation. *Neurobiology of Disease*, *21*(3), 457–467. doi:10.1016/j.nbd.2005.08.006

Jankovic, J. (2008). Parkinson's disease: clinical features and diagnosis. *Journal of Neurology, Neurosurgery & Psychiatry*, *79*(4), 368–376. doi:10.1136/jnnp.2007.131045

Kaltschmidt, B., & Kaltschmidt, C. (2009). NF- B in the Nervous System. *Cold Spring Harbor Perspectives in Biology*, *1*(3), a001271–a001271. doi:10.1101/cshperspect.a001271

Karin, M. (1999). the role of the IkB kinase (IKK) complex. *Oncogene*, 1–8.

Karin, M. (2005). Inflammation-activated Protein Kinases as Targets for Drug Development. *Proceedings of the American Thoracic Society*, *2*(4), 386–390. doi:10.1513/pats.200504-034SR

Kaufman, W. L., Kocman, I., Agrawal, V., Rahn, H. P., Besser, D., & Gossen, M. (2008). Homogeneity and persistence of transgene expression by omitting antibiotic selection in cell line isolation. *Nucleic Acids Research*, *36*(17), e111–e111. doi:10.1093/nar/gkn508

Kaushal, V., & Schlichter, L. C. (2008). Mechanisms of Microglia-Mediated Neurotoxicity in a New Model of the Stroke Penumbra. *Journal of Neuroscience*, *28*(9), 2221–2230. doi:10.1523/JNEUROSCI.5643-07.2008

Kern, C. H., & Smith, D. R. (2010). Preweaning Mn exposure leads to prolonged astrocyte

activation and lasting effects on the dopaminergic system in adult male rats. *Synapse*, *65*(6), 532–544. doi:10.1002/syn.20873

Kigerl, K. A., Gensel, J. C., Ankeny, D. P., Alexander, J. K., Donnelly, D. J., & Popovich, P. G. (2009). Identification of two distinct macrophage subsets with divergent effects causing either neurotoxicity or regeneration in the injured mouse spinal cord. *Journal of Neuroscience*, *29*(43), 13435–13444. doi:10.1523/JNEUROSCI.3257-09.2009

Kim, S. U., & de Vellis, J. (2005). Microglia in health and disease. *Journal of neuroscience research*, *81*(3), 302–313. doi:10.1002/jnr.20562

Kim, Y. S. (2005). Matrix Metalloproteinase-3: A Novel Signaling Proteinase from Apoptotic Neuronal Cells That Activates Microglia. *Journal of Neuroscience*, *25*(14), 3701–3711. doi:10.1523/JNEUROSCI.4346-04.2005

Kim, Y., Kim, B. N., Hong, Y. C., Shin, M. S., Yoo, H. J., & Kim, J. W. (2009). Co-exposure to environmental lead and manganese affects the intelligence of school-aged children. *NeuroToxicology*.

Kimelberg, H. K. (2004). The problem of astrocyte identity. *Neurochemistry International*, *45*(2-3), 191–202. doi:10.1016/j.neuint.2003.08.015

Kovacs, R., Rabanus, A., Otahal, J., Patzak, A., Kardos, J., Albus, K., et al. (2009). Endogenous Nitric Oxide Is a Key Promoting Factor for Initiation of Seizure-Like Events in Hippocampal and Entorhinal Cortex Slices. *Journal of Neuroscience*, *29*(26), 8565–8577. doi:10.1523/JNEUROSCI.5698-08.2009

Kraft, A. D. A., & Harry, G. J. G. (2011). Features of microglia and neuroinflammation relevant to environmental exposure and neurotoxicity. *International Journal of Environmental Research and Public Health*, *8*(7), 2980–3018. doi:10.3390/ijerph8072980

Kuno, R., Yoshida, Y., Nitta, A., Nabeshima, T., Wang, J., Sonobe, Y., et al. (2006). The role of TNF-alpha and its receptors in the production of NGF and GDNF by astrocytes. *Brain Research*, *1116*(1), 12–18. doi:10.1016/j.brainres.2006.07.120

la Riva, de, G. T., Johnson, C. K., Gulland, F. M. D., Langlois, G. W., Heyning, J. E., Rowles, T. K., & Mazet, J. A. K. (2009). Association of an unusual marine mammal mortality event with Pseudo-nitzschia spp. Blooms along the southern California coastline. *Journal of wildlife diseases*, *45*(1), 109–121.

Lalo, U., Pankratov, Y., Wichert, S. P., Rossner, M. J., North, R. A., Kirchhoff, F., & Verkhratsky, A. (2008). P2X1 and P2X5 subunits form the functional P2X receptor in mouse cortical astrocytes. *Journal of Neuroscience*, *28*(21), 5473–5480. doi:10.1523/JNEUROSCI.1149-08.2008

Lawson, L. J. L., Perry, V. H. V., Dri, P. P., & Gordon, S. S. (1990). Heterogeneity in the distribution and morphology of microglia in the normal adult mouse brain. *Neuroscience*, *39*(1), 151–170.

Lee Mosley, R., Benner, E. J., Kadiu, I., Thomas, M., Boska, M. D., Hasan, K., et al. (2006). Neuroinflammation, oxidative stress, and the pathogenesis of Parkinson's disease. *Clinical Neuroscience Research*, *6*(5), 261–281. doi:10.1016/j.cnr.2006.09.006

Lee, D. J., Hsu, M. S., Seldin, M. M., Arellano, J. L., & Binder, D. K. (2012a). Decreased expression of the glial water channel aquaporin-4 in the intrahippocampal kainic acid model of epileptogenesis. *Experimental Neurology*, *235*(1), 246–255. doi:10.1016/j.expneurol.2012.02.002

Lee, K.-W., Zhao, X., Im, J.-Y., Grosso, H., Jang, W. H., Chan, T. W., et al. (2012b). Apoptosis Signal-Regulating Kinase 1 Mediates MPTP Toxicity and Regulates Glial Activation. (M. R.

Cookson, Ed.)*PLoS ONE*, *7*(1), e29935. doi:10.1371/journal.pone.0029935.g006
Lee, S. C., Liu, W., Dickson, D. W., Brosnan, C. F., & Berman, J. W. (1993). Cytokine production by human fetal microglia and astrocytes. Differential induction by lipopolysaccharide and IL-1 beta. *Journal of immunology (Baltimore, Md. : 1950)*, *150*(7), 2659–2667.
Lee, S.-J. (2008). Origins and effects of extracellular alpha-synuclein: implications in Parkinson's disease. *Journal of Molecular Neuroscience*, *34*(1), 17–22. doi:10.1007/s12031-007-0012-9
Lema Tomé, C. M., Tyson, T., Rey, N. L., Grathwohl, S., Britschgi, M., & Brundin, P. (2012). Inflammation and α-Synuclein's Prion-like Behavior in Parkinson's Disease—Is There a Link? *Molecular Neurobiology*, *47*(2), 561–574. doi:10.1007/s12035-012-8267-8
Li, Z.-W., Omori, S. A., Labuda, T., Karin, M., & Rickert, R. C. (2003). IKK beta is required for peripheral B cell survival and proliferation. *Journal of immunology (Baltimore, Md. : 1950)*, *170*(9), 4630–4637.
Liu, M., Cai, T., Zhao, F., Zheng, G., Wang, Q., Chen, Y., et al. (2009). Effect of Microglia Activation on Dopaminergic Neuronal Injury Induced by Manganese, and Its Possible Mechanism. *Neurotoxicity Research*, *16*(1), 42–49. doi:10.1007/s12640-009-9045-x
Liu, X. X., Sullivan, K. A. K., Madl, J. E. J., Legare, M. M., & Tjalkens, R. B. R. (2006). Manganese-induced neurotoxicity: the role of astroglial-derived nitric oxide in striatal interneuron degeneration. *Toxicological sciences : an official journal of the Society of Toxicology*, *91*(2), 521–531. doi:10.1093/toxsci/kfj150
Losi, G., Cammarota, M., & Carmignoto, G. (2012). The role of astroglia in the epileptic brain. *Frontiers in pharmacology*, *3*, 132. doi:10.3389/fphar.2012.00132
Madl, J. E., Duncan, C. G., Stanhill, J. E., Tai, P.-Y., Spraker, T. R., & Gulland, F. M. (2013). Oxidative Stress and Redistribution of Glutamine Synthetase in California Sea Lions (Zalophus californianus) with Domoic Acid Toxicosis. *Journal of comparative pathology*. doi:10.1016/j.jcpa.2013.07.012
Magness, S. T., Jijon, H., Van Houten Fisher, N., Sharpless, N. E., Brenner, D. A., & Jobin, C. (2004). In vivo pattern of lipopolysaccharide and anti-CD3-induced NF-kappa B activation using a novel gene-targeted enhanced GFP reporter gene mouse. *Journal of immunology (Baltimore, Md. : 1950)*, *173*(3), 1561–1570.
Malatesta, P., Hack, M. A., Hartfuss, E., Kettenmann, H., Klinkert, W., Kirchhoff, F., & Götz, M. (2003). Neuronal or glial progeny: regional differences in radial glia fate. *Neuron*, *37*(5), 751–764.
Mastroeni, D., Grover, A., Leonard, B., Joyce, J. N., Coleman, P. D., Kozik, B., et al. (2009). Microglial responses to dopamine in a cell culture model of Parkinson's disease. *Neurobiology of Aging*, *30*(11), 1805–1817. doi:10.1016/j.neurobiolaging.2008.01.001
Matyash, V., & Kettenmann, H. (2010). Heterogeneity in astrocyte morphology and physiology. *Brain Research Reviews*.
McCarty, M. F. (2006). Down-regulation of microglial activation may represent a practical strategy for combating neurodegenerative disorders. *Medical Hypotheses*, *67*(2), 251–269. doi:10.1016/j.mehy.2006.01.013
Meissner, W. G., Frasier, M., Gasser, T., Goetz, C. G., Lozano, A., Piccini, P., et al. (2011). Priorities in Parkinson's disease research, 1–17. doi:10.1038/nrd3430
Menezes-Filho, J. A., Novaes, C. de O., Moreira, J. C., Sarcinelli, P. N., & Mergler, D. (2011). Elevated manganese and cognitive performance in school-aged children and their mothers.

Environmental Research, *111*(1), 156–163. doi:10.1016/j.envres.2010.09.006
Miller, J. A., Trout, B. R., Sullivan, K. A., Bialecki, R. A., Roberts, R. A., & Tjalkens, R. B. (2011). Low-dose 1-methyl-4-phenyl-1,2,3,6-tetrahydropyridine causes inflammatory activation of astrocytes in nuclear factor-κB reporter mice prior to loss of dopaminergic neurons. *Journal of neuroscience research*, *89*(3), 406–417. doi:10.1002/jnr.22549
Minghetti, L., Ajmone-Cat, M. A., De Berardinis, M. A., & De Simone, R. (2005). Microglial activation in chronic neurodegenerative diseases: roles of apoptotic neurons and chronic stimulation. *Brain Research Reviews*, *48*(2), 251–256. doi:10.1016/j.brainresrev.2004.12.015
Mondal, S., Roy, A., Jana, A., Ghosh, S., Kordower, J. H., & Pahan, K. (2012). Testing NF-κB-based Therapy in Hemiparkinsonian Monkeys. *Journal of Neuroimmune Pharmacology*, *7*(3), 544–556. doi:10.1007/s11481-012-9377-9
Moreno, J. A., Streifel, K. M., Sullivan, K. A., Hanneman, W. H., & Tjalkens, R. B. (2011). Manganese-induced NF-κB activation and nitrosative stress is decreased by estrogen in juvenile mice.
Moreno, J. A., Streifel, K. M., Sullivan, K. A., Legare, M. E., & Tjalkens, R. B. (2009a). Developmental exposure to manganese increases adult susceptibility to inflammatory activation of glia and neuronal protein nitration. *Toxicological sciences : an official journal of the Society of Toxicology*, *112*(2), 405–415. doi:10.1093/toxsci/kfp221
Moreno, J. A., Sullivan, K. A., Carbone, D. L., Hanneman, W. H., & Tjalkens, R. B. (2008). Manganese potentiates nuclear factor-kappaB-dependent expression of nitric oxide synthase 2 in astrocytes by activating soluble guanylate cyclase and extracellular responsive kinase signaling pathways. *Journal of neuroscience research*, *86*(9), 2028–2038. doi:10.1002/jnr.21640
Moreno, J. A., Yeomans, E. C., Streifel, K. M., Brattin, B. L., Taylor, R. J., & Tjalkens, R. B. (2009b). Age-dependent susceptibility to manganese-induced neurological dysfunction. *Toxicological Sciences*, *112*(2), 394–404. doi:10.1093/toxsci/kfp220
Mulligan, S. J., & MacVicar, B. A. (2004). Calcium transients in astrocyte endfeet cause cerebrovascular constrictions. *Nature*, *431*(7005), 195–199. doi:10.1038/nature02827
Nagatsu, T., & Sawada, M. (2005). Inflammatory process in Parkinson's disease: role for cytokines. *Current pharmaceutical design*, *11*(8), 999–1016.
Najjar, S., Pearlman, D., Miller, D. C., & Devinsky, O. (2011). Refractory epilepsy associated with microglial activation. *The neurologist*, *17*(5), 249–254. doi:10.1097/NRL.0b013e31822aad04
Nakajima, K., & Kohsaka, S. (1993). Functional roles of microglia in the brain. *Neuroscience research*.
Neal, A. P., & Guilarte, T. R. (2012). Mechanisms of Heavy Metal Neurotoxicity: Lead and Manganese. *J Drug Metab Toxicol S*, *5*, 2. doi:10.4172/2157-7609.S5-002
Nedergaard, M., & Verkhratsky, A. (2012). Artifact versus reality--how astrocytes contribute to synaptic events. *Glia*, *60*(7), 1013–1023. doi:10.1002/glia.22288
Ngugi, A. K., Kariuki, S. M., Bottomley, C., Kleinschmidt, I., Sander, J. W., & Newton, C. R. (2011). Incidence of epilepsy: A systematic review and meta-analysis. *Neurology*, *77*(10), 1005–1012. doi:10.1212/WNL.0b013e31822cfc90
Nimmerjahn, A. (2009, March 27). Astrocytes going live: advances and challenges. *The Journal of Physiology*. J Physiol. doi:10.1113/jphysiol.2008.167171
O'Callaghan, J. P., & Sriram, K. (2005). Glial fibrillary acidic protein and related glial proteins as biomarkers of neurotoxicity. *Expert Opinion on Drug Safety*, *4*(3), 433–442.

doi:10.1517/14740338.4.3.433
Oeckl, P., Lattke, M., Wirth, T., Baumann, B., & Ferger, B. (2012). Astrocyte-specific IKK2 activation in mice is sufficient to induce neuroinflammation but does not increase susceptibility to MPTP. *Neurobiology of Disease*, *48*(3), 481–487. doi:10.1016/j.nbd.2012.06.010
Olanow, C. W. (2004). Manganese-induced parkinsonism and Parkinson's disease. *Annals of the New York Academy of Sciences*, *1012*, 209–223.
Ong, W. Y. W., Leong, S. K. S., Garey, L. J. L., Reynolds, R. R., & Liang, A. W. A. (1996). An immunocytochemical study of glutamate receptors and glutamine synthetase in the hippocampus of rats injected with kainate. *Experimental Brain Research*, *109*(2), 251–267.
Ortinski, P. I. P., Dong, J. J., Mungenast, A. A., Yue, C. C., Takano, H. H., Watson, D. J. D., et al. (2010). Selective induction of astrocytic gliosis generates deficits in neuronal inhibition. *Nature Neuroscience*, *13*(5), 584–591. doi:10.1038/nn.2535
Ouchi, Y., Yagi, S., Yokokura, M., & Sakamoto, M. (2009). Neuroinflammation in the living brain of Parkinson's disease. *Parkinsonism & related disorders*, *15 Suppl 3*, S200–4. doi:10.1016/S1353-8020(09)70814-4
Parpura, V., Heneka, M. T., & Montana, V. (2012). Glial cells in (patho)physiology - Parpura - 2012 - Journal of Neurochemistry - Wiley Online Library. *Journal of …*.
Perea, G., & Araque, A. (2010). GLIA modulates synaptic transmission. *Brain Research Reviews*, *63*(1-2), 93–102. doi:10.1016/j.brainresrev.2009.10.005
Perea, G., Navarrete, M., & Araque, A. (2009). Tripartite synapses: astrocytes process and control synaptic information. *Trends in Neurosciences*, *32*(8), 421–431. doi:10.1016/j.tins.2009.05.001
Perez, F. A., & Palmiter, R. D. (2005). Parkin-deficient mice are not a robust model of parkinsonism. *... Academy of Sciences of the United …*.
Perl, D. P., & Olanow, C. W. (2007). The neuropathology of manganese-induced Parkinsonism. *Journal of neuropathology and experimental neurology*, *66*(8), 675–682. doi:10.1097/nen.0b013e31812503cf
Petroff, O., Errante, L. D., Rothman, D. L., & Kim, J. H. (2002). Glutamate–glutamine Cycling in the Epileptic Human Hippocampus - Petroff - 2002 - Epilepsia - Wiley Online Library. *…*.
Powell, E. M., & Geller, H. M. (1999). Dissection of astrocyte-mediated cues in neuronal guidance and process extension. *Glia*, *26*(1), 73–83.
Przedborski, S., Jackson-Lewis, V., Djaldetti, R., Liberatore, G., Vila, M., Vukosavic, S., & Almer, G. (2000). The parkinsonian toxin MPTP: action and mechanism. *Restorative neurology and neuroscience*, *16*(2), 135–142.
Pulido, O. M. (2008). Domoic Acid Toxicologic Pathology: A Review. *Marine Drugs*, *6*(2), 180–219. doi:10.3390/md20080010
Ramsdell, J. S. (2010). Neurological Disease Rises from Ocean to Bring Model for Human Epilepsy to Life. *Toxins*, *2*(7), 1646–1675. doi:10.3390/toxins2071646
Ransohoff, R. M., & Perry, V. H. (2009). Microglial Physiology: Unique Stimuli, Specialized Responses. *Annual Review of Immunology*, *27*(1), 119–145. doi:10.1146/annurev.immunol.021908.132528
Rehni, A. K., Singh, T. G., Kalra, R., & Singh, N. (2009). Pharmacological inhibition of inducible nitric oxide synthase attenuates the development of seizures in mice. *Nitric Oxide*, *21*(2), 120–125. doi:10.1016/j.niox.2009.06.001
Rogawski, M. A., & Löscher, W. (2004). The neurobiology of antiepileptic drugs for the

treatment of nonepileptic conditions. *Nature Medicine*.
Saijo, K., Winner, B., Carson, C. T., Collier, J. G., Boyer, L., Rosenfeld, M. G., et al. (2009). A Nurr1/CoREST Pathway in Microglia and Astrocytes Protects Dopaminergic Neurons from Inflammation-Induced Death. *Cell*, *137*(1), 47–59. doi:10.1016/j.cell.2009.01.038
Santamaria, A. B. (2008). Manganese exposure, essentiality & toxicity. *Indian Journal of Medical Research*.
Sastre, M. (2010). NSAIDs: how they work and their prospects as therapeutics in Alzheimer's disease. *Frontiers in Aging Neuroscience*. doi:10.3389/fnagi.2010.00020
Sauer, B. (1998). Inducible Gene Targeting in Mice Using the Cre/ lox System. *Methods*, *14*(4), 381–392.
Scallet, A. C., Schmued, L. C., & Johannessen, J. N. (2005). Neurohistochemical biomarkers of the marine neurotoxicant, domoic acid. *Neurotoxicology and Teratology*, *27*(5), 745–752. doi:10.1016/j.ntt.2005.06.018
Schmittgen, T. D., & Livak, K. J. (2008). Analyzing real-time PCR data by the comparative CT method. *Nature protocols*.
Scholin, C. A., Gulland, F., Doucette, G. J., Benson, S., Busman, M., Chavez, F. P., et al. (2000). Mortality of sea lions along the central California coast linked to a toxic diatom bloom. *Nature*, *403*(6765), 80–84. doi:10.1038/47481
Seifert, G., & Steinhäuser, C. (2011). Neuron–astrocyte signaling and epilepsy. *Experimental Neurology*. doi:10.1016/j.expneurol.2011.08.024
Sigel, A., Sigel, H., & Sigel, R. K. O. (2007). *Metal Ions in Life Sciences*. Wiley.
Silvagni, P. A., Lowenstine, L. J., Spraker, T., Lipscomb, T. P., & Gulland, F. M. D. (2005). Pathology of Domoic Acid Toxicity in California Sea Lions (Zalophus californianus). *Veterinary Pathology*, *42*(2), 184–191. doi:10.1354/vp.42-2-184
Silver, J., & Miller, J. H. (2004). Regeneration beyond the glial scar. *Nature Reviews Neuroscience*, *5*(2), 146–156. doi:10.1038/nrn1326
Sofroniew, M. V., & Vinters, H. V. (2010). Astrocytes: biology and pathology. *Acta Neuropathologica*, *119*(1), 7–35. doi:10.1007/s00401-009-0619-8
Spranger, M., Schwab, S., Desiderato, S., Bonmann, E., Krieger, D., & Fandrey, J. (1998). Manganese Augments Nitric Oxide Synthesis in Murine Astrocytes: A New Pathogenetic Mechanism in Manganism? *Experimental Neurology*, *149*(1), 277–283. doi:10.1006/exnr.1997.6666
Sriram, K. (2006). Deficiency of TNF receptors suppresses microglial activation and alters the susceptibility of brain regions to MPTP-induced neurotoxicity: role of TNF. *The FASEB Journal*, *20*(6), 670–682. doi:10.1096/fj.05-5106com
Streifel, K. M., Moreno, J. A., Hanneman, W. H., Legare, M. E., & Tjalkens, R. B. (2012). Gene deletion of nos2 protects against manganese-induced neurological dysfunction in juvenile mice. *Toxicological Sciences*, *126*(1), 183–192. doi:10.1093/toxsci/kfr335
Streit, W. J. W. (2002). Microglia as neuroprotective, immunocompetent cells of the CNS. *Glia*, *40*(2), 133–139. doi:10.1002/glia.10154
Sugama, S., Yang, L., Cho, B. P., DeGiorgio, L. A., Lorenzl, S., Albers, D. S., et al. (2003). Age-related microglial activation in 1-methyl-4-phenyl-1, 2, 3, 6-tetrahydropyridine (MPTP)-induced dopaminergic neurodegeneration in C57BL/6 mice. *Brain Research*, *964*(2), 288–294.
Sutherland, R. J., Hoesing, J. M., & Whishaw, I. Q. (1990). Domoic acid, an environmental toxin, produces hippocampal damage and severe memory impairment. *Neuroscience Letters*,

120(2), 221–223.
Takano, T., Oberheim, N., Cotrina, M. L., & Nedergaard, M. (2009). Astrocytes and Ischemic Injury. *Stroke*, *40*(3, Supplement 1), S8–S12. doi:10.1161/STROKEAHA.108.533166
Tansey, M. G., McCoy, M. K., & Frank-Cannon, T. C. (2007). Neuroinflammatory mechanisms in Parkinson's disease: Potential environmental triggers, pathways, and targets for early therapeutic intervention. *Experimental Neurology*, *208*(1), 1–25. doi:10.1016/j.expneurol.2007.07.004
Tieu, K. K. (2011). A guide to neurotoxic animal models of Parkinson's disease. *Cold Spring Harbor perspectives in medicine*, *1*(1), a009316–a009316. doi:10.1101/cshperspect.a009316
van Loo, G., de Lorenzi, R., Schmidt, H., Huth, M., Mildner, A., Schmidt-Supprian, M., et al. (2006). Inhibition of transcription factor NF-κB in the central nervous system ameliorates autoimmune encephalomyelitis in mice. *Nature Immunology*, *7*(9), 954–961. doi:10.1038/ni1372
Verina, T., Kiihl, S. F., Schneider, J. S., & Guilarte, T. R. (2011). Manganese exposure induces microglia activation and dystrophy in the substantia nigra of non-human primates. *NeuroToxicology*, *32*(2), 215–226. doi:10.1016/j.neuro.2010.11.003
Verkhratsky, A., & Butt, A. (2007). Glial Neurobiology - Alexei Verkhratsky, Arthur Butt - Google Books.
Vezzani, A., Aronica, E., Mazarati, A., & Pittman, Q. J. (2011). Epilepsy and brain inflammation. *Experimental Neurology*. doi:10.1016/j.expneurol.2011.09.033
Waldbaum, S., & Patel, M. (2010). Mitochondria, oxidative stress, and temporal lobe epilepsy. *Epilepsy Research*, *88*(1), 23–45. doi:10.1016/j.eplepsyres.2009.09.020
Wang, Y., Zaveri, H. P., Lee, T.-S. W., & Eid, T. (2009). The development of recurrent seizures after continuous intrahippocampal infusion of methionine sulfoximine in rats. *Experimental Neurology*, *220*(2), 293–302. doi:10.1016/j.expneurol.2009.08.034
Woolf, A., Wright, R., & Amarasiriwardena, C. (2002). A child with chronic manganese exposure from drinking water. *Environmental Health …*.
Wyss-Coray, T., & Mucke, L. (2002). Inflammation in neurodegenerative disease--a double-edged sword. *Neuron*, *35*(3), 419–432.
Zabka, T. S., Goldstein, T., Cross, C., Mueller, R. W., Kreuder-Johnson, C., Gill, S., & Gulland, F. M. D. (2009). Characterization of a degenerative cardiomyopathy associated with domoic acid toxicity in California sea lions (Zalophus californianus). *Veterinary Pathology*, *46*(1), 105–119. doi:10.1354/vp.46-1-105
Zhang, P., Hatter, A., & Liu, B. (2007). Manganese chloride stimulates rat microglia to release hydrogen peroxide. *Toxicology Letters*, *173*(2), 88–100. doi:10.1016/j.toxlet.2007.06.013
Zhang, P., Wong, T. A., Lokuta, K. M., Turner, D. E., Vujisic, K., & Liu, B. (2009). Microglia enhance manganese chloride-induced dopaminergic neurodegeneration: role of free radical generation. *Experimental Neurology*, *217*(1), 219–230. doi:10.1016/j.expneurol.2009.02.013
Zhang, S., Zhou, Z., & Fu, J. (2003). Effect of manganese chloride exposure on liver and brain mitochondria function in rats. *Environmental Research*, *93*(2), 149–157. doi:10.1016/S0013-9351(03)00109-9
Zhang, W. W., Wang, T. T., Pei, Z. Z., Miller, D. S. D., Wu, X. X., Block, M. L. M., et al. (2005). Aggregated alpha-synuclein activates microglia: a process leading to disease progression in Parkinson's disease. *FASEB Journal*, *19*(6), 533–542. doi:10.1096/fj.04-2751com
Zhao, F., Cai, T., Liu, M., Zheng, G., Luo, W., & Chen, J. (2008). Manganese Induces

Dopaminergic Neurodegeneration via Microglial Activation in a Rat Model of Manganism. *Toxicological Sciences*, *107*(1), 156–164. doi:10.1093/toxsci/kfn213

Zhuo, L., Theis, M., Alvarez-Maya, I., Brenner, M., Willecke, K., & Messing, A. (2001). hGFAP-cre transgenic mice for manipulation of glial and neuronal function in vivo. *genesis*, *31*(2), 85–94. doi:10.1002/gene.10008